Raman Spectroscopy for Monitoring Aqueous Phase Hydrogen Sulphide Scavenging Reactions with 1,3,5-tri-(2-hydroxyethyl)-hexahydro-s-triazine

By Leah Nygaard Johansen & Lykke Kloster

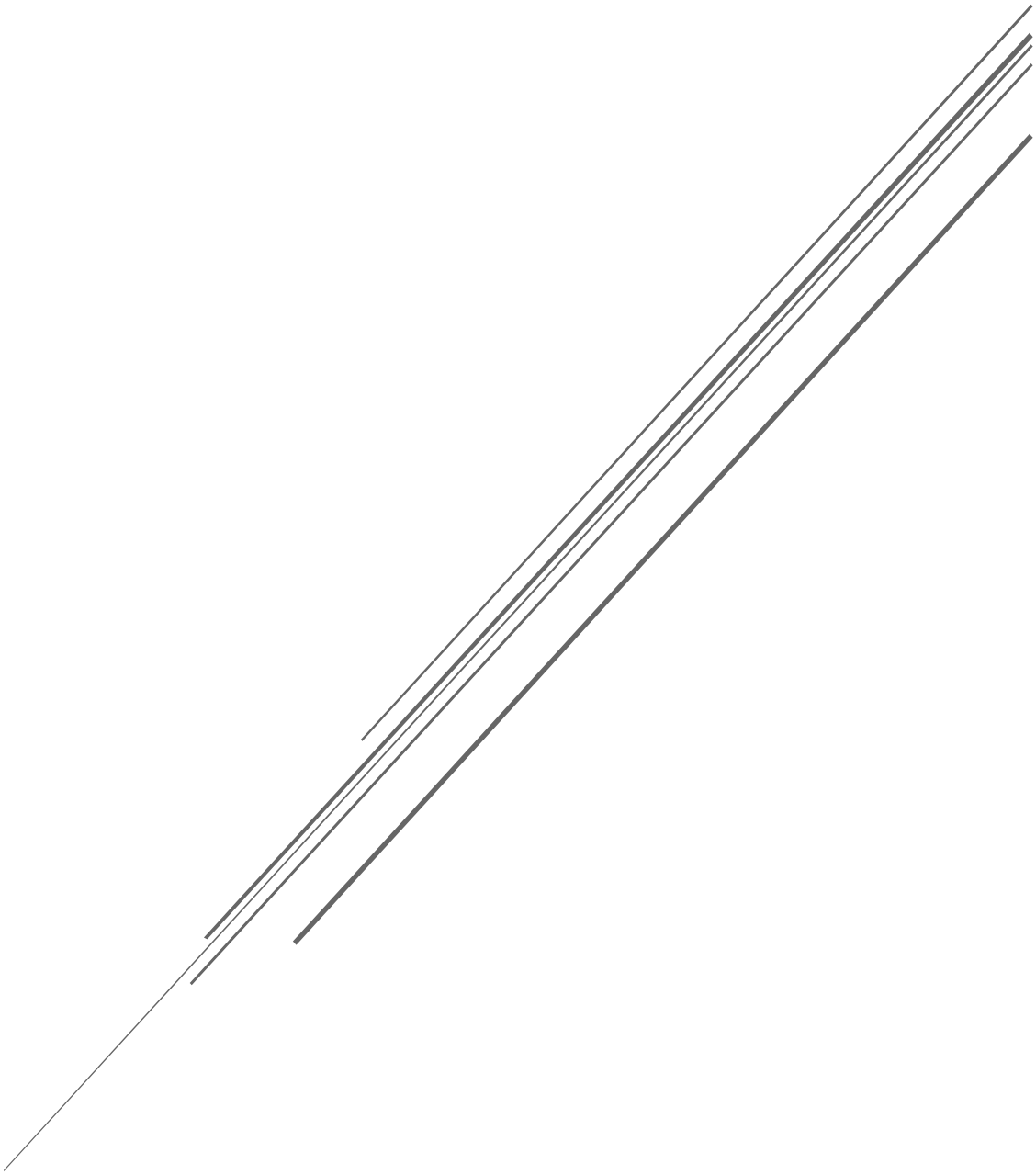

Aalborg University Esbjerg
Master Thesis

Title page

Specialization:	Chemical Engineering
Title:	Raman Spectroscopy for Monitoring Aqueous Phase Hydrogen Sulphide Scavenging Reactions with 1,3,5-tri-(2-hydroxyethyl)-hexahydro-s-triazine
University:	Aalborg University Esbjerg
Supervisors:	Rudi P. Nielsen, Marco Maschietti, Sergey Kucheryavskiy, Anders Andreasen
Collaborators:	Ramboll Energy
Project period:	01.09-2018 – 07.06-2019
Semester:	9th and 10th
Date of hand in:	07.06-2019
Authors:	Leah Nygaard Johansen
	Lykke Kloster

Preface

This project is a master thesis concerning the use of the H_2S scavenger 1,3,5-tri-(2-hydroxy-ethyl)-hexahydro-s-triazine and which factors influencing the scavenging reaction. The challenges within this subject has been numerous, which has only made this project more intriguing and highlighted the importance of this research. Furthermore, this project has attracted attention from outside of Aalborg University Esbjerg when being presented as a poster at the Danish Hydrocarbon Research and Technology Centre, DHRTC, conference in November 2018. Additionally, selected results from this project were published in a paper in Chemical Engineering Transactions vol. 76, 2019, AIDIC with title, Raman Spectroscopy for Monitoring Aqueous Phase Hydrogen Sulphide Scavenging Reactions with Triazine: A Feasibility Study. The article was presented with a poster at the ICheaP 14 conference in Bologna, Italy, May 2019.

The sources used are referred to using the Harvard style and the literature list is found in the end of the report. Following the literature list appendices are attached which cover data deemed non-essential for the report. Figures of all experiments are attached as electronic files. Raw experimental data is attached as a digital file.

We would like to thank DHRTC and the Otto Mønsted Fonds for funding our attendance at the ICheaP 14 conference in Bologna. Also, a big thanks to Anders Andreasen from Ramboll Energy, Field Development, Studies and FEED, Esbjerg, Denmark for great input and co-supervision on this project.

Enjoy reading

Leah Nygaard Johansen and Lykke Kloster

Aalborg University Esbjerg 2019

Abstract

In the offshore oil and gas industry an aqueous scavenger solution of triazine is often used to remove the toxic gas H_2S. Though triazine has been used for decades in the industry, only limited kinetics data is available for the scavenging reaction.

In this project it was attempted to develop a methodology and experimental setup for obtaining kinetics data with the help of Raman spectroscopy and check feasibility of both for online monitoring of the aqueous phase reaction between 1,3,5-tri-(2-hydroxyethyl)-hexahydro-s-triazine (HET) and HS^-, and a setup for obtaining kinetics data is attempted developed.

Raman spectroscopy demonstrated development of specific peaks in the spectra indicating the reaction. Relating the intensity of the peaks to a concentration of HET and HS^-, it was possible to quantify the consumption of reactants over time. Experiments in the pH range of 10.3 and 8.5 was conducted and indicated that the scavenging reaction is pH dependent and is faster at lower pH. At pH 11 no reaction was observed within two hours. HS^-/HET conversion ratios between 1 and 2 indicate that a second scavenging reaction is occurring, which was found to be the reaction between thiadiazine and HS^-.

Four different setups were tested, varying how the acid was added to the system. None of the tested setups proved adequate, as they all had insurmountable disadvantages. Based on the experimental data a kinetics expression dependent on concentration of H^+ and HET is proposed.

Contents

Introduction

The production of oil and gas is vital for the modern society, albeit the industry is often made the villain of the environmental issues the world faces in current times. Even though the industry is not the sole cause for the environmental concerns, it is a contributor, and in as much should limit its environmental footprint. There are many ways the oil and gas production influence the environment negatively, but one of them is the use and discharge of chemicals in the offshore industry. One problematic chemical used offshore is the so-called H_2S-scavenger, which is used to reduce the hydrogen sulphide in the gas streams.

As many oil reservoirs offshore, i.e. in the North Sea, mature, more seawater is introduced to the reservoirs to maintain pressure. The injecting of seawater into the reservoirs results in growth of sulphur reducing bacteria, SRB. These bacteria reduce sulphates in the seawater to the pungent gas dihydrogen sulphide, H_2S. Along with the production fluid H_2S is pumped up from the reservoir causing corrosion to pipelines, health risks to platform workers and contamination of the final product. It is consequently very important to remove H_2S from the production stream. The most common method for removing smaller amounts of H_2S; concentrations of 1000 ppm or less, corresponding to 50 kg/day (Buhaug, 2002), is using water soluble, non-regenerative scavengers often based on derivatives of s-triazines. These scavengers convert H_2S into less toxic chemicals, scavenger products, and are injected directly into the production pipes (Kelland, 2014), cf. Figure 1.

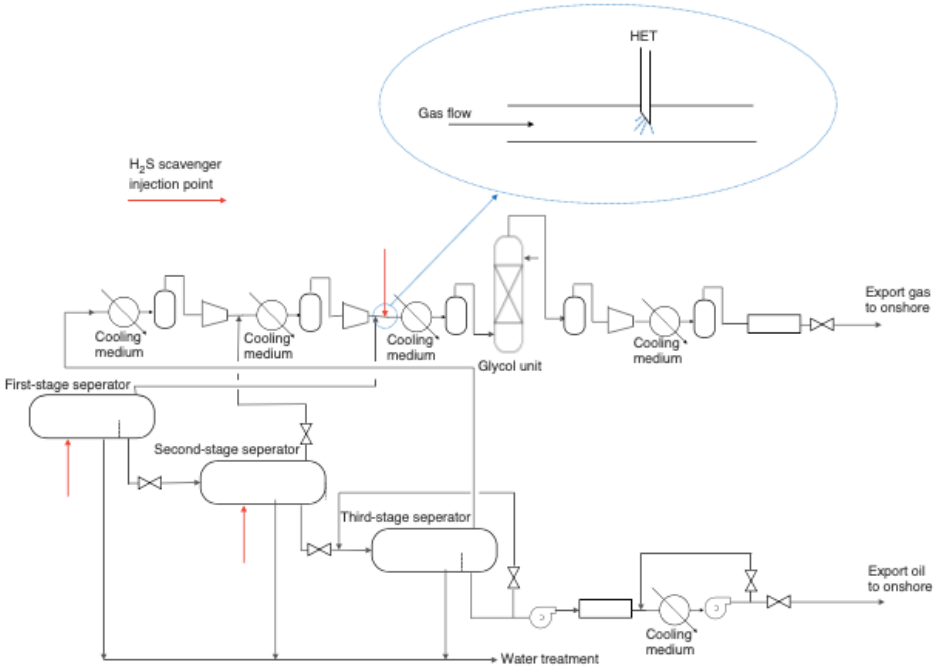

Figure 1: Illustration of the separation process in the North Sea and injection points of the HET scavenger inspired from (Bothamly, 2004)

In the North Sea aqueous solutions of scavengers are injected directly into the production streams, at several points, in the separators and in the gas phase after separation of the production fluids, yet before the dehydration tower, cf. Figure 1 . When injected the aqueous scavenger is either dispersed in the gas stream as small droplets or poured through an injection quill, making the scavenging of H_2S a heterogenous reaction; first part is the absorption of gas into the injected liquid; second part is the reaction in the aqueous phase (Murison et al., 2016).

Though these scavengers have been used for decades, the reaction kinetics of the reaction between H_2S and scavenger is not well defined, and scavengers are often added based on an experienced based theory that requires knowledge of the H_2S concentration; on most platforms this is based on measurements of the export gas. In recent years methods for establishing the H_2S concentrations has been under development, and one promising method is the use of electrochemical H_2S-sensors. These sensors are to be placed before the injection of scavenger, to provide information on the initial concentration of H_2S. However, the sensors and the current techniques only measure the presence of H_2S, and thereby if the H_2S is being removed from the gas phase. It does not measure if the sulphur is indeed transformed into less toxic chemicals, or if it is simply absorbed into the aqueous phase. Based on these techniques it therefore not possible to obtain the optimal conditions for scavenging, as the kinetics for the

reaction is still unknown. The need for a deeper understanding of the scavenging reaction in general, as well as the reaction kinetics is therefore pertinent. Even if the sensors were used to smart regulate, where a feed forward, FF, signal is used to regulate the amount of injected scavenger based on online measurements of H_2S concentration, an over injection of scavenger is still probable, as lack of knowledge leads to the “better safe than sorry”-approach often being utilized.

Over injection of the scavenger is problematic for several reasons; it is not economical viable; it causes fouling in the system; and it increases the amount of spent and unspent scavenger discharged into the surrounding sea leaving environmental footprints. Therefore, it is important to optimize the use of scavengers, and this optimization can be realised by a thorough understanding of the reaction kinetics of the scavenging reaction.

Chapter 1

H_2S

As described, H_2S is a problem most often caused by the combination of the anaerobe sulphate reducing bacteria, SRB, found the reservoirs and the sulphur containing seawater being injected. Studies indicate that seawater-flooded reservoirs generate far more H_2S, compared to reservoirs not seawater-flooded, making the H_2S problem more likely to occur in the offshore industry.

The presence of H_2S is a three-pronged problem as H_2S is; toxic; corrosive and considered a pollutant of the final product. This means, not only does it cause potential health risks and structural problems, it also lowers the value of the final product.

Health risks

As stated H_2S is toxic and potentially lethal, as the symptoms for H_2S exposure varies with the concentration, cf. Table 1.

Table 1: Health symptoms of H_2S (Agbroko et al., 2017), (Beredskabsstyrelsen)

C_{H2S} [ppm]	Symptoms
0.003-100	Very pervasive rotten egg smell
50-100	Eyes and respiratory irritation
100-200	Anaesthetises of the nasal receptors
250-500	Fluid in lungs, cyanosis, bloodstained cough, pneumonia First lethal cases among lung impaired
500	Headache, vertigo, paralysis of respiratory tract, unconsciousness, paranoia
1000	Respiratory arrest, instantaneous collapse and death

As it is evident from Table 1 even lower concentrations of H_2S can cause discomfort to personnel if the gas is released on the platform, however from above 100 ppm, the gas becomes unnoticeable as the olfactory is paralyzed. At higher concentrations the symptoms are severe and above 1000 ppm death is instantaneous. As this toxic gas is imperceptible to humans at hazardous concentrations, the gas must be removed.

Structural risks

Aqueous H_2S behaves like a weak acid; partly dissociating into hydrogen sulphide and sulphide ions, with dissociation equilibria, cf. reaction 1.1 and 1.2:

$$H_2S + H_2O \rightleftharpoons H_3O^+ + HS^- \qquad PK_a = 7.0 \qquad (1.1)$$

$$HS^- + H_2O \rightleftharpoons H_3O^+ + S^{2-} \qquad PK_a = 14.0 \qquad (1.2)$$

The protonation of H_2S in aqueous solution is pH dependent as it is evident from the Bjerrum diagram, Figure 2.

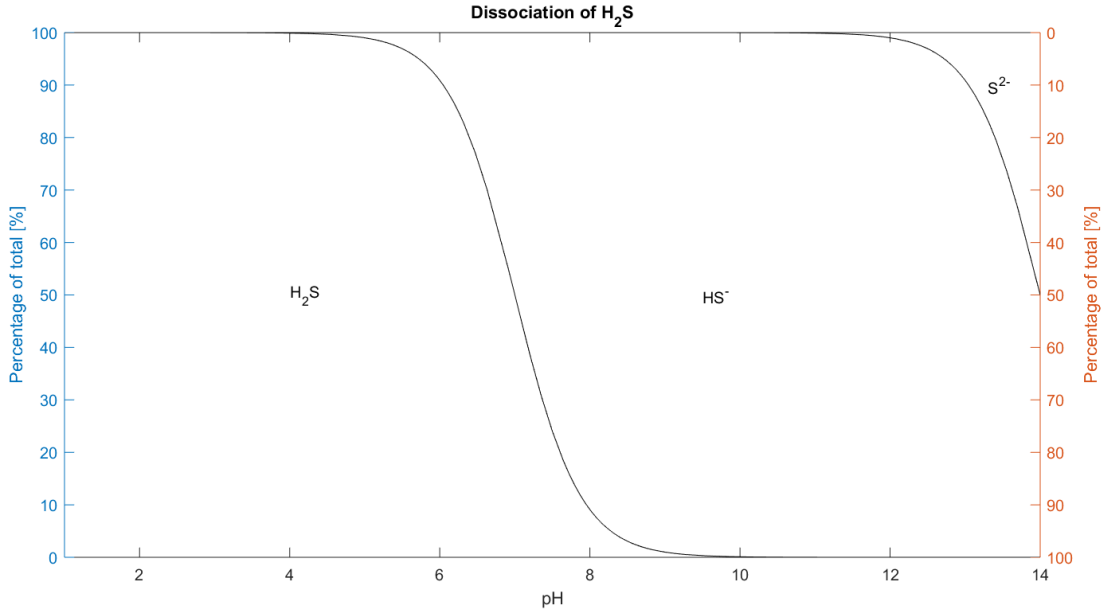

Figure 2: pH dependence of the ionization of H_2S.

From Figure 2 it is evident that only the neutral H_2S gas will be present if pH is below 4, and that no neutral gas will be present above the pH of 10.

As H_2S is a weak acid it will increase corrosion rate on steel pipelines, which impact the structural integrity of the pipes. H_2S is known to cause; pitting, stress cracking corrosion, including sulphide stress cracking and/or deposition of iron sulphide scale (Kelland, 2014).

The explosive nature of H_2S also poses a risk; with LEL and UEL of H_2S of 4% and 44% respectively, H_2S poses a great risk at higher concentrations. Compared to gasoline with LEL at 1,2% and UEL at 7,1%, gasoline is more explosive at lower concentration (mathesongas).

Revenue risks

The last prong of the problem with H_2S is the effect on the quality of the oil and gas sent to the refinery. As the sale specification of natural gas demands a sulphide concentration below 4 ppm (Kelland, 2014), the sulphide must be reduced before export, since, noncompliance of the sale specifications will lead to a monetary fine.

The problem with H_2S presence is most commonly resolved using chemical non-regenerative scavengers, which are added to the production streams and discharged with the produced water. The most common scavenger being triazine based scavengers, as these are relatively cheap and easy to use.

Chapter 2

H_2S scavengers - triazines

The most common method for reducing the amount of H_2S is to use liquid non-regenerative scavengers, as these chemicals are easy to use and do not require additional equipment. The most commonly used scavengers are the class of s-triazines, and most commonly the derivatives of these symmetrical triazines are used.

Triazines are produced by a condensation reaction between an amine and a carbonyl compound. The alkyl groups on the carbonyl compound will be the side groups on the final triazine. The polarity of the side groups determines whether triazine is water or oil soluble. Water soluble triazines are most commonly used due to the easy separation from hydrocarbons making the disposal process easier. One of the most commonly used triazines has an ethanol sidechain, and is formulated from aminoethanol, MEA, and formaldehyde (Agbroko et.al., 2017), cf. Figure 3. This scavenger is called 1,3,5-tri-(2-hydroxyethyl)-hexahydro-s-triazine, a hydroxyethyl-triazine, with designation: HET.

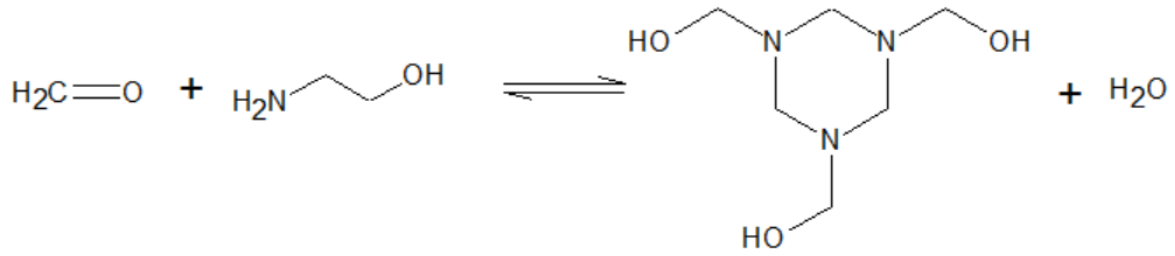

Figure 3: Synthesis of hydroxyethyl-triazine, inspired from (Madsen, 2011)

The reaction requires three moles of formaldehyde and three moles of MEA to synthesize one six-membered ring with three side groups and three water molecules. This reaction is reported to be reversible at low pH, causing a decomposition of the formed triazine molecule into its constituents (Bakke et al., 2001). This reaction is of course unwanted as this makes the scavenger less effective.

2.1 **Problems with scavengers**

HET, and triazines in general, are favourable for several reasons; the reaction products have low toxicity, they reduce H_2S below the threshold limit for sales, 5 ppm, they are H_2S selective and they reduce the H_2S rapidly (Agbroko et. al., 2017), (Kelland, 2014). Yet, HET is not a problem-free chemical to use and tends to be used in excess.

As HET is formulated from formaldehyde, depending on the pureness, the product will contain some traces of formaldehyde. Formaldehyde is a carcinogen and banned in Europe (Kelland, 2014). Furthermore, as seen in Figure 3, the decomposition of HET results in MEA and formaldehyde. This reaction is found to be very pH dependent and, according to the literature, will occur at a pH below 10 (Buhaug, 2002). This causes environmental issues if unspent or decomposed scavenger is discharged into the sea, and decomposition decreases the efficiency of the scavenger, which leads to more scavenger having to be injected.

Though low pH is not favourable due to the decomposition of triazine, high pH is not favourable either as this will lead to fouling problems, caused by scaling. Scale is a problem in the system as this can lead to blocking of equipment and increases the risk of pitting corrosion (Sumestry and Tedjawidjaja, 2013). However, as HET has a high pH, and the resulting MEA as an equally high pH, above 10, the use of HET and other triazines will result in an overall increase of the pH, the amount of scavenger therefore needs to be limited.

Another aspect of the use of scavenger, is that HET tends to lead to precipitation, leading to severe fouling at refineries. The reaction products of HET, both dithiazine and thiadiazine, are suspected of causing additional reaction pathways, which lead to precipitation (Madsen & Søgaard, 2012).

Due to both environmental issues, blockage of pipelines and economic reasons optimizing the use of triazine scavengers has great interest. The scavenging is a heterogenous reaction consisting of absorption and reaction. As the absorption is well-defined in literature (Liss, 1972), the information needed to optimize the scavenging process is the quantitative and qualitative description of the reaction taking place in the aqueous phase.

2.2 H_2S scavenging

The aqueous scavenging reaction of the triazine HET is described in literature as the HET molecule, binding H_2S by substituting one amine with a sulphur molecule (Madsen, 2011), (Buhaug, 2002), cf. Figure 4.

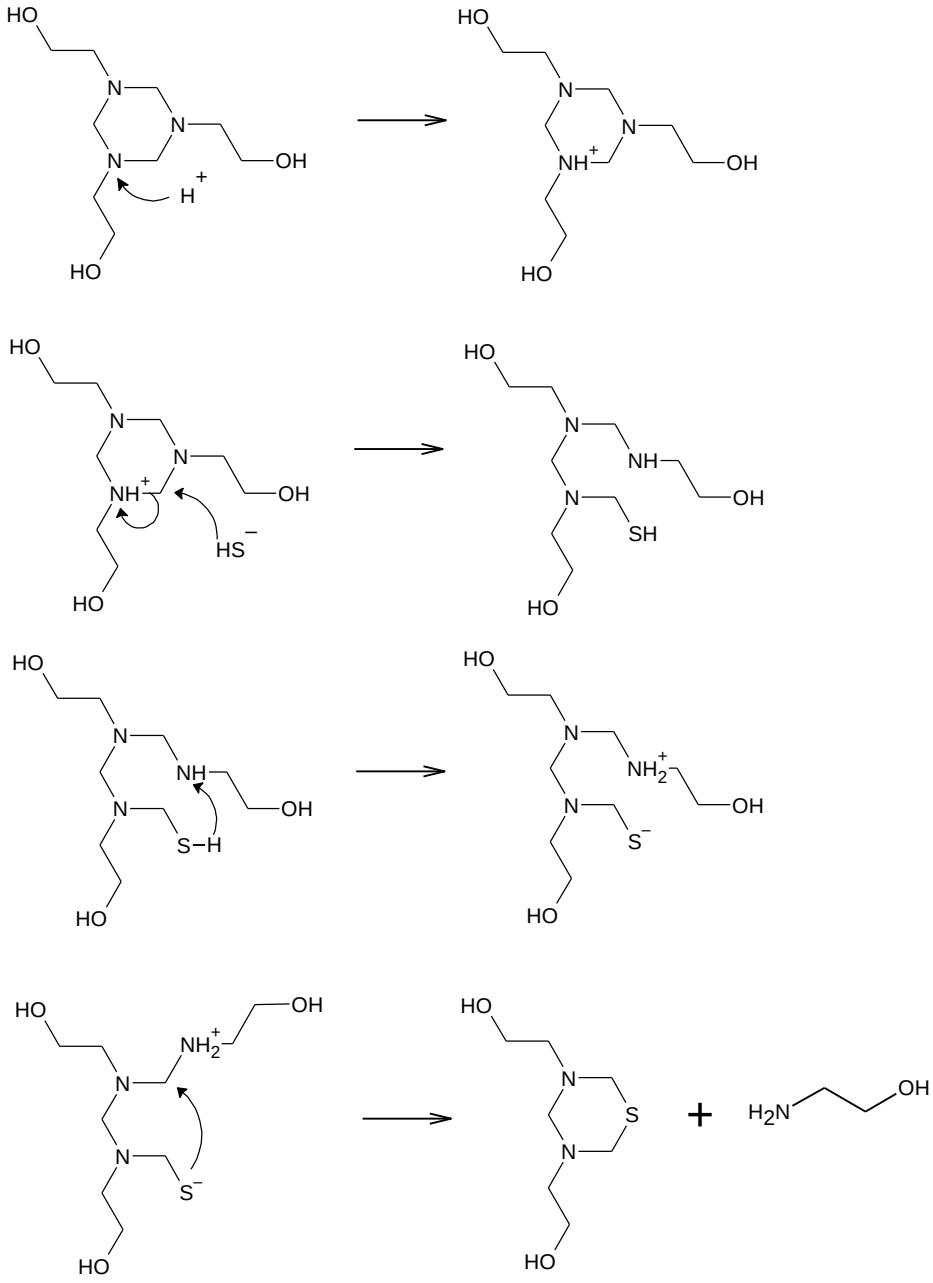

Figure 4: Reaction mechanism for the scavenging reaction between H_2S and triazine inspired from (Madsen, 2011),

The nitrogen molecule is protonated in an acid/base reaction, due to its free lone pair, making the molecule more electrophilic. The electrophilic nature of the molecule will make it

favourable for the positively charged carbon atoms to react with HS^- in a ring opening S_N2-reaction, where the amine side group will be the leaving group.

As the sulphur atom contributes with more electrons to the ring structure and has its electrons situated further from the nucleus, the electrons from sulphur will be shared more efficiently within the molecule compared to nitrogen, making the molecule more stable. According to Madsen 2011 the formed product reacts with HS^- with the same reaction mechanism, creating serial reaction, cf. Figure 5.

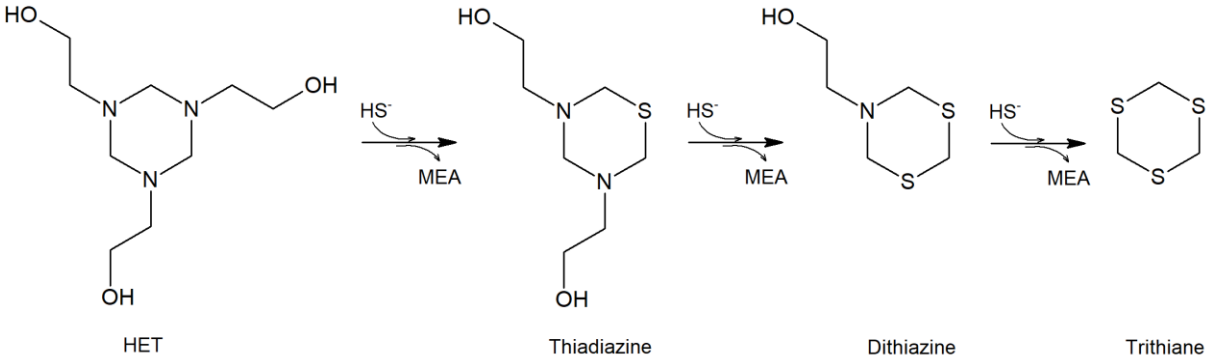

Figure 5: Scavenging pathway for 1,3,5-tri-(2-hydroxyethyl)-hexahydro-s-triazine from (Johansen et al., 2019)

The triazine molecule reacts with HS^- where the nitrogen is substituted with the sulphur atom forming 3,5-di-(2-hydroxyethyl)-hexahydro-1,3,5-thiadiazine, thiadiazine, cf. Figure 5. The thiadiazine molecule further reacts with HS^- forming 5-(2-hydroxyethyl)-hexahydro-1,3,5-di-thiazine, dithiazine. Due to the increased stability of the molecule, the reactivity decreases, hence the reaction rate of thiadiazines reaction with H_2S is lower than triazines reaction rate (Madsen, 2011).

In theory dithiazine further reacts with HS^- to form s-trithiane, yet trithiane is only observed after numerous hours (Madsen, 2012), (Buhaug,2002). It must therefore be assumed that HET theoretically reacts with H_2S two to one, giving a HET to H_2S ratio of 0.5.

However, HET is usually injected in amounts based on an experience-based principle, i.e. equation 2.1(dthreetechnology):

$$0.2\ L\ \cdot C_{H_2S}[ppm] \cdot F\ [MMSCFD] = V_{triazine}\left[\frac{L}{day}\right] \qquad (2.1)$$

The concentration of H_2S refers to the concentration needed to be removed from the stream, and MMSCFD is a typical flow unit used offshore; million standard cubic feet per day. For a

flowrate of 1 MMSCFD and a concentration of 1000 ppm H_2S, corresponding to 995 ppm removal, the equation results in a molar HET to H_2S ratio of 0.56, which is 11 % more HET than theoretically needed. Even with accurate measurements of the initial concentration of H_2S the use of equation 2.1 will still lead to a theoretical 10 % overdosing of HET, making the need for optimization of HET relevant.

2.3 Kinetics of aqueous scavenging reaction

As the reaction scheme in Figure 5 and the reaction mechanisms in Figure 5 is repeatedly described in literature, the qualitative aspect of the scavenging reaction is considered well-defined. However, there are little to no data on the quantitative aspect of the reaction, the only data reported is for excess of HS^- and constant pH (Buhaug, 2002), (Johansen et al., 2019). Making the subject of theoretical and practical importance.

As described HET has two reaction pathways; either it reacts with sulphide or it decomposes into its constituents, cf. Figure 6.

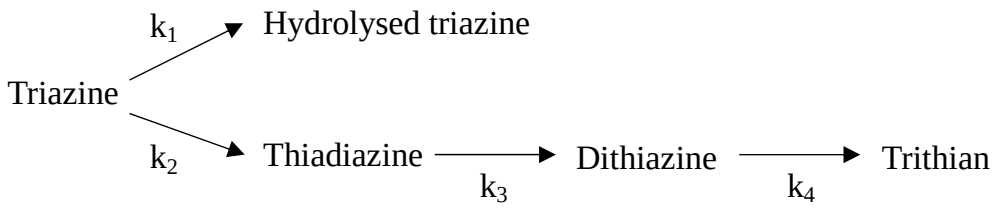

Figure 6: General reaction pathways of triazine inspired from (Madsen,2011)

Figure 6 indicates the reaction pathways of HET, and to examine the full reaction rate of the consumption of triazine both pathways must be taking into consideration. In a study performed by J. Buhaug both pathways were investigated, and it was found that the forming of trithiane does not occur, and therefore does not need to be considered in a study of reaction kinetics (Buhaug, 2002), (Madsen, 2011).In the study the proposed reaction rate for the consumption of HET due to scavenging was as equation 2.2:

$$-r_{HET} = k \cdot C_{HET} \cdot C_{HS^-} \cdot C_{H^+} \qquad (2.2)$$

Based on the assumed reactions, cf. reaction 2.1 and 2.2 (Buhaug, 2002):

$$HET + H^+ \rightarrow HET^+ \quad (2.1)$$

$$HET^+ + HS^- \rightarrow Thiadiazine \quad (2.2)$$

In the investigation of the kinetics J. Buhaug (Buhaug, 2002) used the following setup:

- The reactions have HS^- in excess
- pH is constant

The reactions are considered first order since pH is kept stable and an excess of HS^- is used, however, triazine is commonly in excess, and the scavenging reaction results in an increase of pH as the acidic sulphur species is removed and the alkaline MEA is formed.

The data on the reaction kinetics of the scavenging reaction is still lacking regarding the effects of pH, temperature and concentration of sulphide.

The study of the kinetics of the aqueous phase requires an analytical method that is both able to quantify and identify the reactants and products. To avoid having to sample and stopping the reaction and having to evaporate the water from the samples to preform analysis the analytical method Raman spectroscopy is a possibility. Raman spectroscopy is already used in the food industry for fast on-line monitoring of products (Berg et al., 2013), as it is not affected by the presence of water, nor does it need sampling or other preparation of the solution before measuring.

Chapter 3

Raman Spectroscopy

Raman spectroscopy is a vibrational and rotational spectroscopic technique based on inelastic scattering of monochromatic light in the range of 380-1050 nm. Raman analysis may both be used for samples of liquid, gas, or solid or any form of in-betweens or combinations. Raman can be applied to monitor the progression of batch, semi-batch or continuous reactions, at small as well at large scale. It can be used above sample, through glass, or in direct contact with the sample, e.g. directly on the surface or submerged.

In Raman spectroscopy a sample is illuminated by a laser beam where all scattered light is collected to obtain the Raman spectrum of the sample. Most of all incident photons undergo elastic Rayleigh scattering, and is when a molecule absorbs and emits a photon with identical frequency v_0; this signal is of no use for molecular characterisation. Stokes signal appears when a molecule absorbs a photon with frequency v_0 and emits it with the reduced frequency of v_0-v_m, cf. Figure 7. Anti-stokes signal appears if the molecule is already excited, at the time of interaction. It will then emit the light at a higher frequency of v_0+v_m. It is the signals Stokes and anti-Stokes that produces the Raman signal, and is used in the Raman spectrum.

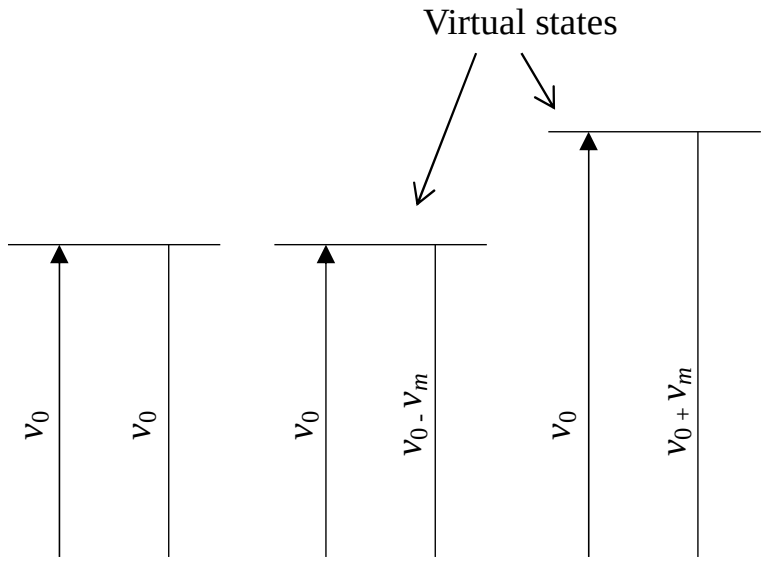

Figure 7: Frequencies of emitted light - Rayleigh scattering, Stokes and anti-Stokes

Spectral wise Raman provides well-resolved bands that are easily and quickly collected over the entire spectral range, 50-4000 cm^{-1}. Bands and peaks can be assigned to functional groups

and for quantitative work univariate calibration models are enough. Raman spectroscopy performs well on compounds with double or triple bonds, different isomers, sulphur-containing and symmetric species (Socrates, 2001). Most importantly, the Raman spectrum of water is very weak enabling direct measurement in aqueous samples.

Subtle changes to the position and shape of Raman bands are indicative of small changes in the local chemical environment. This is both an advantage, as this makes Raman very sensitive and suitable for complex chemical reactions and a disadvantage as small changes in the environment or laser wavelength can appear as wavenumber shifts and be mistaken for chemical changes. This disadvantage of stability can be minimized by mathematically align reference spectrum or pseudo-reference peaks (Bakeev, 2010).

Raman spectroscopy is widespread for process monitoring in pharma and food industry, but limited research has been published on using Raman spectroscopy for monitoring of scavenging reactions (Berg et al. 2013). Recently Perez-Pineiro et al. (Perez-Pineiro et al., 2018) investigated the use of Raman spectroscopy to quantify amounts of HET and dithiazine in spent triazine samples off-line. The results indicated potential for early stages of the scavenging process while later stages of the reaction indicate that the MEA by-product might cause chemical interference (Perez-Pineiro et al., 2018). As Raman has already proven useful in other areas as well as in the study of the scavenging reaction, it should be a viable candidate as an analytical method able to follow the scavenging reaction and providing much needed quantitative data.

Chapter 4

Problem statement

Hydrogen sulphide is as, it was already mentioned, a huge problem in the offshore oil and gas industry. As it is corrosive and toxic, it causes problem for the safety of the crew and structural integrity. It therefore needs to be removed and discarded off as cheaply and safely as possible. One method of doing this is by using the non-regenerative scavenger called HET which is injected into the gas pipeline right after the separation trains and before the glycol unit. The HET scavenger is currently one of the most commonly used offshore, yet very little information regarding the kinetics of the scavenging reaction is known. Due to this lack in knowledge there is a tendency to utilize a "better safe than sorry" practice when it comes to dosing of the scavenger, leading to gross overdosing of the chemical. This leads to a loss of money and greater environmental impacts, hence there is a clear need for an optimization of the scavenger consumption. However, an optimization can only be realized if the kinetics of the reaction is well defined.

Therefore, one of the main questions when dealing with scavengers is: Why is there very little information available on the kinetics of a chemical that has been used for decades?

To understand the kinetics of the scavenging reaction between HET and HS^-, a method based on Raman spectroscopy has been developed in this project. This was done by proposing and answering the questions:

1. Is Raman spectroscopy a feasible method to investigate the scavenging reaction between HET and HS^-?
2. Which factors, if any, are the most important for the reaction kinetics; temperature, pH, concentration of reactants?

The first step in this project was to see if Raman can track changes in the chemicals during a reaction. The second step was to identify any problems associated with the use of Raman. After checking the feasibility of Raman to track the reaction and clarifying any issues with the use, next step was to develop a setup, which makes possible to identify and quantify the reactants and products of the reaction and use these data to obtain knowledge about the reaction kinetics of the scavenging reaction.

Chapter 5

Experimental work

The scavenging of hydrogen sulphide in the offshore environment is as described divided into two separate steps; the absorption of the gaseous H_2S into the aqueous scavenger solution and the reaction between HET and HS^- in the aqueous solution. As the absorption of gaseous H_2S is well defined in literature, the focus of this project will be the reaction occurring in the aqueous solution of scavenger.

As described in the problem statement, several steps must be taken in order to fully understand the problems connected with the scavenging reaction. The experimental work is divided into several different segments. The segments are thought of as a guidance through the choices made based on a proposed question. After every segment the answer to the proposed question will be either 'yes' or 'no' which will lead to the next question. The proposed questions and their pathways are explained in Figure 8.

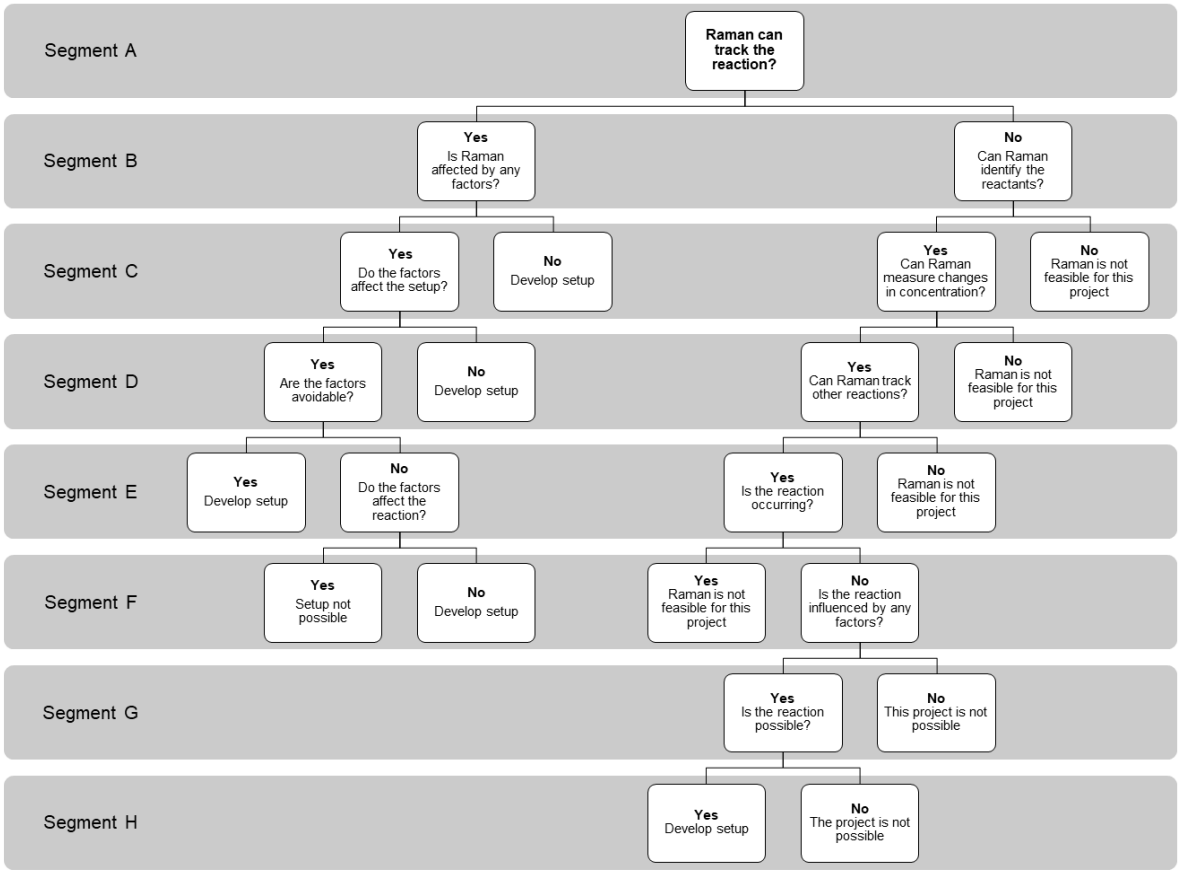

Figure 8: Pathway of experimental design divided into segments from A to H.

Segment A is to investigate if Raman can track the scavenging reaction. This is expected based on recent research for off-line quantification of HET and scavenger products and due to the application of process monitoring in the food and pharma industry (Berg et al.). The next segments depend on the result of the prior segments, if Raman is not able to track the reaction it must be identified why, if Raman can track the reaction it must be investigated what may influence the signal to develop a setup for obtaining kinetics data. The expectations for the experimental work are that Raman can track the reaction and that it is possible to develop a setup which can provide reliable and repeatable kinetics data.

For the all experimental segments the same assumptions and considerations were made.

5.1 Experimental basics

For the experiments conducted throughout this project some general consideration and choices are made regarding the setup and chemicals used.

The general steps of the experimental method are:

1. Make aqueous solutions of HET and HS^-
2. Mix the two solutions together
3. Reaction carried out in batch mode
4. Acquire and analyse the spectra

The exact setup varied throughout the experiments; however, the basic conceptual setup was identical and is illustrated in Figure 9:

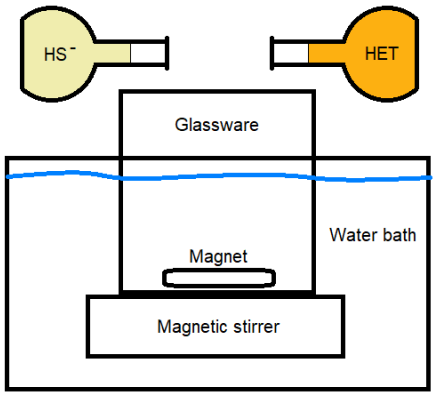

Figure 9: Basic conceptual setup

The temperature was kept constant using a water bath, and the solutions were kept homogeneous using a magnet and magnetic stirrer inside the water bath. Different glassware was used for different experiments, with volumes in the range of 10-100 ml.

In all the experiments, some decisions were made, mainly regarding the availability of scavenger as well as how to dissolve HS^- in water and the presence of oxygen.

The availability of scavengers

To investigate the kinetics of the scavenger reaction it is necessary to have the pure scavenger chemical HET. On the other hand, this chemical has limited availability. It was however possible to obtain a very limited amount of HET with a purity of 75 %. This was not ideal as the last 25 % of the solution is unknown. Some of the 25 % impurities are suspected of being water or aminoethanol, MEA, as this is one of the constituents of HET. It was considered to synthesize HET in the laboratory, however, there was no available method of ensuring the synthesized product was HET.

The limited amount of HET was taken into consideration during the experimental work to preserve as much HET as possible. For this reason, another scavenger was used for the preliminary studies. This other scavenger was another derivative of the s-triazine, with methyl as side groups, thereby creating a methanol amine triazine, MMAT. The physical and chemical data for the two triazines are listed in Table 2.

Table 2: Physical and chemical data of HET and MMAT

	HET	MMAT
Chemical formula	1,3,5-tri-(2-hydroxyethyl)- hexahydro-s-triazine	1,3,5-Trimethylhexahydro-1,3,5-triazine
CAS number	4719-04-4	108-74-7
Supplier	Sigma-Aldrich	Sigma-Aldrich
MW	219.33 g/mol	129.24 g/mol
Purity	75 %	99 %
Density	1.19 g/cm^3	0.919 g/cm^3
Appearance	Yellow viscous liquid	Clear colourless liquid

The MMAT-scavenger is expected to react as the original HET, though the leaving group will be different. Since MMAT was available in copious amounts, this scavenger was used instead of the HET, for some of the experiments.

Sulphide

To ensure the presence of H_2S in the solution sulphur salt was dissolved in water. The dissolution of salt meant that it was possible to be in control of the amount of sulphide in the system. However, the downside of using any salts as a basis for the sulphide is the addition of ions to the system, this could potentially have unwanted effects on the reaction; it raises the overall ionic strength of the solutions, which changes the activity of the chemicals. It may affect the reactivity of the chemicals in the solution when increasing the ionic strength (Arnaut et al., 2007). The ionic strength is not accounted for in this project.

Two salts were available for this: Na_2S and NaHS, cf. Table 3.

Table 3: Physical and chemical data of Na_2S and NaHS

	Na_2S	NaHS
Chemical formula	$Na_2S \cdot x\ H_2O$	$NaHS \cdot x\ H_2O$
CAS number	27610-45-3	207683-19-0
Supplier	VWR Prolab Chemicals	Honeywell
Product code	83756.230	101750961
Water content [mol/mol]	~ 4.5	~ 1.6
Molecular weight [g/mol]	160.91	83.99
Purity [%]	61	N/A
Solubility in water	570 g/L	620 g/L

The water content of the two salts was found by using ICP to measure the sodium content of a solution with a known amount of salt. From the sodium content it could be estimated how much water was in the chemical.

Both Na_2S and NaHS will, when being dissolved in water, yield one mole of hydrogen sulphide per mole salt. However, according to J.E Doeller (Doeller, 2005) and F. Bashipour (Bashipour, 2017) NaHS tends to not completely dissociate into HS^-, and therefore Na_2S, was initially chosen for the experiments.

Other Chemicals

The data for chemicals used in the project is listed in Table 4.

Table 4: Physical and chemical data of MEA, HCl and formaldehyde

	MEA	HCl	Formaldehyde
Chemical formula	C_2H_7NO	HCl	CH_2O
CAS	141-43-45	7647-01-0	50-00-0
Supplier	Sigma-Aldrich	Fisher Scientific	Sigma-Aldrich
Molecular weight	61.08	36.46 g/mol	30.03 g/mol
Purity	≥ 98 %	36-38% w/w in water	37% w/w in water
Density	1.01 g/mL	1.20 g/mL	1.09 g/mL
Appearance	Clear liquid	Clear liquid	Clear liquid

Oxygen

In the offshore environment the presence of oxygen would not be a factor. There are several reasons as to why oxygen is undesired offshore and should be removed from the system. In an experimental setup the problem is the oxidation of sulphide Östlund & Alexander states that oxygen oxidizes sulphide to sulphite and sulphate (Östlund & Alexander, 1963). Both are un-wanted in the reaction system as this would obscure the sulphide being scavenged; a decrease in concentration of sulphide could then be attributed to both the scavenger reaction as well as the oxidation of sulphide. Even though the presence of oxygen is a nuisance, it was experienced challenging to avoid, cf. Appendix 1.

On the other hand, as stated in literature the oxidation rate depends on the oxygen/sulphide-ratio (Östlund & Alexander, 1963), (Cline & Richards, 1969); at 25 ℃ and a ratio of 10 the half-life was found to be approximately 17 minutes (Östlund & Alexander, 1963) and 65 hours if the ratio is less than 4 and the temperature is 9.8 °C (Cline & Richards, 1969). The measured concentration of oxygen in the demineralized water were 9 mg/L as a maximum, cf. Appendix 1, giving a maximum oxygen/sulphide-ratio of 0.1, making oxidation negligible in this case.

5.2 Spectral data

Raman was chosen as the analytical technique in this project, and the spectrometer available had specifications as stated in Table 5.

Table 5: Specifications on the Raman spectrometer used

Spectrometer	RXN1
Vendor	Kaiser Optical systems, Inc., MI, USA
Excitation light source	785 nm laser
Probe	Fibre connected non-contact probe
Spectral range (Raman shift)	3425 to 100 cm^{-1}
Resampling interval	1 cm^{-1}

The optimal settings for spectra acquisition were evaluated experimentally. Exposure times of 1, 2, 3 and 5 seconds was tested, and 5 seconds was chosen as this provided the best signal-to-noise ratio. Exposure times above 5 seconds was not tested, as it was desired to obtain spectra as close to one another as possible.

To reduce variation in the measurements, it was chosen to accumulate a total of 3 scans, to provide 1 average spectrum. The measurements were obtained in aqueous solutions, and though the solutions were assumed homogeneous, local variations are to be expected. Taking the average of three different scans therefore provided a more descriptive result of the solution at the current time. The accumulation of 3 scans with exposure times of 5 seconds resulted in each Raman spectrum being the average spectrum of the solution over the duration of 20 seconds. The 5 additional seconds are due to delays between each scan.

It was desired to have measurements as close timewise as possible, however, with the exposure time and accumulation settings, Raman preformed most stable with sampling intervals of 1 minute. The intervals with 20, 30, 40 and 50 seconds have been also tested, however, shorter intervals resulted in uneven spacing of the measurements. For all experiments throughout the project identical settings were used, cf. Table 6.

Table 6: Settings used for Raman

Sampling interval	1 minute
Exposure time	5 seconds
Accumulation of scans	3 scans

Pre-processing

After obtaining the spectral data, spectra were pre-processed to minimize noise, correct baseline and to account for any discrepancies with the positioning of the Raman probe (global intensity effect), making the data more comparable. As with the Raman settings, the optimal pre-processing settings were based on experimental data.

To minimize noise the smoothing Savitzky-Golay filter was used. This filter is based in convolution to fit adjacent points to a polynomial (Eilers, 2003). For the project the linear polynomial was selected. The number of adjacent points (filter width) was tested between 5 and 27; the lower the filter width the lower the signal-to-noise ratio a high filter width was therefore best. However, the higher filter width smoother the peaks made them less distinguishable. The filter width providing the highest signal-to-noise ratio without losing the shape of the peaks was 11.

To correct the baseline the Alternating Least Squares (ALS) method was chosen (Eilers, 2003). This method uses a smoothing parameter, lambda, and a penalty. The smoothing parameter was chosen as 1000, several higher values were tested, however, as the higher value the smoother curve, higher values resulted in less distinguishable peaks. The penalty limits the difference between smoothed curve and the fitted data, and was chosen as 0.001, higher values was tested, but 0.001 was found to provide the clearest peaks.

To normalize the data, and, thereby, make spectra more comparable, Standard Normal Variate (SNV) was chosen. This method corrects global intensity effect which can be caused e.g. different distance between probe and sample. SNV normalizes each spectrum individually by subtracting the average of the total spectrum from each Raman shift and dividing it by the standard deviation (Rinnan et.al., 2009).

The pre-processing was carried out using MATLAB 2018b and the toolbox “mdatools” (Kucheryavskiy, 2019), with identical settings, cf. Table 7.

Table 7: Pre-processing used to pre-process Raman spectra

Purpose	Tool	Settings
Minimize noise	Savitzky-Golay smoothing filter	filter width = 11 points linear fit
Correct baseline	ALS baseline correction	penalty = 0.001 lambda = 1000
Normalization	Standard Normal Variate (SNV)	

5.3 Segment A

The first step to evaluate the scavenging reaction is to validate if Raman spectroscopy can monitor the scavenging reaction, cf. Figure 10. Research show that Raman can quantify HET and the scavenging products off-line. However, no research is available for Raman spectroscopy to online monitor the scavenging reaction. This needs to be investigated.

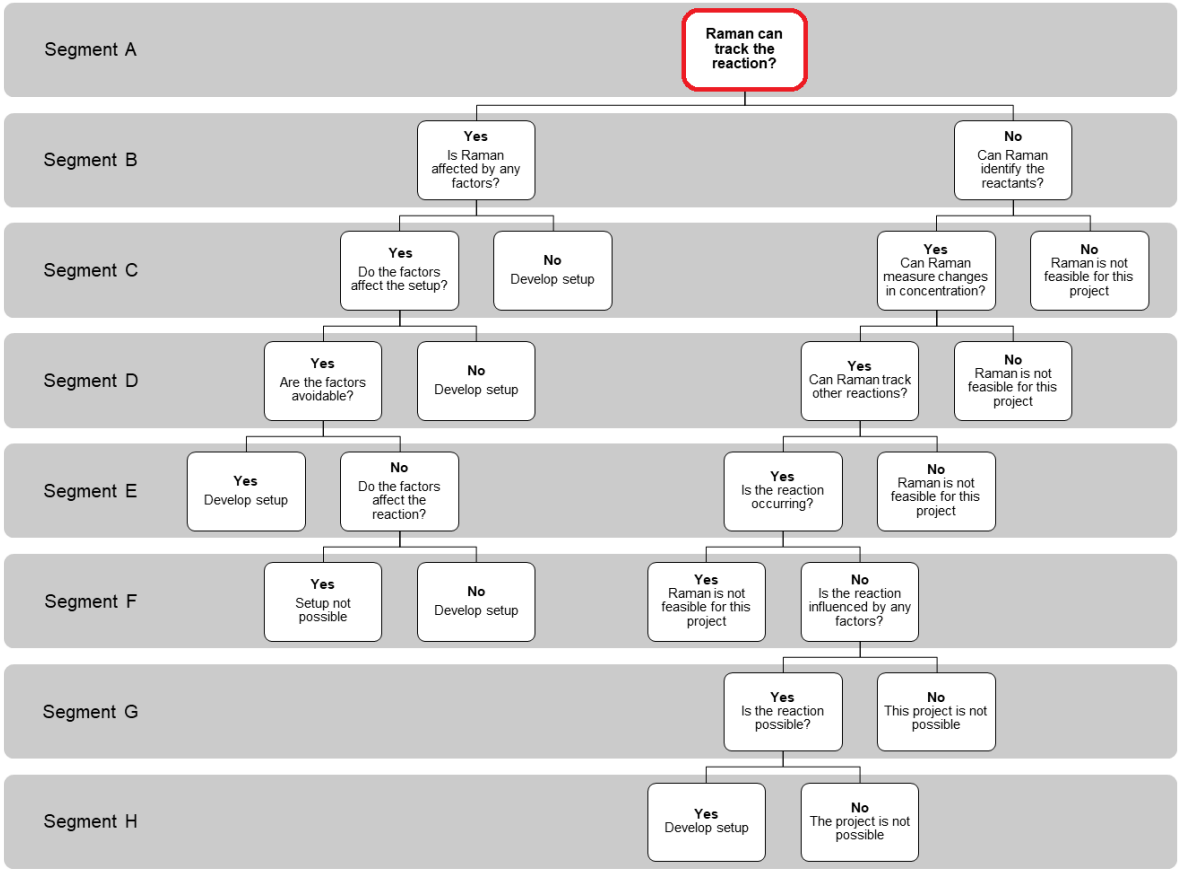

Figure 10: Segment A; Red indicates the current segment, blue the answered segments.

For validation of Raman spectroscopy, the primary method was, as before mentioned, making solutions of aqueous MMAT and HS^-, mixing them and acquire data to analyse.

As one of the aims of the study was to observe the effect of pH on the reaction, it was decided to keep the pH stable at 12 using a phosphate buffer, Na_2HPO_4/Na_3PO_4. This buffer was chosen as this is the buffer used in previous studies of the scavenging reaction (Buhaug, 2002), (Madsen, 2011).

The HET and HS^- solutions were made and heated separately, the time of mixing was set as t = 0.

The glassware in this experimental setup was a measuring cylinder, 100 ml, and the Raman probe was positioned just above the aqueous solution, as illustrated in Figure 11.

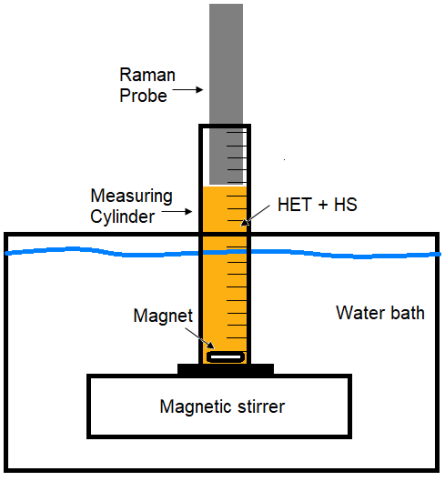

Figure 11: Setup for segment A

Several experiments were conducted with different concentrations of reactants and temperatures, cf. Table 8 for the combinations. The experimental specifications for all experiments are found in Appendix 2.

Table 8: Conducted experiments using the MMAT and Na_2S at different temperatures with reaction time of 5 min.

Experiment	Time [min]	C_{MMAT} [M]	C_{HS^-} [M]	T [°C]
A.1	5	0.023	0.015	35
A.2	5	0.015	0.015	25
A.3	5	0.023	0.023	35
A.4	5	0.015	0.023	25
A.5	5	0.023	0.015	25
A.6	5	0.023	0.023	35
A.7	5	0.023	0.015	35
A.8	5	0.023	0.015	25
A.9	5	0.023	0.023	25
A.10	5	0.015	0.015	25
A.11	5	0.015	0.015	35
A.12	5	0.015	0.015	35
A.13	5	0.023	0.023	25
A.14	5	0.015	0.023	25
A.15	5	0.015	0.023	35
A.16	5	0.015	0.023	35
A.17	**30**	**0.005**	**0.048**	**22**
A.18	**210**	**0.005**	**0.048**	**22**

Experiments A.17 and A.18 are identical in chemicals, concentrations and temperature as the one reportedly used by J. Buhaug (Buhaug, 2002) in their studies of the kinetics.

Results and discussion

Several attempts at tracking the scavenging reaction were conducted, but none were successful. The pre-processed spectrum of experiment A.15 is plotted in Figure 12 and is indictive of the overall trend for all the experiments in segment A. Spectra of all experiments are attached digitally.

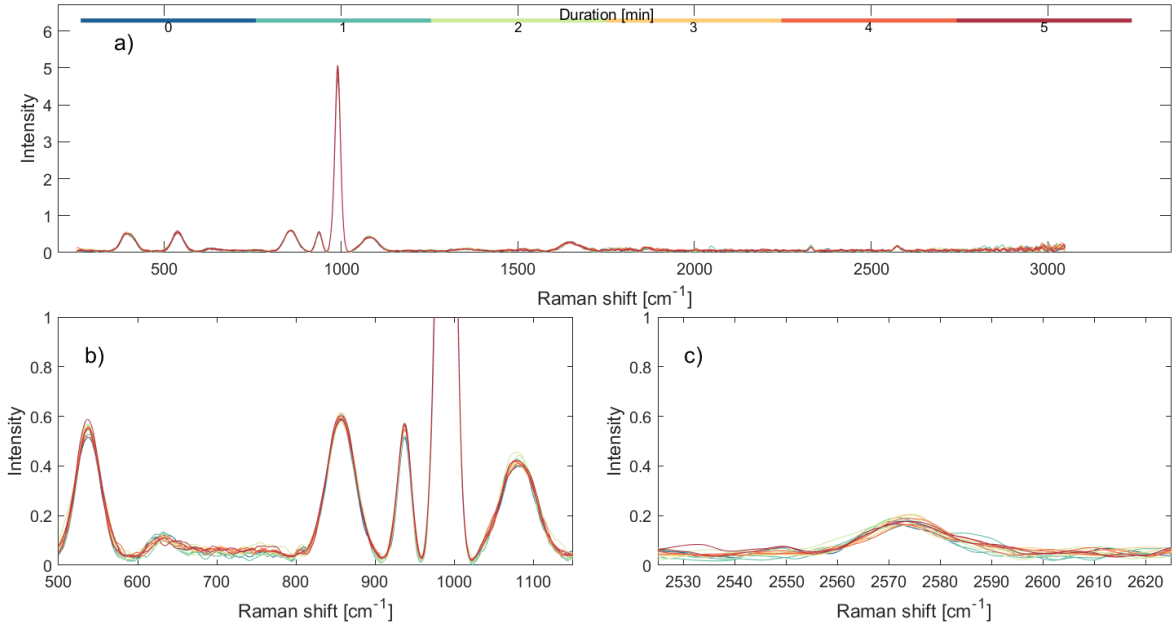

Figure 12: Raman spectrum experiment A.15. This spectrum is indictive of the experiments of segment A.

As it is evident from Figure 12 there are no discernible changes in the spectra indicating any chemicals decreasing in concentration. There were no changes in the spectra for any experiments in segment A. It must therefore be concluded that the answer to segment A is ‘no’. At this point Raman is not able to track the scavenging reaction. It therefore needs to be scrutinised why no reaction is observed. Starting with investigating Raman.

5.4 **Segment B**

It is evident from segment A that the scavenging reaction is not observable, and the answer to segment A must therefore be ‘no’. This leads to the next segment where it must be investigated why no reaction is observed, cf. Figure 13.

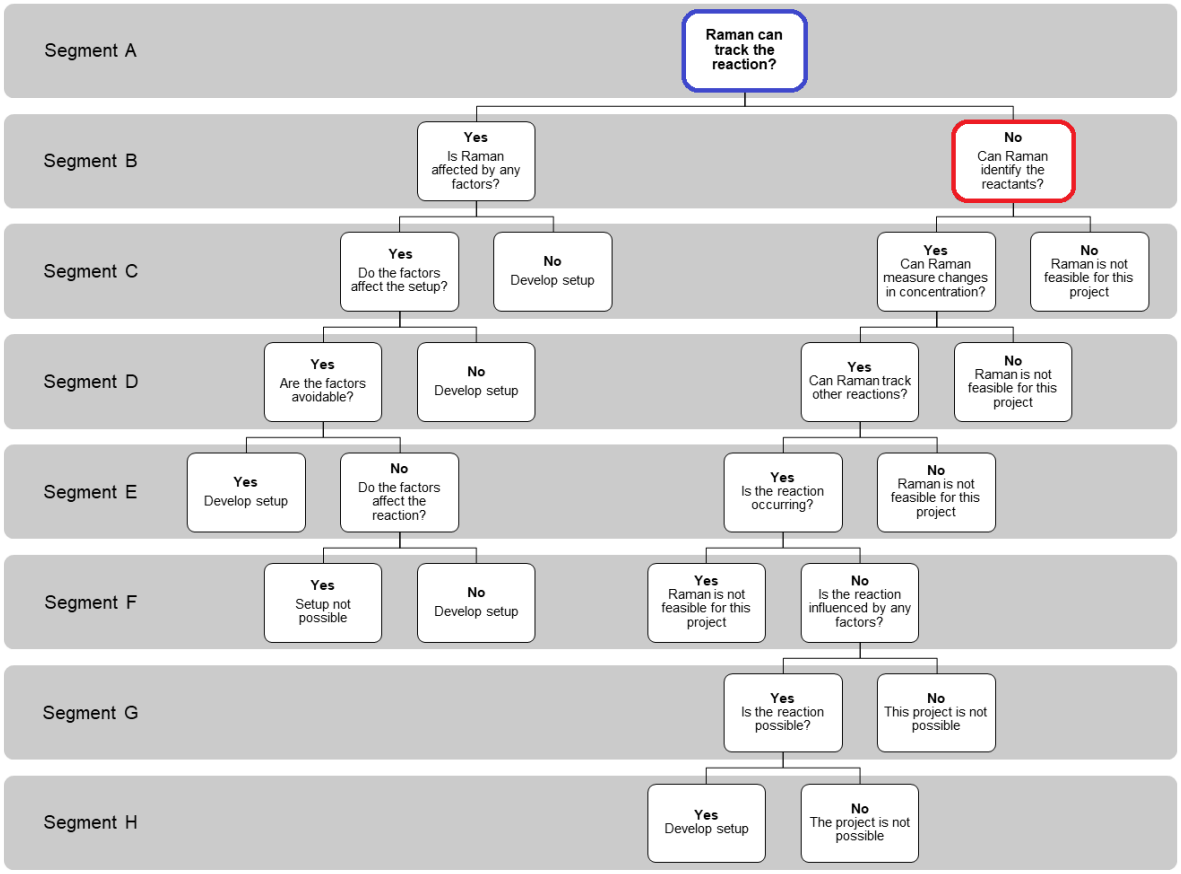

Figure 13: Segment B; Red indicates the current segment, blue the answered segments.

Segment B therefore poses the question; can Raman identify the reactants?

To ensure that Raman can identify and distinguish between the reactants aqueous solutions are prepared of all reactants.

HS^-

HS^- has only one chemical bond and therefore only one band in the Raman spectra, cf. Figure 14. The band is positioned at 2572 cm^{-1} (Socrates, 2001).

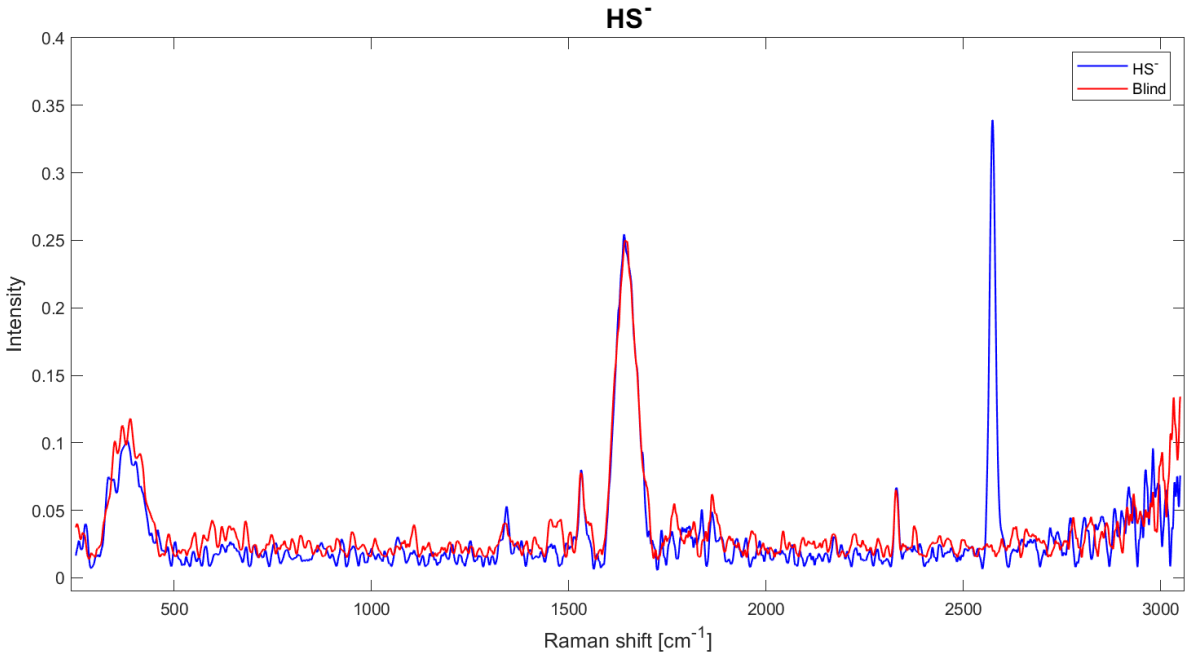

Figure 14; Raman spectra of HS- (blue) and a reference spectra (red)

As illustrated in Figure 14 there is a strong peak at band 2572 cm^{-1}. This peak is an identification peak of HS^-. The peaks at 400 and 1600 cm^{-1} are present both in the HS^- solution and in the water sample and are suspected of being response from the glassware. The peak at 2400 cm^{-1} is expected to be caused by either water or the glassware, and not a part of the reactant's spectra.

HET and MMAT

The ring structure of HET and MMAT are the same but has different side groups, some peaks are therefore expected to be identical cf. Figure 15.

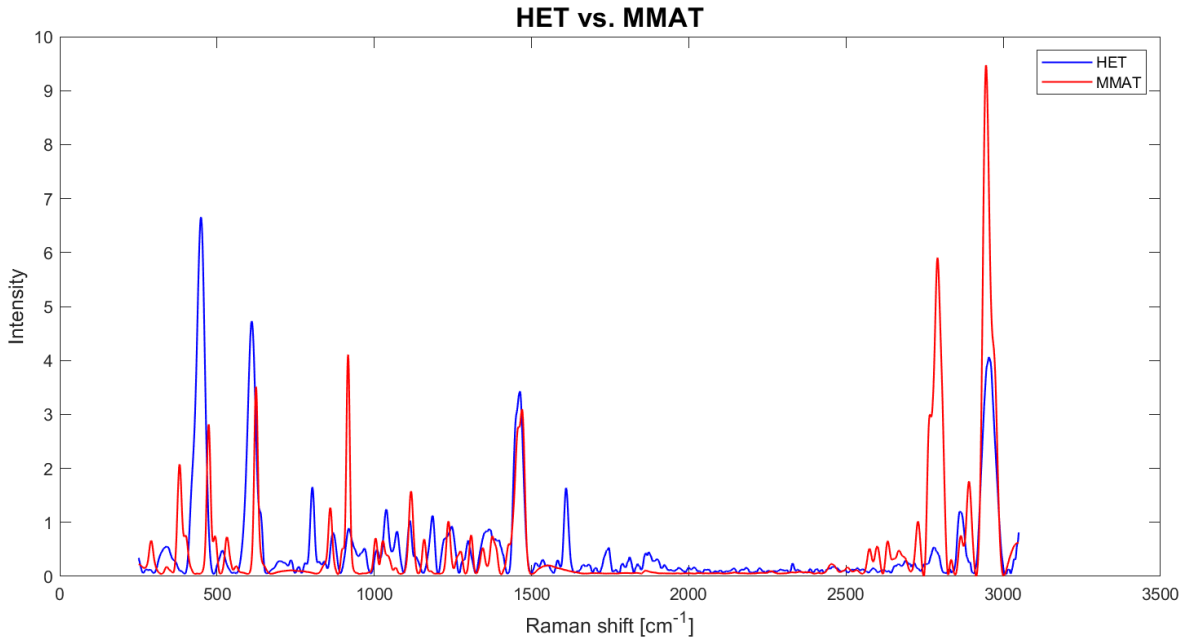

Figure 15 Raman spectra of the used HET (blue) and MMAT (red)

Bands from 980 to 1000 cm^{-1} are referred to as symmetric triazine, peaks at 1300 to 1500 cm^{-1} are described as tertiary amines (Socrates, 2001). Peaks for symmetric triazine and tertiary amines are present in both the HET and MMAT spectra, cf. Figure 15. The peak at 2700 cm^{-1} correspond to the bond energies of N-CH_3 (Socrates, 2001) and therefore this peak must refer specifically to MMAT. The peaks at 3000 cm^{-1} are indicative of water. The peak around 800 cm^{-1} is only present in the HET spectrum and the peak at 1600 cm^{-1} is considered a HET peak due to the side group, MEA, cf. Figure 15. In this spectrum the peak around 1400 cm^{-1} is considered a glass or water peak, and not important for either reactants.

HET and MEA

Spectra of HET and its scavenging by-product MEA was acquired to investigate if MEA and HET interferes, cf. Figure 16. The two molecules are expected to have peaks at the same Raman shifts, as MEA is a constituent of HET. Though it is possible that aliphatic MEA, with a primary nitrogen atom, has a slightly different Raman shift as the nitrogen atom is no longer a tertiary amine.

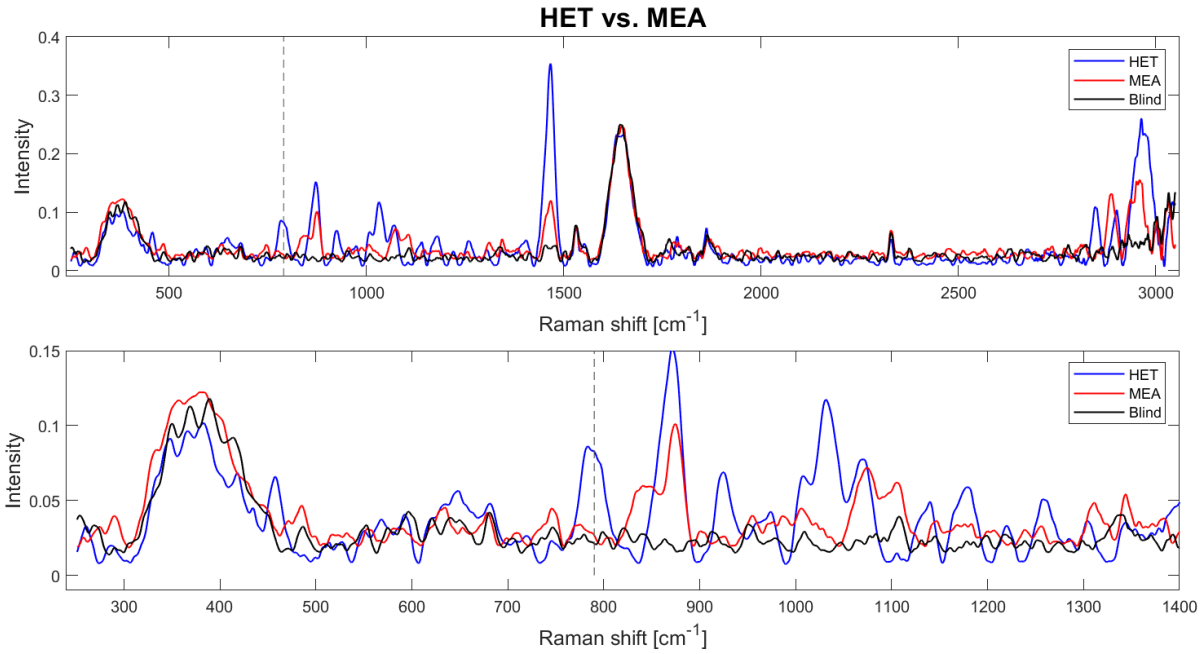

Figure 16 Raman spectra of HET (blue), MEA (red), and demineralized water (black)

As evident from Figure 16, most MEA peaks are obscured by HET peaks and it is difficult to separate the two molecules. The peak at 1600 cm^{-1} is glass or water and not of interest to the spectrum for the reactants. The HET used has a purity of 75 %, and MEA is suspected to one impurity in the last 25 %, albeit most is expected to be water. The suspected presence of MEA in HET could explain the challenges in clearly identifying MEA in the presence of HET, as the molecule would be present in both HET and MEA solutions. The peak at 1100 cm^{-1} indicates an aliphatic amine and therefore refers to MEA. HET has a peak at 790 cm^{-1}, which is described as C-N stretch in literature. As this is only present in HET, and not MEA, the C-N bond must indicate the ring structure. The HET peak just above 1000 cm^{-1} is considered as a 1,3,5-trisubstitued ring (Socrates, 2001).

Perez-Pinero et al., 2018 uses the peak 870 cm^{-1} as a HET indication peak, though the paper state that this peak might be obscured by MEA, which is evident from Figure 16. Perez-Pinero et al., 2018 also report that HET peaks at 1025 cm^{-1} are often obscured by alcohols, and the peak at 921 cm^{-1} tends to disappear in spent samples.

Indicator peaks

The peaks that are not obscured by other chemicals are chosen as indicator peaks for each reactant, cf. Table 9.

Table 9: Indicator peaks for reactants in the scavenger reaction and glass

Chemical	Indicator peak [cm^{-1}]
HS^-	2572
HET	790
MMAT	2700
MEA	1100

Raman spectroscopy can identify and distinguish between the different reactants, as each reactant has significant identification peaks. Therefore, this is not the reason for the lack of observable reactions.

5.5 Segment C

As concluded from segment B, Raman can distinguish between the different chemical compounds HS^-, MMAT, HET, and MEA. The Raman spectra indicates peaks important to identify the different chemicals. The answer to segment B is therefore 'yes', cf. Figure 17.

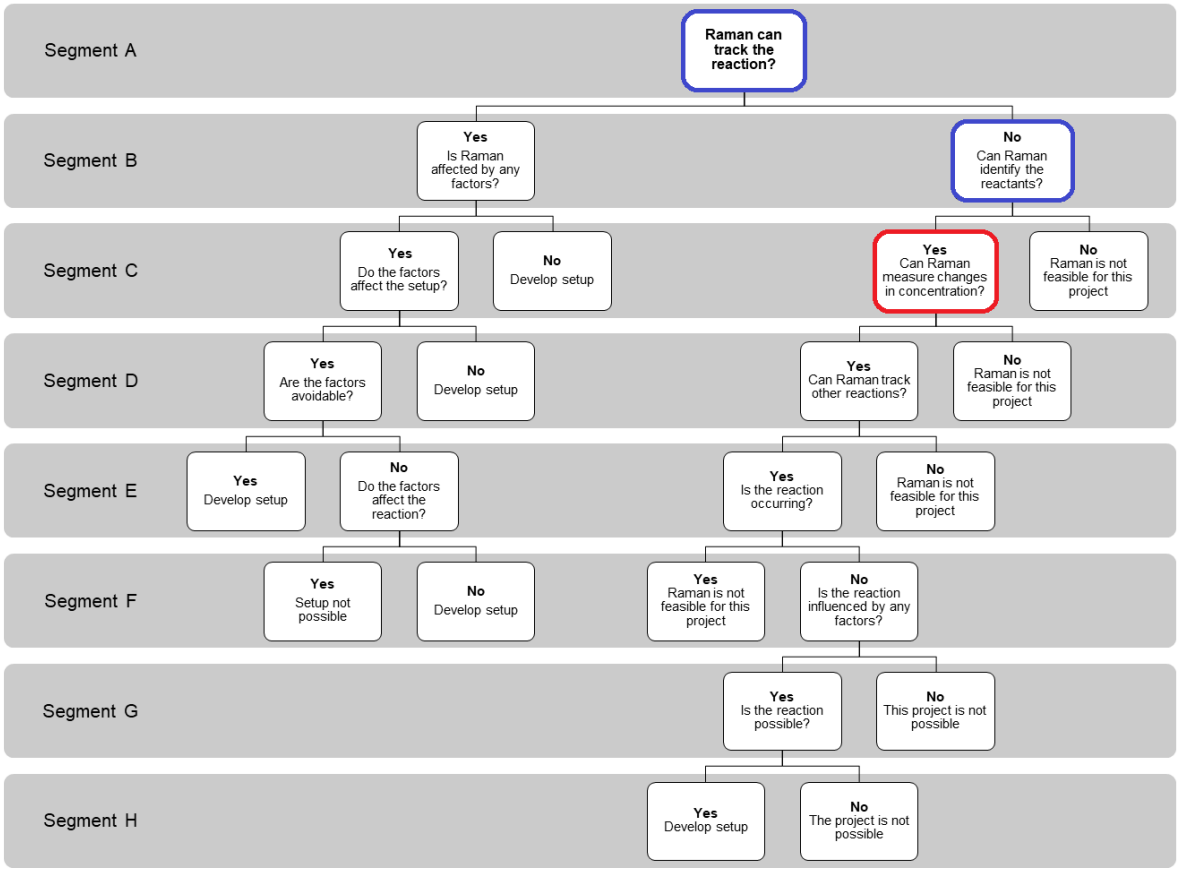

Figure 17: Segment C; Red indicates the current segment, blue the answered segments.

Segment C therefore poses the question; Can Raman measure changes in concentration?

To ensure it is possible to track changes in concentration using Raman spectroscopy, calibrations were carried out.

These calibrations consisted of acquiring spectra of the reactants at three different concentration levels. If a change in the intensity of the peaks were observed, a regression correlating the intensity of the signal to a concentration was performed.

As mentioned in segment B and summarized in Table 9 different indicator peaks are chosen for each reactant. HS^- has one indicator peak, the peak at 2572 cm^{-1}, and is expected to be the only peak to change. HET has several peaks expected to change with changes in concentration.

However, peaks present in both MEA and HET must be removed as influencing factors of the calibration, due to interference. To ensure that MEA is not influencing the calibration solutions containing both HET and MEA different concentrations are prepared and scanned with Raman, cf. Table 10.

Table 10: Concentrations of HET and MEA for calibration experiments

Combination	HET [M]	MEA [M]
1	0.38	0.19
2	0.38	0
3	0	0.38
4	0.19	0.38
5	0.19	0.19
6	0	0
7	0.19	0
8	0	0.19
9	0.38	0.38

The combination of concentration levels listed in Table 10 limited the effects of MEA on the calibration of HET.

To calibrate HS^-, solutions were prepared with Na_2S, at concentration levels identical to the ones of HET, listed in Table 10. In Figure 18 the spectra for the calibration sets are illustrated.

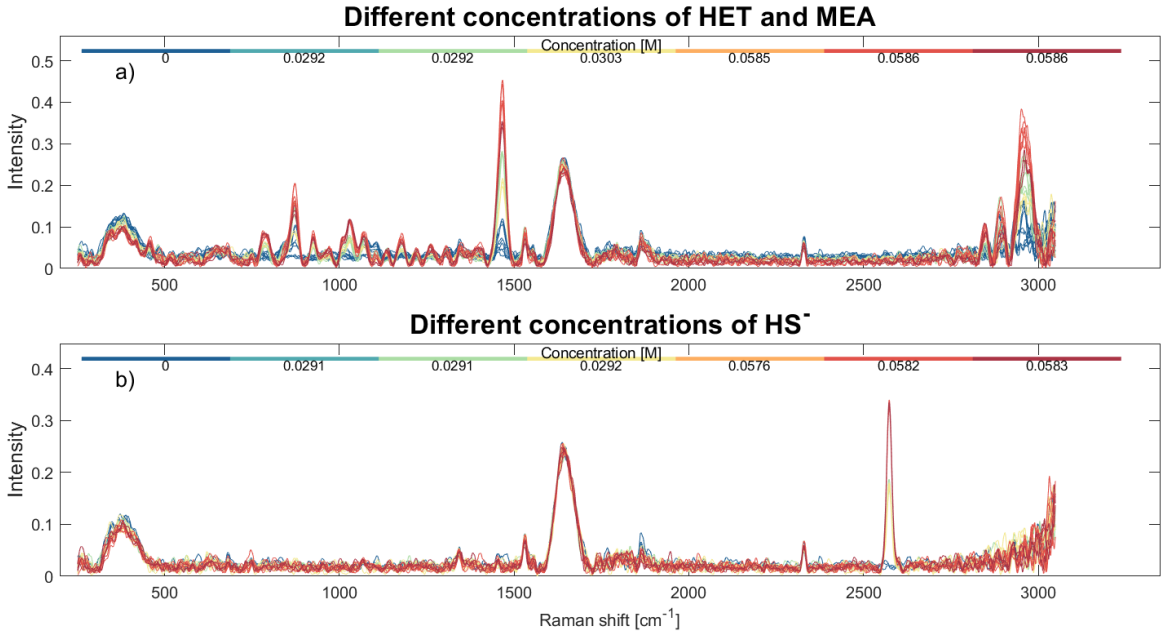

Figure 18: Spectra of different concentration levels of HS^- and for a solution of HET and MEA

As it is evident from Figure 18 Raman can register changes in concentration. From Figure 18 the intensity of peak 2572 cm^{-1} appears to double as the concentration doubles, and this is the

only peak changing. This indicates that there is a linear correlation between the intensity and the concentration. HET has several peaks changing with concentration, and as expected MEA influence some of the peaks indictive of HET, peak 1400 cm^{-1}, and these should therefore not be included in the calibration.

To ensure optimal correlation of peak intensity and concentration all peaks are used in the calibration using the mathematical linear regression method called Partial Least Squares, PLS. PLS was chosen since it is useable when number of objects is higher than the number of observations (Kucheryavskiy, 2019). The PLS method provides a predictive model for many factors, in this case Raman shifts, that are colinear with the predictions (Kucheryavskiy, 2019). The method locates the Raman shifts most predictive of the expected concentration and correlates the intensity linearly to the concentration. PLS is used on both HS^-, HET and MEA. For the calibration of HS^-, cf. Figure 19.

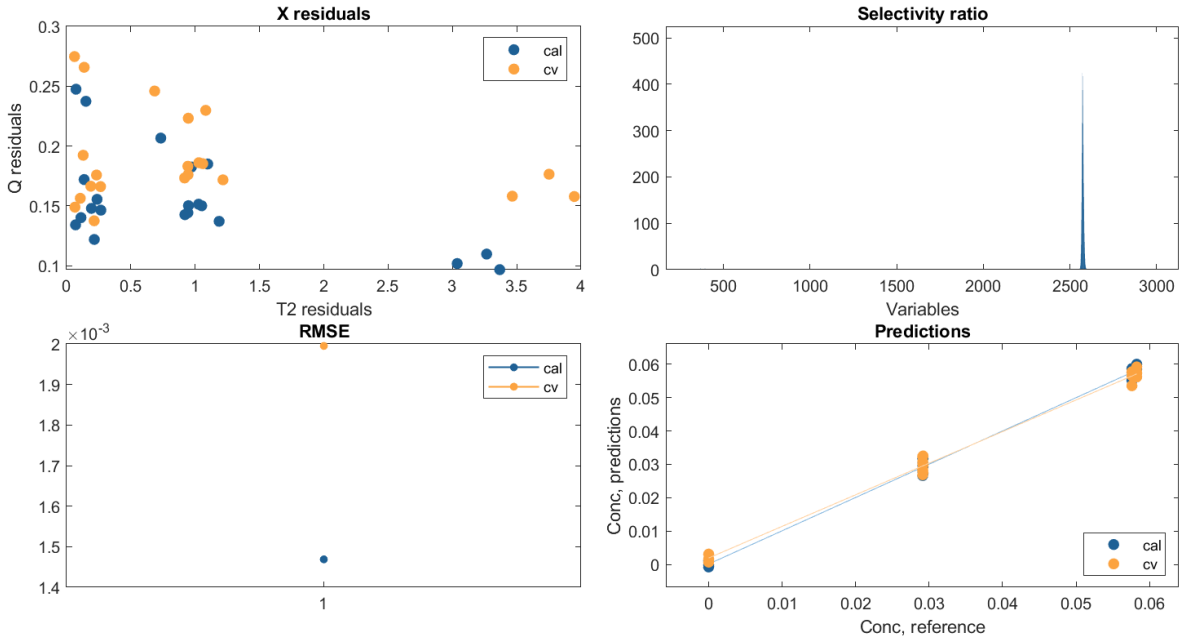

Figure 19: PLS model of HS^-. The concentrations are in molar.

As it is evident from Figure 19, there is a linear correlation between concentration and intensity, with an R^2-value of 0.993 and a RPD of 10.4, cf. Appendix 3. And as expected the peaks around 2572 cm^{-1} are solely indictive of the sulphur species.

Using PLS on the data for HET, a similar linear correlation is evident, cf. Figure 20.

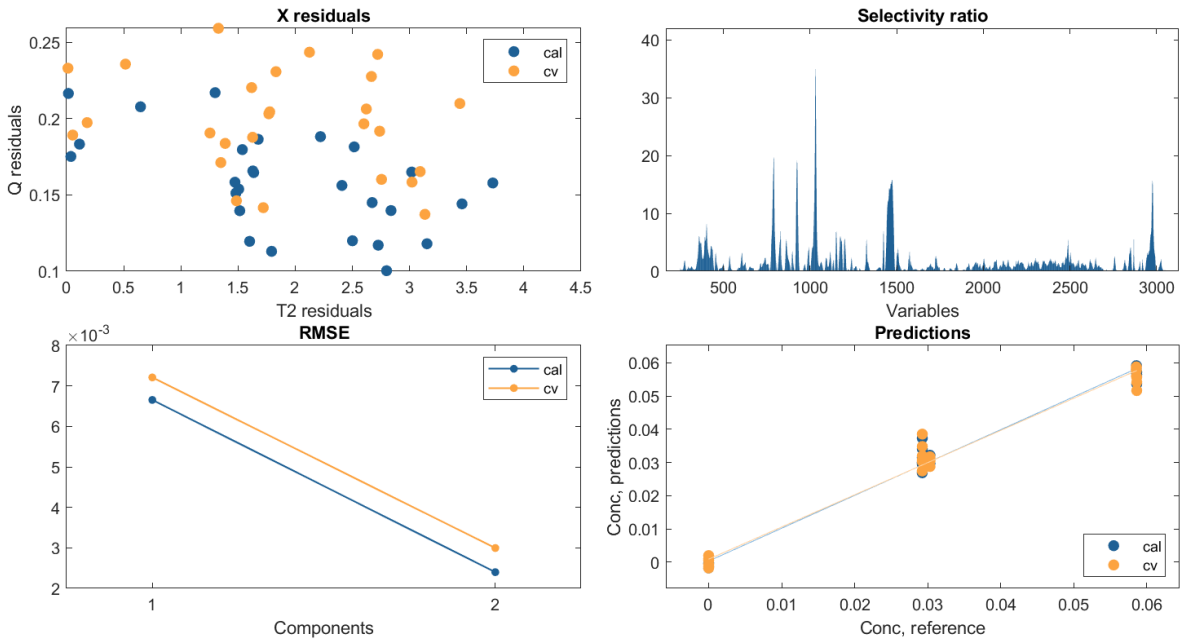

Figure 20: PLS model of HET. The concentrations are in molar.

From Figure 20 it is evident that several peaks influence the concentration profile, cf. Figure 20b. If these peaks are compared with the peaks said to identify MEA and HET, the selected peaks are not overlapping with MEA. Therefore, the calibration should not take any change in MEA concentration into account. The linear correlation has a R^2 value of 0.985 and an RPD of 8.14, cf. Appendix 3.

The calibration for MEA is available in Appendix 3.

It is possible to definitively show a linear correlation between the intensity of several peaks and the concentration of the reactants. Raman can track changes in the concentrations of the reactants.

5.6 **Segment D**

It is concluded from segment C that it is possible to correlate the concentration of HS^- and HET to the intensity of peaks in the Raman spectra. This validates that Raman can track changes in concentration of chemical species. Therefore, the answer is, 'yes', Raman can measure changes in concentration, cf. Figure 21.

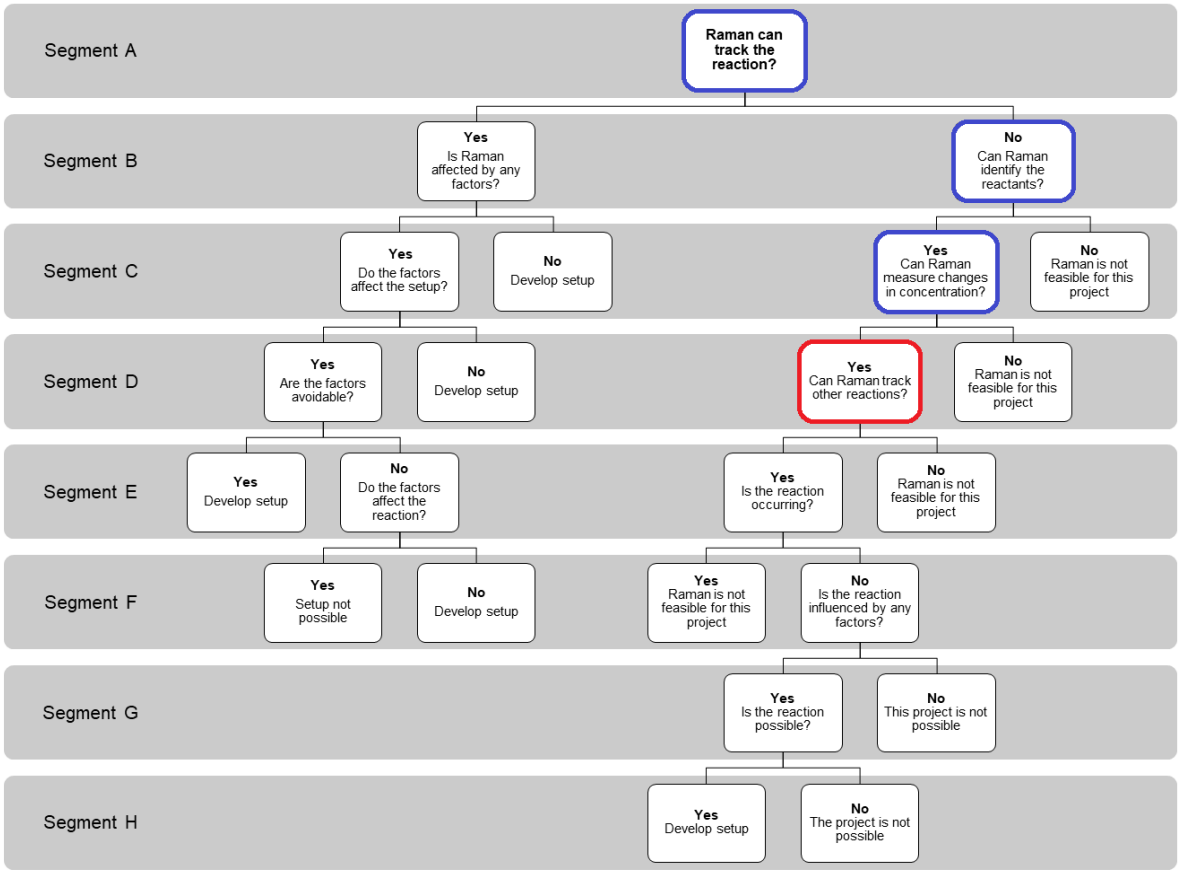

Figure 21: Segment D; Red indicates the current segment, blue the answered segments.

Segment D therefore poses the question; Can Raman track other reactions?

To ensure that Raman can track changes in concentration over a period, two different experiments were carried out:

1. Evaporation of sulphur species
2. Gas-experiment

The first experiment is to ensure that Raman can track changes in concentration if only one chemical compound is present. The second experiment is performed using gaseous H_2S instead of the sodium salt to ensure that Raman can track changes in the chemicals studied.

Evaporation of sulphur species

During the project a H_2S sensor from Unisense A/S (SulfiLogger™) became available and was used as a cross-validation of Raman spectroscopy. Albeit the sensor is not a validated method to track the concentration of H_2S, and the cross-validation is therefore used cautiously; if an observable change in H_2S concentration using the sensor is also detectable using Raman, the sensor will support that Raman is able to monitor a change in concentration.

The sensor is electrochemical and selective towards H_2 and mercaptans (Unisense A/S). As the sensor is only able to detect H_2S and not HS^- a new setup was required, cf. Figure 22. Furthermore, a calibration on H_2S was necessary, cf. Appendix 3. An almost closed system was needed to ensure that H_2S gradually evaporated from the system, therefore, a flow cell was used, cf. Figure 22.

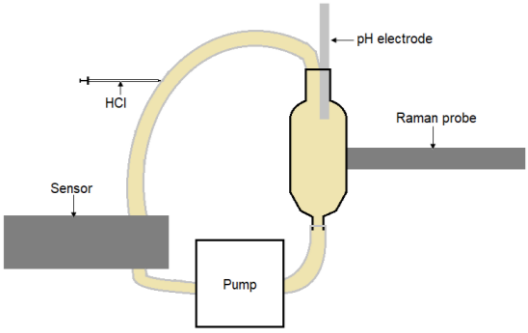

Figure 22: Setup of sensor experiments

A Na_2S solution was used to fill the system after which the system was closed. HCl was added to the system using a syringe, achieving a pH of 6, ensuring most of the sulphide was gaseous H_2S, cf. Figure 2. The system was monitored using Raman and the sensor and the results were as follows from Figure 23.

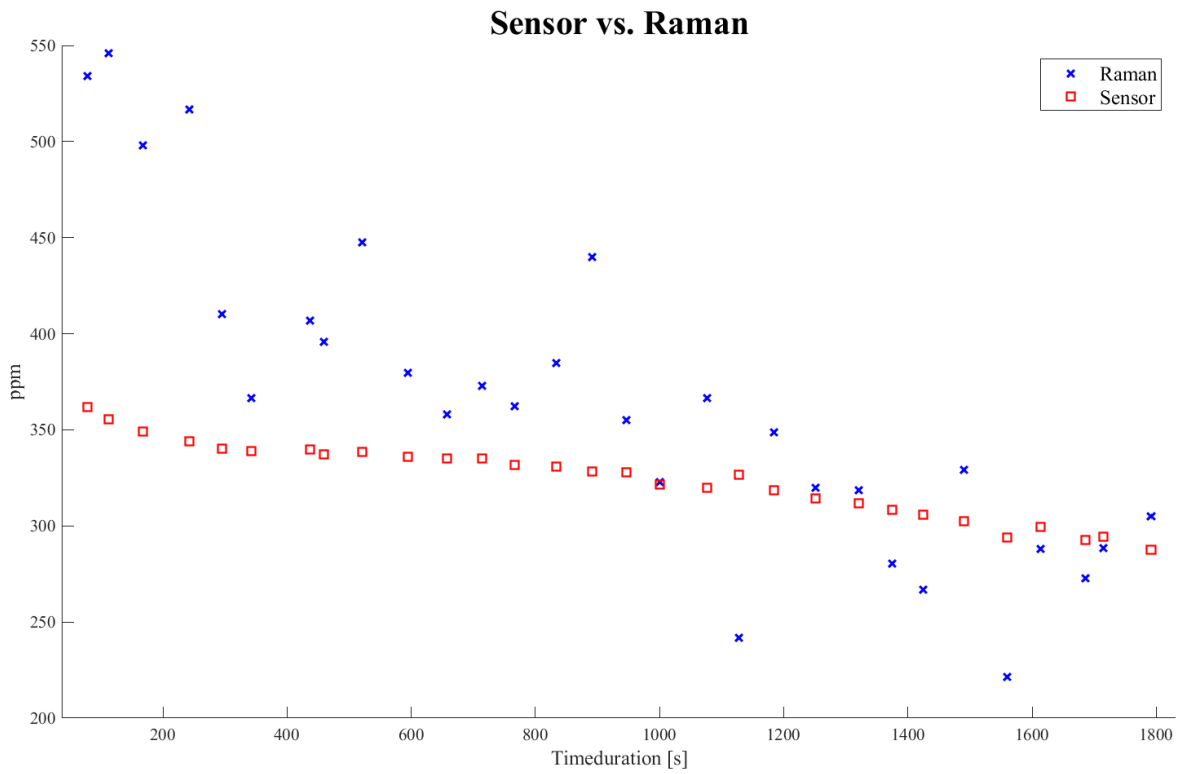

Figure 23: H_2S concentration over time measured by H_2S-sensor (red) and Raman (blue)

As it is evident from Figure 23 a decrease in both the Raman signal and sensor is observed. However, the initial concentrations of H_2S vary with 200 ppm. One reason for this is Raman measures on the entire system, whereas, the sensor measures gaseous H_2S which permeates the membrane. The sensor provides a more stable signal, compared to an oscillating Raman signal. The oscillations in the Raman signal, and the different concentrations of the two analytical techniques, can be explained by the calibration of the equipment. The sensor was calibrated by Unisense using H_2S gas, and Raman was calibrated by the project group using Na_2S and HCl, cf. Appendix 3. The calibration of Raman on a gas proved to be challenging. To measure the concentration of H_2S the alkaline solution of HS^- ions needed to be acidified. Here it was a challenge to reach the same pH for the repeated experiments. The deviations may have contributed to the differences between the two analytical techniques.

Regardless, Raman can track changes in concentration of a single chemical compound over time.

Gas-experiment

Raman can detect changes in concentration of different solutions and of the same compound over time. However, it must be shown that Raman can track changes of concentrations in a solution with several chemicals over time. In several of the previous qualitative studies, a different method of mixing sulphur and HET was used, i.e. using neutral H_2S-gas and bubbling it through a HET-solution. This method is not a viable choice for kinetic studies, as there is little to no control over the flow of gas, and thereby with the initial or even instantaneous concentrations of sulphur. It is however a useful method to qualitatively show a change over time, and to identify the reaction products.

This required a different setup of experiment, cf. Figure 24.

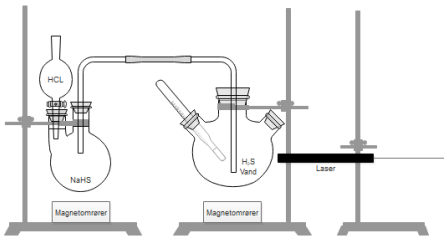

Figure 24: Setup for gas-experiment acquired from (Gammelby et.al., 2018)

100 ml of 0.036 M aqueous solution of MMAT was prepared and a total of 0.12 moles of H_2S was bubbled through at ambient temperature. The H_2S gas was bubbled through by adding HCl to 10 g of NaHS and passing the gas through the MMAT solution. A Raman spectrum was acquired every 30 seconds for a total of 15 minutes.

The initial pH was 9 and decreased to 7 at the end of the experiment.

This experiment provided the spectra in Figure 25.

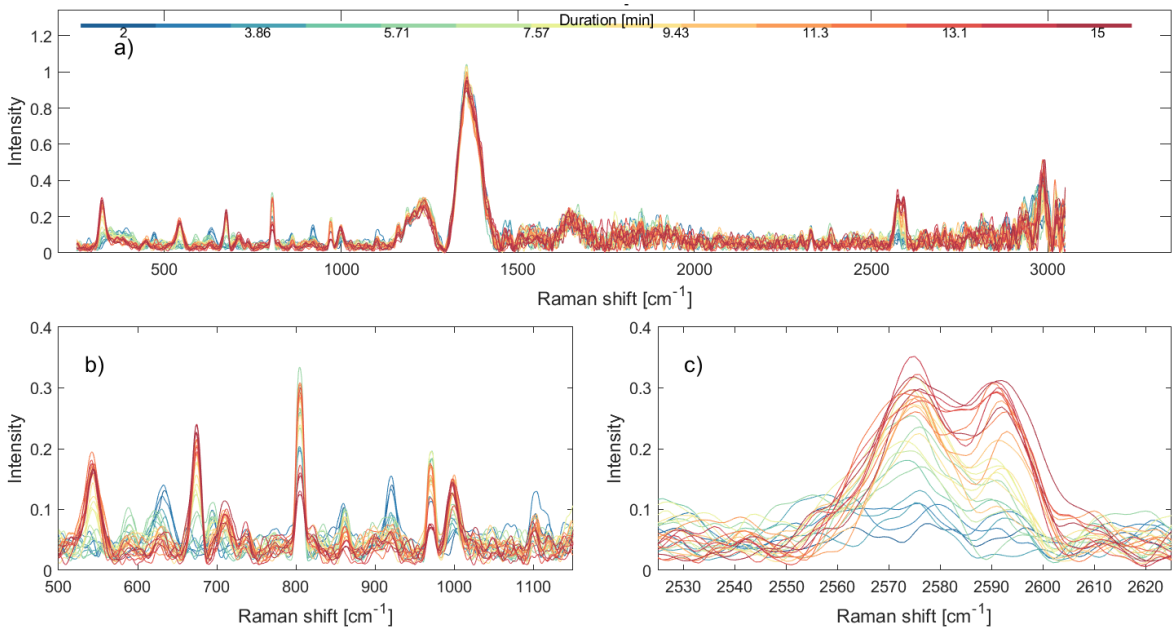

Figure 25: Raman spectra of gas experiment

As evident from Figure 25 a reaction happening; Some peaks are decreasing while others increase, and new peaks are formed. The HS^- peak at 2572 cm^{-1}, Figure 25c, is present and increases over time, the peak at 2590 cm^{-1} evolves as well, and this peak is indictive of H_2S (Socrates, 2001).The two sulphur species increase over time, due to the excess of H_2S bubbled through the system. At pH 7 the H_2S:HS^- ratio will be 1, cf. Figure 2. New peaks are formed, at Raman shift 550 and 675 cm^{-1}.

The spectra in Figure 25 prove that Raman can track changes in intensity over time, as well as track the forming new peaks and thereby of new chemicals.

5.7 Segment E

In segment D it is evident that Raman can track the evaporation of H_2S from the solution. Moreover, an experiment where H_2S is bubbled through a triazine solution indicates a reaction. Here the intensity of peaks either increases or decreases during the reaction proving that Raman can track a reaction. The answer to segment D is therefore, 'yes', cf. Figure 26.

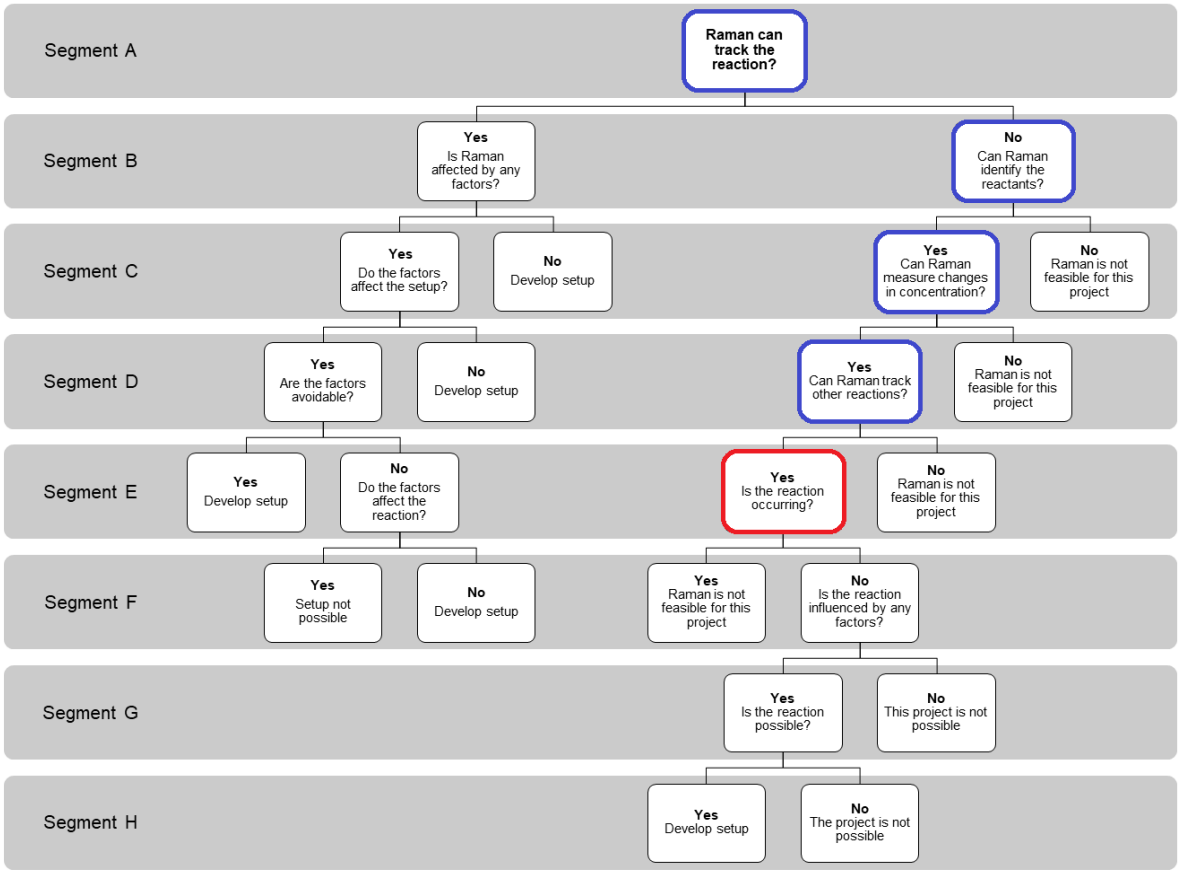

Figure 26: Segment E; Red indicates the current segment, blue the answered segments.

As Raman is proven feasible to track the scavenging reaction another reason must be found to why no reaction was observed in segment A. Therefore, it is important to investigate if the scavenging reaction is occurring.

Segment E therefore poses the question; Is the scavenging reaction occurring?

To ensure that the scavenging reaction is occurring, two options was considered:

1. Ensure that the buffer used is not interfering with the reaction
2. Investigate if the concentrations are out of the range of the reaction

First step is to ensure that the buffer used is not interfering with the reaction, this is done by testing the reaction without buffer. Next step is to investigate if the concentrations are out of the range of the reaction, i.e. too low or too high. This is achieved by testing different concentration levels of the reactants.

For all experiments in segment E the same experimental setup was used, cf. Figure 27.

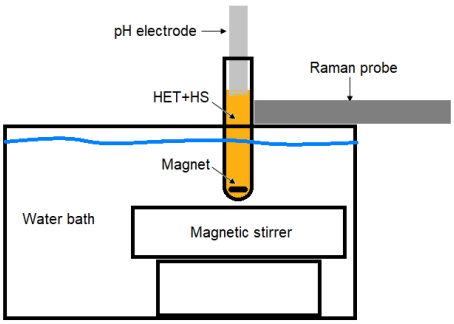

Figure 27: Setup for experiments conducted in segment E

In the new setup, the glassware chosen was a glass vial, as this ensured less chemicals spent. The smaller vial, however, results in the Raman probe having to be on the outside of the vial. It was tested if the glass vial did interfere with the Raman signal, where the glass in turn results in an interference in the Raman signal. But as these tests also showed, was that the glass peaks are not covering any indictive peaks and are therefore not a problem to use.

Buffers:

The first suspect of why no reaction appears to be happening is the buffer in question; the phosphate buffer. Firstly, it needs to be established that this buffer does not obscure any of the indicator peaks for neither HET nor HS^-. Secondly, it needs to be ensured that the buffer itself does not obstruct the reaction from happening, i.e. does the reaction occur with no buffer present.

To make sure the phosphate buffer does not obscure any of the indicator peaks the spectrum of buffer and HET was investigated, cf. Figure 28.

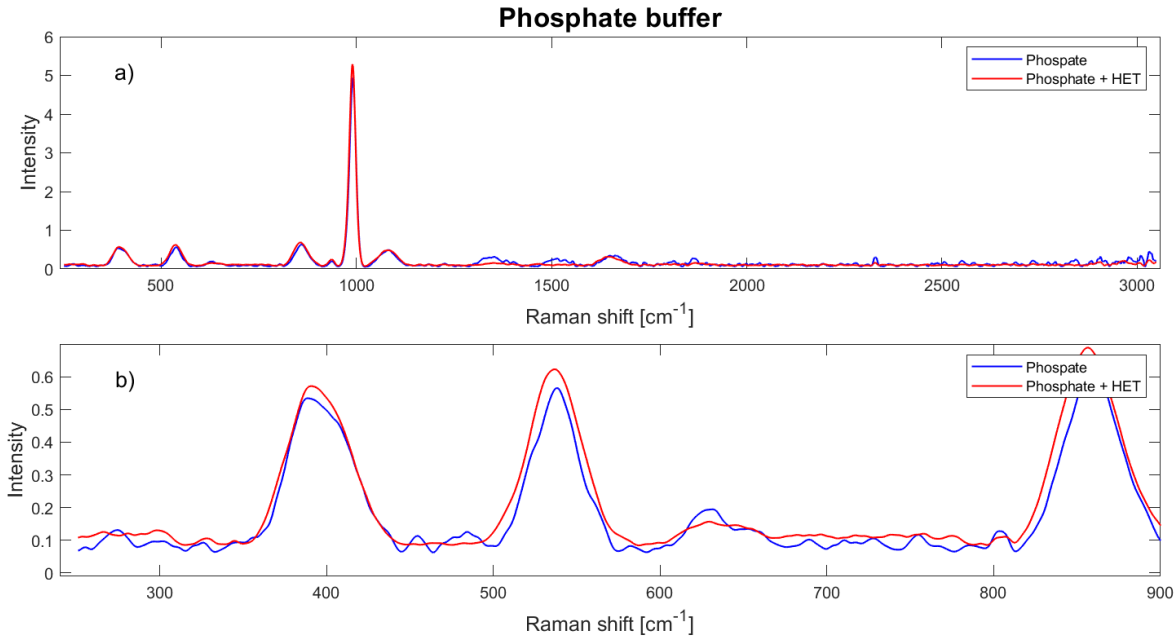

Figure 28: Raman spectra of phosphate buffer (blue) and a solution of phosphate and HET (red)

From Figure 28 it is evident that the buffer peaks are around Raman shift 1000 cm^{-1}, thus they do not obscure the indicator peaks at 790 and 2572 cm^{-1}. The peak at 1100 cm^{-1}, MEA, is however obstructed by the buffer. However, the HET indicator peak at 790 cm^{-1}, is not visible in Figure 28 this is contributed to the concentration of buffer needed to keep pH stable. A concentration of 2 M phosphate equals a signal from the buffer so strong, that the scavenger peaks disappears in noise and are therefore not easily discernible. This makes the phosphate buffer an undesirable choice as this will make the data less clear.

The peaks indicating the scavenger is obscured by the high concentration of buffer. It was therefore tested if the reaction would happen if HET and sulphide solutions were prepared in demineralized water. Several experiments were carried out, cf. Table 11. The pH was 12 throughout the experiments, and all experiments were carried out at ambient temperature.

Table 11: HS^- concentration and temperature for experiments carried out in demineralized water

Experiment	Time [min]	$C_{scavenger}$ [M]	C_{HS^-} [M]	T [°C]
E.1	5	0.034 (HET)	0.003	22
E.2	5	0.034 (HET)	0.003	22
E.3	5	0.034 (HET)	0.003	22
E.4	5	0.024 (MMAT)	0.03	22
E.5	5	0.024 (MMAT)	0.03	22

However, no reaction was observable, even without the buffer interfering. There were no changes in any of the indicator peaks, nor in any other peaks. The phosphate buffer is not at fault for the lack of reaction.

It was, however, as a precaution, chosen to investigate the reaction without the presence of buffer.

Concentrations

Since the buffer had no effect on the lack of reaction it was investigated if the concentrations were too low for a reaction to occur. Therefore, the concentrations were increased to ensure collisions between the reactants. Several concentrations were examined, cf. Table 12. Each experiment consisted of preparing MMAT and Na_2S solutions in demineralized water at ambient temperature. The time of mixing was taken as the starting point of the reaction. in each the pH remained 12 throughout.

Table 12: Experiments carried out in demineralized water

Experiment	Time [min]	pH	C_{MMAT} [M]	$C_{Sulphur\ salt}$ [M]	T [°C]
E.6	15	12	0.071	0.303 (Na_2S)	22
E.7	5	12	0.071	0.202 (NaHS)	22
E.8	20	12	0.071	0.057 (Na_2S)	22

None of the concentration levels examined yielded any changes in the Raman spectra, or pH, and therefore a reaction was yet to be observed.

5.8 **Segment F**

When investigating the scavenging reaction in segment E, no reaction was observed when changing the concentration of the reactants. It is therefore suspected that other factors must have an influence on the scavenging reaction.

As no reaction is occurring, the answer to segment E, is therefore 'no', cf. Figure 29.

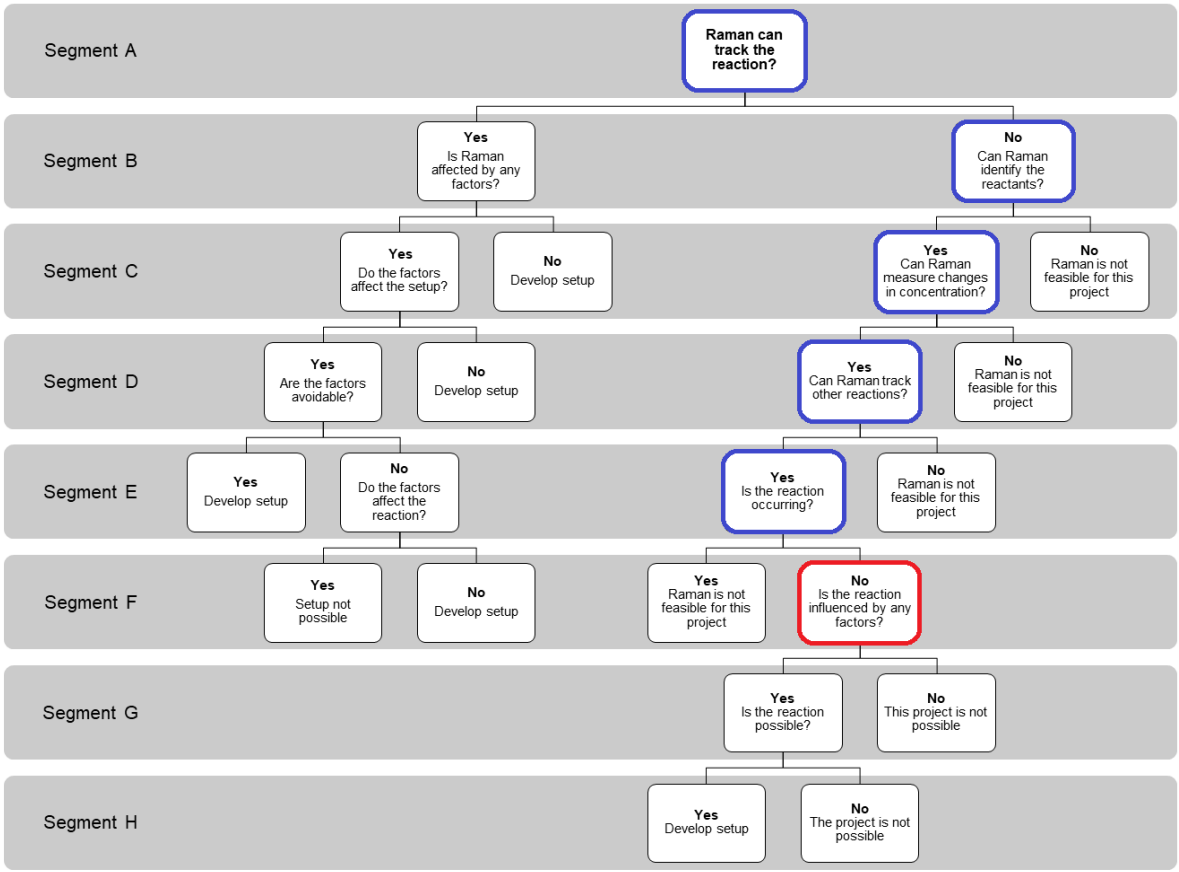

Figure 29: Segment F; Red indicates the current segment, blue the answered segments.

Segment F therefore poses the question; Is the scavenging reaction influenced by any factors?

As the concentration did not affect the reactions occurrence, the two other factors to be examined were temperature and pH.

Raising the temperature will increase the kinetic energy of the molecules and when the molecules collide the minimum energy barrier, the activation energy, is easier overcome. From the reaction mechanism, cf. Figure 4, it is evident that the triazine molecule must be protonated before further reacting. If the pH is lowered more hydrons will be available in the solution to protonate the triazine molecule.

The effect of these factors was tested by preparing solutions of HET and Na_2S at ambient temperature. The two solutions were then preheated to the set temperature, and mixed in a vial, setup is illustrated in Figure 30.

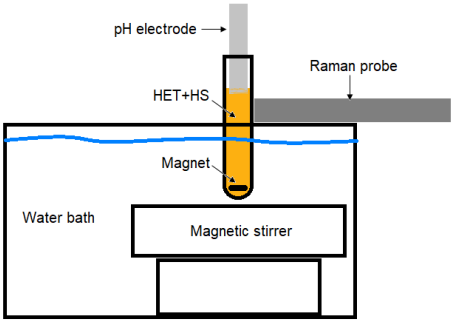

Figure 30: Setup for experiments conducted in segment F

For the experiments where only temperature is a factor, the time of mixing was set as the starting time of the reaction. For experiments where pH is a factor, the time of setting pH was considered starting time. The pH was adjusted with HCl. Kinetic studies in batch reactors are conducted under constant-volume conditions. HCl is not expected to change the volume of the solution when added, which was tested and confirmed, cf. Appendix 4. Three different values of pH are measured during an experiment. pH_{before}, is the pH measurement directly after mixing HET and HS^-. $pH_{initial}$, is the pH measured directly following addition of acid. pH_{final}, is the pH value measured when the experiment is stopped.

Firstly, the factors, temperature and pH, was investigated separately to see which one or if both has an effect on the reaction, cf. Table 13.

Table 13: Experiment where only one factor is changed. First pH, secondly temperature

Experiment	Time [min]	pH_{before}	$pH_{initial}$	pH_{final}	C_{HET} [M]	C_{HS^-} [M]	T [°C]	Reaction
F.1	30	12.89	7.5	8	0.030	0.050	22	No
F.2	60	12.99	12.99	12.81	0.343	0.621	50	No

As it is evident from Table 13 experiment F.1 conducted at a lower pH and the experiment F.2 conducted at higher temperature did not yield any observable reactions. Separately increasing temperature and lowering pH show no effect on the reaction. It was therefore further investigated if both increasing the kinetic energy while adding more acid to the system would yield a reaction. Therefore, the temperature was increased to 40 °C and pH was lowered, cf. Table 14.

Table 14: Experimetns conducted at 40 °C and lower pH

Experiment	Time [min]	pH_{before}	$pH_{initial}$	pH_{final}	C_{HET} [M]	C_{HS^-} [M]	T [°C]	Reaction
F.3	15	12.99	0.5	0.5	0.171	0.311	40	No
F.4	30	12.99	7	11	0.342	0.621	40	No
F.5	60	12.99	8.49	11.28	0.342	0.621	50	Yes
F.6	120	12.99	9.3	10.5	0.342	0.410	50	Yes

Experiment F.4 yielded an increase in pH, however this did not appear to have any effect on the reaction. Due to the lack of reaction the temperature was increased to 50 °C, further increasing the kinetic energy. The pH for experiment F.5 was initially 8.5 increasing to 11.3 throughout the reaction. The experiment was repeated, experiment F.6, and tracked for 120 minutes, yielding the same increase in pH, and the same changes in the Raman spectrum, cf. Figure 31.

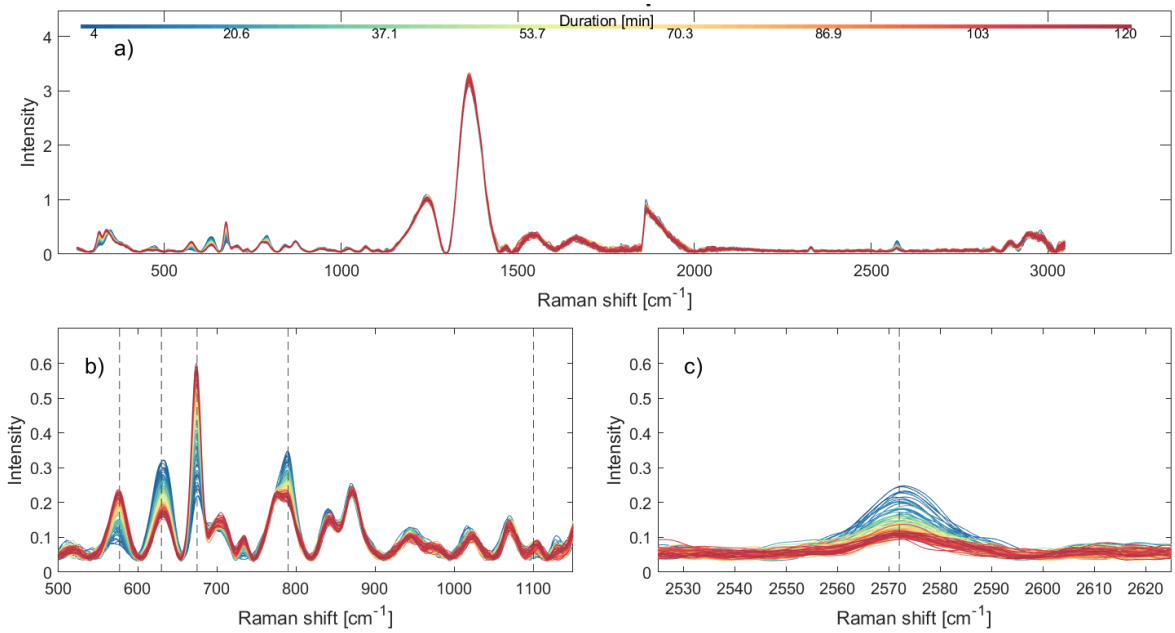

Figure 31: Raman spectra of experiment F.6 which is indictive of experiments where a reaction is observed

Figure 31 illustrate a clear change in several peaks. This indicates a reaction happening. The peak indicating the sulphur species, cf. Figure 31c, is clearly decreasing in intensity and thereby in concentration. From Figure 31b, it is evident that the indicator peaks are decreasing in intensity, and new peaks are being formed. The forming peaks are located around Raman shifts 575 cm^{-1} and 675 cm^{-1}.

A reaction occurs if pH and temperature is decreased and increased, respectively. However, it needs to be further investigated if the observed reaction is a scavenging reaction, and not a combination of evaporation of sulphide and hydrolysis of the scavenger, as per the literature.

5.9 Segment G

In segment F, it was found that no reaction occurred when separately increasing temperature and lowering pH. Yet, if both increasing the temperature while at the same time adding acid to the solution a reaction is observed in the Raman spectra. This indicates that the reaction is affected by two factors, temperature and pH. The answer to segment F is therefore 'yes', cf. Figure 32.

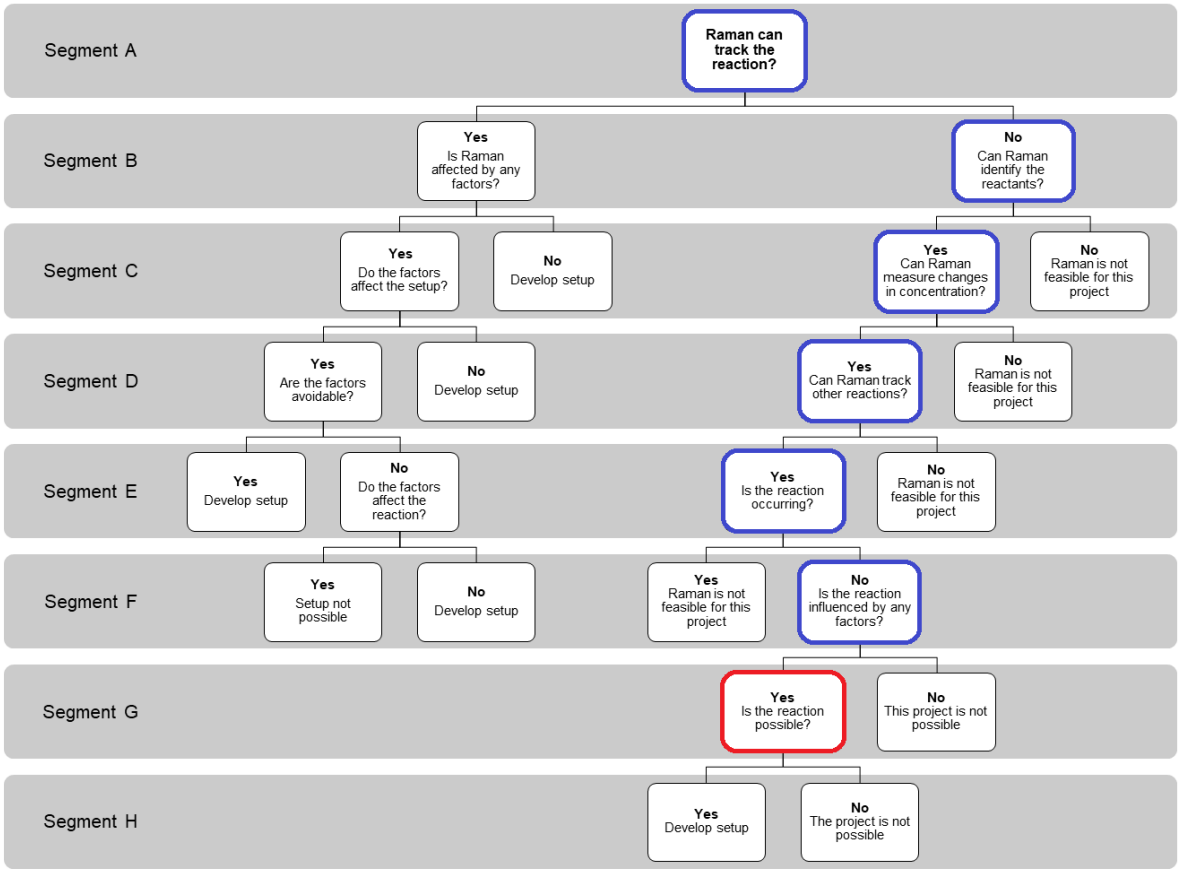

Figure 32: Segment G; Red indicates the current segment, blue the answered segments.

However, triazine show a tendency to hydrolyse into its two constituents, cf. Figure 3. The hydrolysis is reported to be pH dependent (Buhaug, 2002) and therefore it needs to be ensured that the reaction observed in segment F is the scavenging reaction and not the hydrolysis of HET, due to the lowering of pH.

Segment G therefore poses the question; Is the scavenging reaction possible?

As the experiments with high temperature and low pH showed changes in the Raman spectra, a reaction is occurring, however, there are two options as to what is occurring in the Raman spectrum:

1. A scavenger reaction is occurring
2. The HET is decomposing due to the low pH, and the observed decrease of HS^- is due to evaporation of the neutral gas.

Only the first option is desired in this project and the possibility of the second option must be investigated.

This is done by first investigating if H_2S evaporates at lower pH, and second by investigating if HET decomposes at lower pH values. And finally, to ensure that the reaction is a scavenger reaction the forming peaks are identified.

Evaporation of H_2S

To investigate if the simultaneous changes in concentration of HS^- and HET are caused by evaporation of Sulphur, a solution of HS^- was prepared and heated.

It was then observed with Raman for two hours, yielding no visible change, cf. Figure 33.

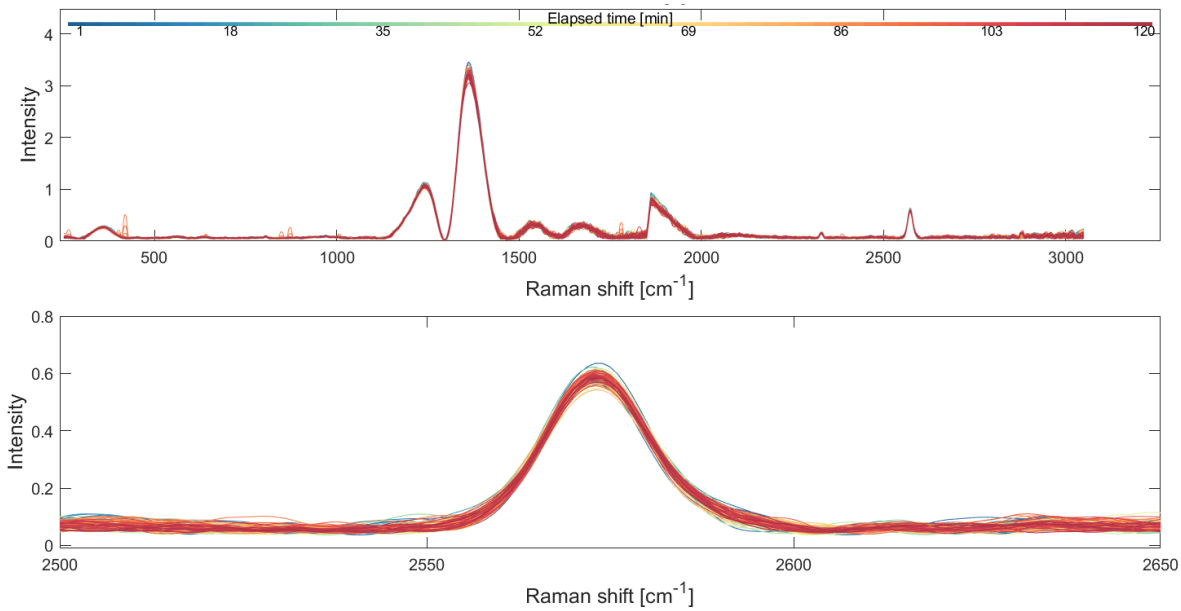

Figure 33: Investigation into if HS^- evaporates from solution

There is no observable change in the Raman spectra over time. Therefore, the change in HS^- evident in Figure 31 is not caused by the evaporation of H_2S.

Decomposition of HET

Previous studies of HET show that the chemical hydrolyses at low pH values. In order to ensure that this hydrolysis was not causing a change in the Raman spectra, solutions of HET was prepared and the pH lowered by adding HCl, cf. Table 15. The hydrolysis was studied at both ambient temperature and at 50 ℃, and at pH levels between 6.5 and 10, and as low as 0.3.

Table 15: Hydrolyses experiments conducted at different pH, HET concentration and temperature

Experiment	Time [min]	pH_{before}	$pH_{initial}$	pH_{final}	C_{HET} [M]	T [°C]
G.1	30	10.5	9.28	9.42	0.068	22
G.2	30	10.5	8.93	8.99	0.205	22
G.3	30	10.5	7.45	7.59	0.137	22
G.4	30	10.5	9.03	9.12	0.137	22
G.5	30	10.5	7.94	7.97	0.317	22
G.6	30	10.5	7.96	8.06	0.205	22
G.7	30	10.5	6.87	6.97	0.205	22
G.8	30	10.5	7.97	8.1	0.137	22
G.9	30	10.5	6.99	6.99	0.137	22
G.10	120	10.5	7.0	7.0	0.345	50
G.11	120	10.5	0.6	0.3	0.345	50

The solutions were observed for a period of 30-120 minutes and at pH levels above 6.5 no change in the spectrum was observed for experiment G.1 to G.10, cf. Figure 34.

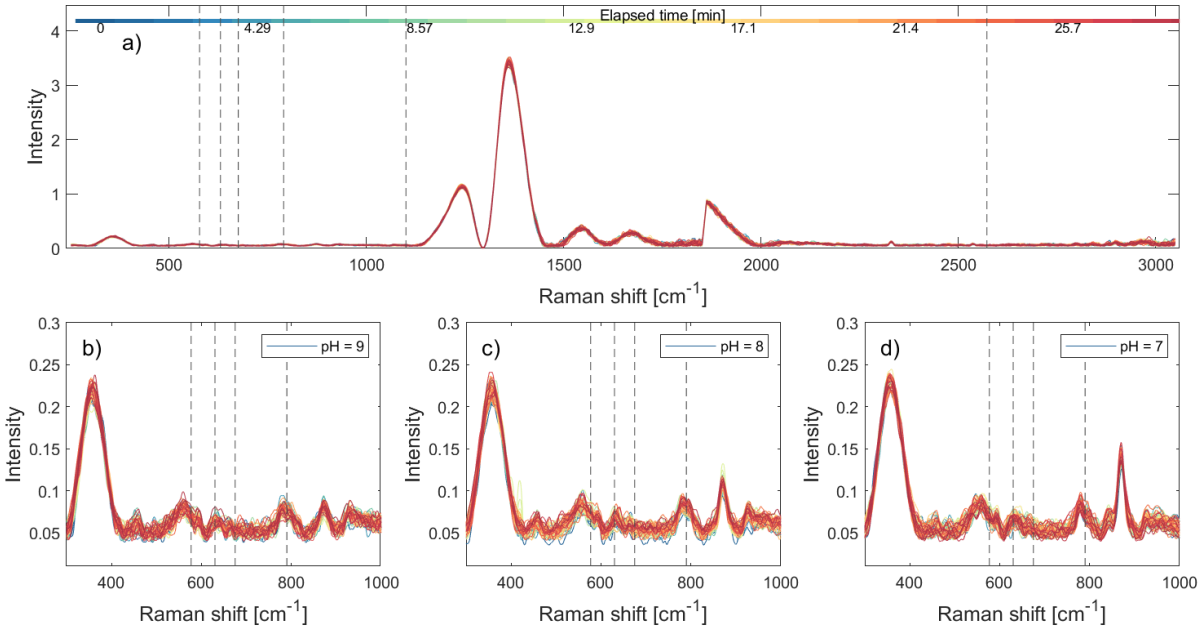

Figure 34: General Raman spectra of the hydrolysis experiments G.1 to G.10

As it is evident from Figure 34 no changes in the HET peaks are observed even at low pH values. This indicates that the changes in the Raman spectra, is not caused by the hydrolysis of HET. However, at pH 0.6 a change was observed, cf. Figure 35.

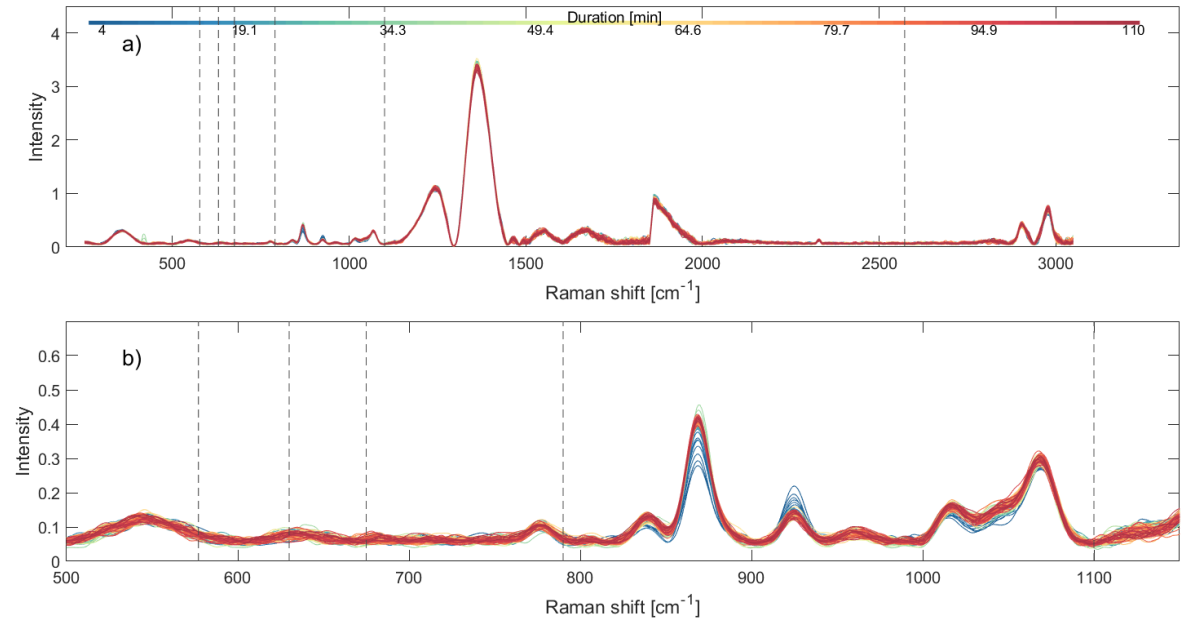

Figure 35: Raman spectra of hydrolysis experiment at pH 0.6, experiment G.11.

As it is evident from Figure 35 peaks at Raman shift 880 and 930 cm^{-1} are increasing and decreasing, respectively, with time, which indicates a reaction occurring. Furthermore, the indicator peak at 790 cm^{-1} is not visible in this spectrum. As the first spectrum is acquired after the

setting of pH, this could indicate a fast hydrolysis of HET at low pH. However, the indicator peak for MEA is not increasing, which is unexpected, as the hydrolysis is considered to yield MEA and formaldehyde. The peaks at 1200-1500 cm^{-1} is response from the glass vial. However, the reaction is compared with the spectrum of formaldehyde, cf. Figure 36 an increase in the formaldehyde peaks are visible.

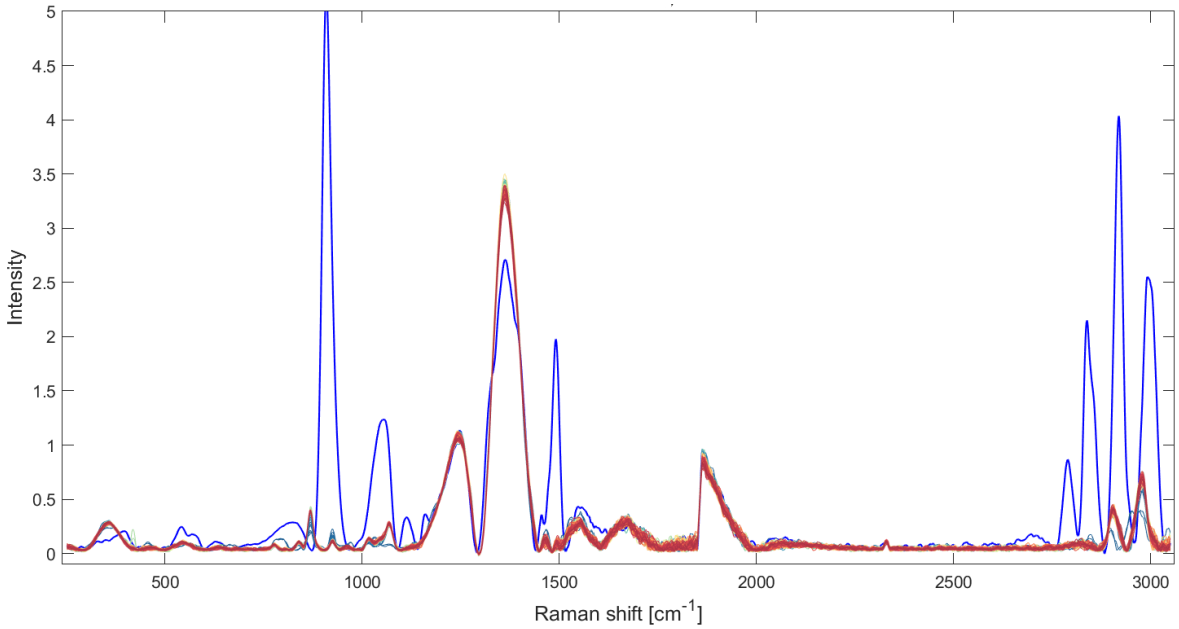

Figure 36: Spectrum of pure formaldehyde (blue) and experiment G.11

As evident from Figure 36 an increase in the peak around 1050 cm^{-1} is visible. This peak overlaps with a peak from formaldehyde, indicating an increase in the concentration of formaldehyde. However, a strong formaldehyde peak at 930 cm^{-1} appears to be decreasing, indicating another reaction. The peak has not been identified. The spectrum for formaldehyde is of higher concentration than the HET in the reaction spectrum. This accounts for the general intensity difference between the formaldehyde spectrum and the reaction spectrum.

Regardless, at the pH levels to be studied in this project, pH > 7, HET does not hydrolyse.

Identification of peaks

Even though it was established that the most likely explanation of the changes in the Raman spectra is that a scavenger reaction is occurring, the theory still needed to be verified. It was therefore attempted to identify the peaks changing throughout the reaction, cf. Figure 37, to ensure that the reaction occurring yielded expected molecules, specifically C-S, bonds, cf. Figure 5.

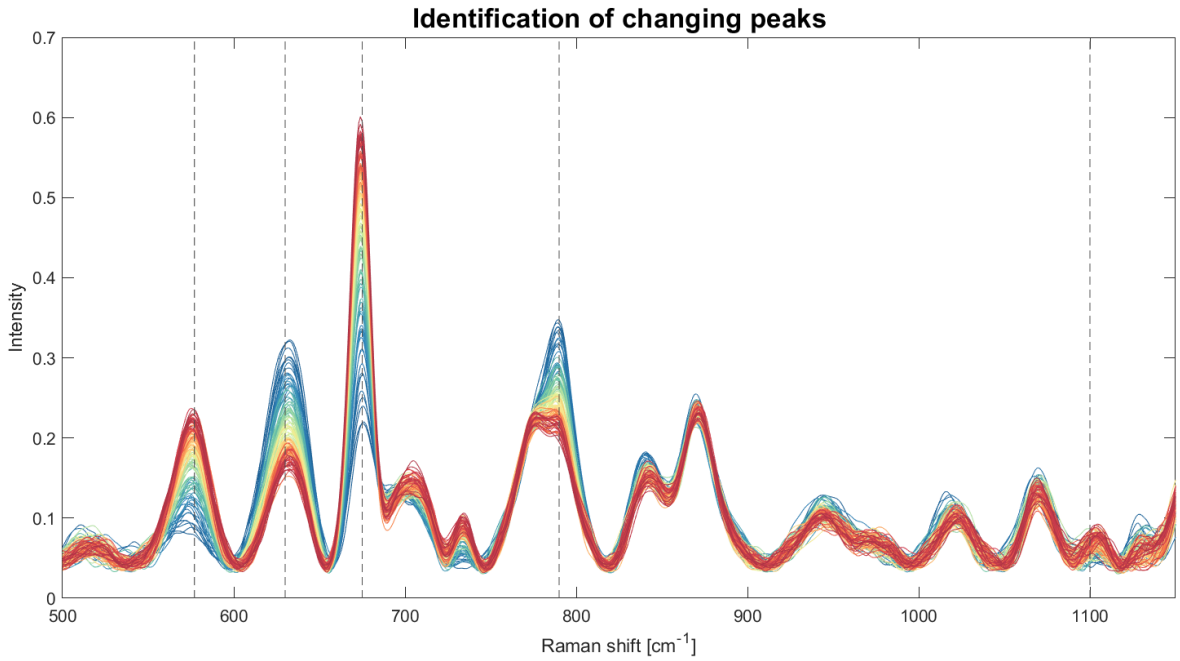

Figure 37: Raman spectra of experiment G.11

The HET peak at 790 cm^{-1} is as described a C-N bond in the triazine ring. Throughout the scavenging reaction the Nitrogen atom should be substituted with a Sulphur atom and should result in a decrease in the C-N bonds in the ring structure. A decrease in the 790 cm^{-1} peak is evident from Figure 37, making the scavenging likely. Another decreasing peak is at 630 cm^{-1}, however, this peak cannot be definitively identified. The MEA indicator peak at 1100 cm^{-1} is increasing which also indicates the substitution of sulphur for nitrogen in the triazine-ring. The peak at 675 cm^{-1}, identified as a C-S-C bond (Socrates, 2001), is increasing, indicating the scavenging reaction occurring. This peak is also described as the indicator peak for the scavenger product, dithiazine, by Perez-Pineiro et al. However, as it is C-S-C-bond, it would be present in both the HET-HS^- reaction and in the thiadiazine-HS^- reaction. It is therefore denoted as a product peak and not assigned a specific product. The peak increasing at 577 cm^{-1} is identified as a C-S stretch, and is also present in dithiazine (Perez-Pineiro,2018), however, it appears to be formed later in the reaction, compared to 675 cm^{-1}, which could indicate this peak, 577 cm^{-1}, being an indicator peak of dithiazine.

The identification of important scavenger peaks proves that the reaction occurring is a scavenger reaction, and the reaction is therefore possible, the answer to segment G is therefore ‘yes’, cf. Figure 38.

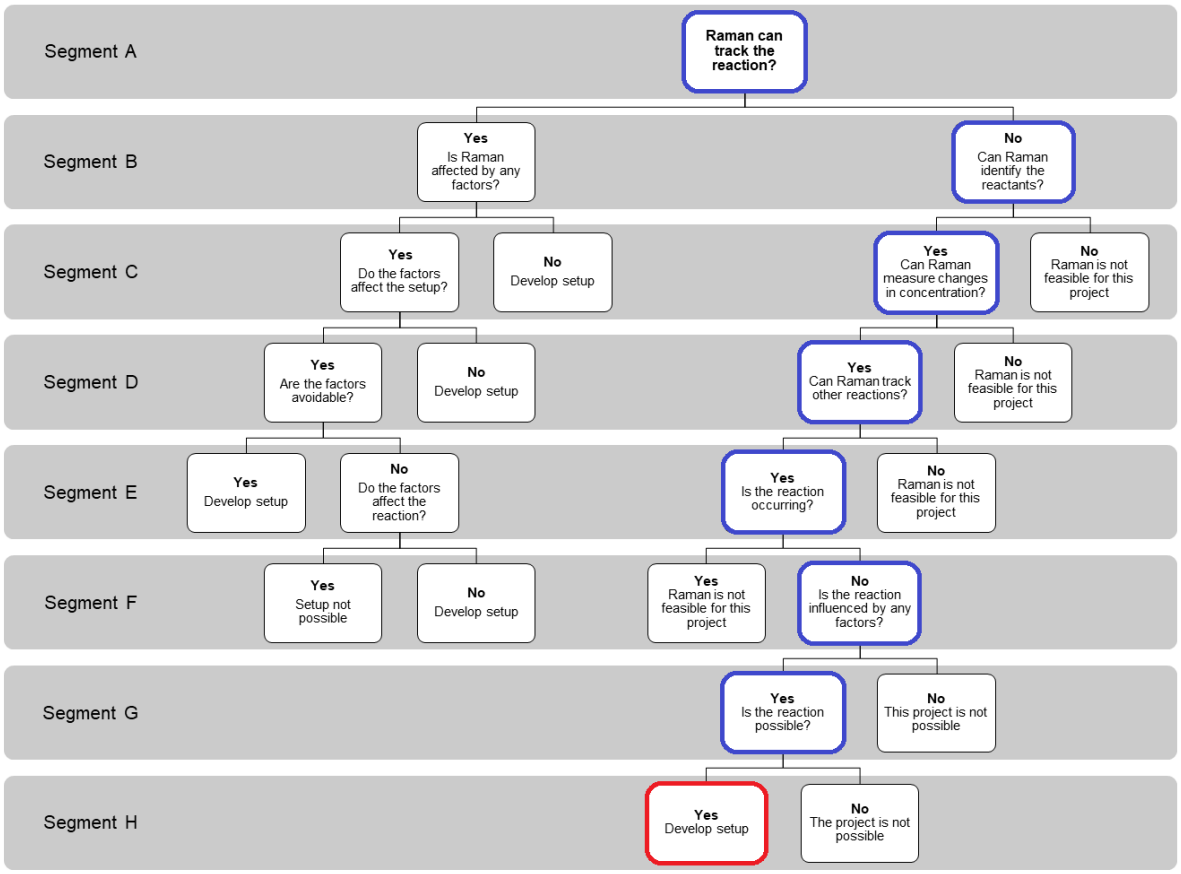

Figure 38 Segment H; Red indicates the current segment, blue the answered segments.

Throughout the segments, valuable information on the scavenger reaction is obtained. For the scavenger reaction to occur temperature must be increased to above ambient temperature and pH must be lowered from pH 11. Therefore, segment H prompts the development of the setup, however this requires revisiting Segment B.

5.10 **Segment B - revisited**

After investigations of both Raman and the scavenging reaction Raman has proven able to track the scavenging reaction. However, for this reaction to occur temperature and pH was the two important factors. The answer to Segment A now is therefore, ‘yes’, Raman can track the reaction, cf. Figure 39.

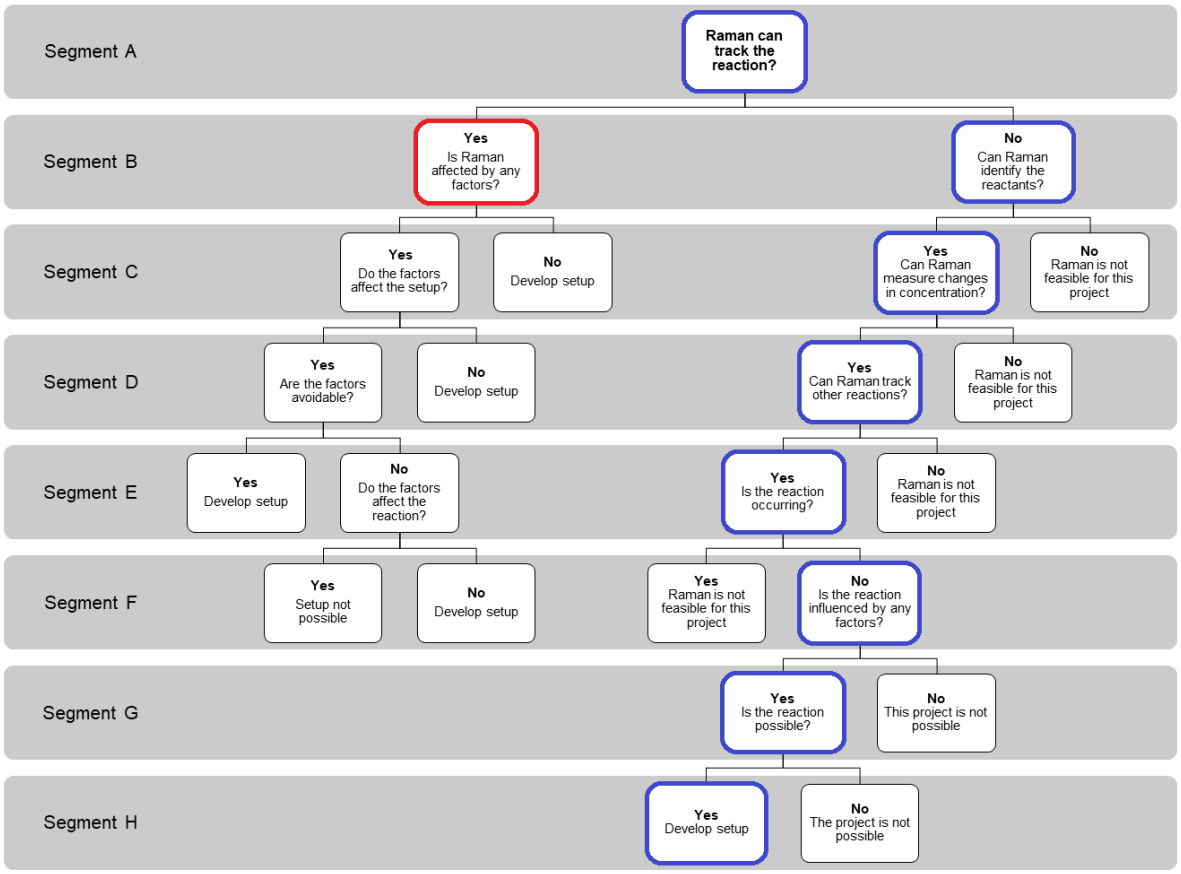

Figure 39: Segment B- revisited; Red indicates the current segment, blue the answered segments.

Segment B-revisited, therefore, poses the question; Is Raman affected by any factors?

To ensure that Raman is not influenced by any factors, several experiments were carried out, testing the effect of temperature, stirring, flow and glassware on the Raman signal.

Temperature

To investigate if the temperature has any effect on the Raman spectrum, a solution of HS^- was prepared and sealed in a glass vial. The sulphur was chosen as it has one very distinctive peak. The prepared solution of HS^- was then scanned with Raman at ambient temperature, then it was heated to 50℃ and scanned again. From these spectra it was evident that there was no change in the Raman signal regardless of the temperature. Therefore, temperature change would not affect the Raman signal.

Stirring or flow

It was examined if flow or stirring cause any interference with the Raman signal.

To investigate this issue, a solution of HS^- was prepared and then scanned, first without stirring and then with; no discernible differences were present in the Raman spectrum. This indicates that stirring does not affect the Raman signal, and spectra with and without agitation of the solutions are fully comparable. The same results were achieved when examining if flow had any influence.

Glassware

The glassware chosen is expected to have an effect; if the laser beam must pass through the glassware it would yield a different spectrum, compared to a spectrum were the laser beam does not pass through glass. However, it had to be investigated if this could have any effect on Raman's ability to track the scavenging reaction, and if there was a need to recalibrate if the setup changed.

To determine how the Raman signal changes scans through different types of glassware was obtained, cf. Figure 40.

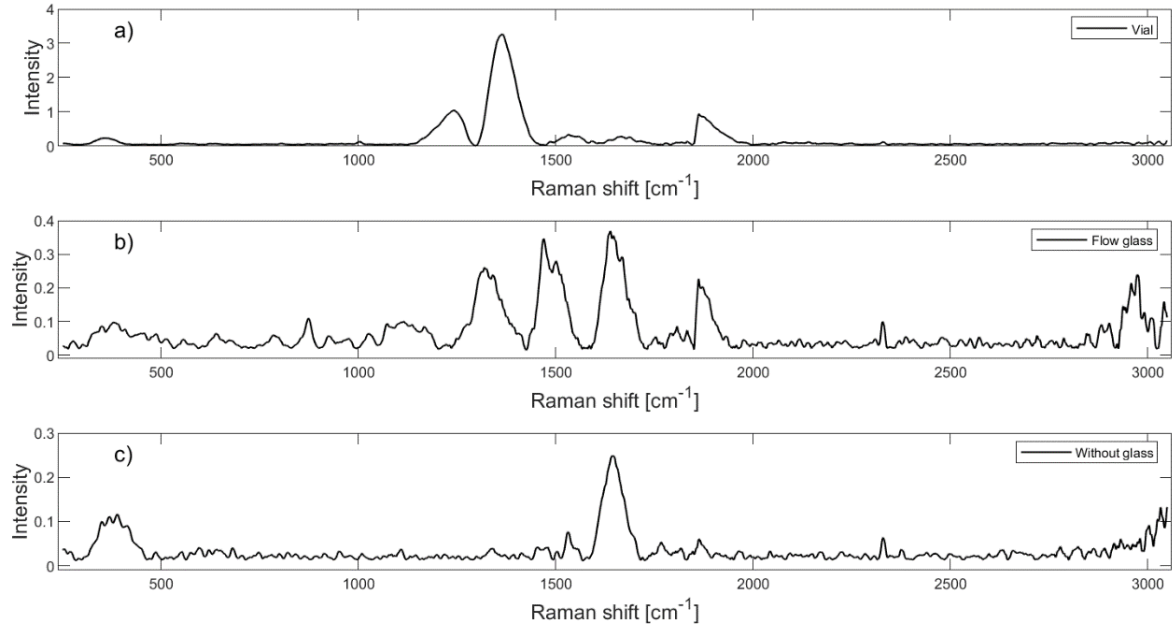

Figure 40 Raman signal through different glassware a) the vial used b) the glass used for the sensor experiment c) Raman probe submerged into demineralized water

As it is evident from Figure 40 each type of glassware has its own unique Raman signal. It is therefore preferable to acquire the scans without the interference of glassware when possible, however, it poses few problems to scan through the glassware. One of the problems with scanning through glassware is that the peaks decrease in intensity and some minor changes may be

obscured by the glass. If the setup is changed and the position of the Raman probe changes a new calibration of the peaks is needed in order to quantify the data.

Raman is influenced by the glassware, but not by neither temperature nor stirring or flow.

5.11 Segment C – revisited

As evident from segment B – revisited, the Raman signal is not influenced by temperature or stirring. However, the glassware used for the setup is important. For the glassware it is important that it does not obscure any peaks and that the signal to noise ratio is as low as possible. As Raman is influenced by glassware, the answer to Segment B is, 'yes', cf. Figure 41.

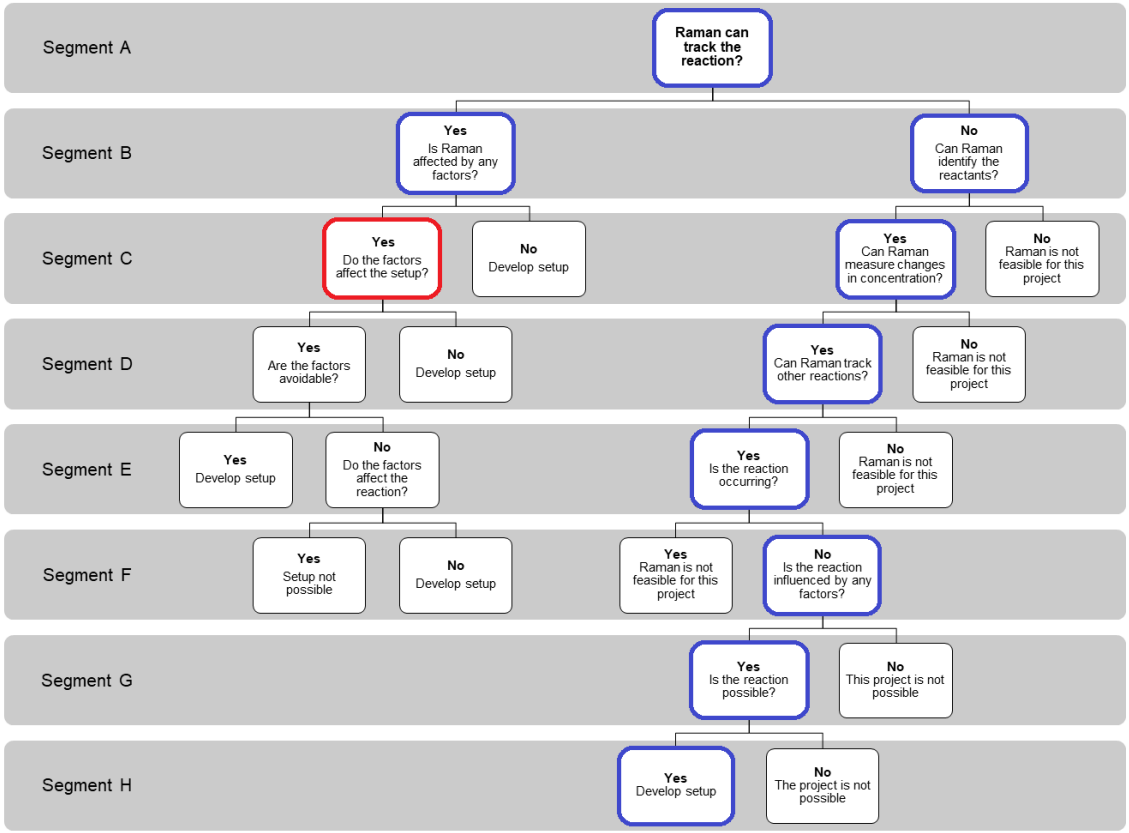

Figure 41: Segment C - revisited

Segment C-revisited, therefore, poses the question; Does the factors affect the setup?

Important parameters are low signal to noise ratio, and no glass peaks obscuring the scavenging reactants and products. However, if the calibration of the chemicals is done using the same, appropriate, glassware the affect will be eliminated. Segment C – revisited therefore prompts the development of the setup.

Chapter 6

Developing the setup

To obtain reliable kinetics data, it is necessary to be able to obtain reproduceable result from a well-defined reaction. This campaign therefore aims at developing a reproduceable method to obtain reliable kinetics data.

As it has already been shown, the reaction is strongly dependent on temperature and pH to initialize the reaction. The method therefore must include:

- Setting of the pH
- Control over the four parameters:
    - Temperature
    - pH
    - Concentration of HET and HS^-

It is first investigated if it is possible to use buffers as a method for keeping pH stable, then it is described how the calibration of the product peak is performed. And finally, the developed methods are described.

1.1.1 Buffers

Setting and keeping pH stable is possible using buffers, however, any buffer used would have to be:

1. Not overlapping any reactants or products in the Raman spectrum
2. Not overshadowing any peaks in the Raman spectrum
3. Not reacting with any reactants or products
4. Able to keep pH constant
5. Have buffer potential within the desired pH range

As the desired pH range is between 8 and 10, the buffer needs pKa values at about 9 in order to keep the desired pH values. The first buffer tested was a phosphate buffer, as this was the buffer of choice in previous experiments, and it has already proven to be neither overlapping nor reacting with any of the chemicals involved in the reaction.

In this project the buffers available was:

1. Phosphate, Na_2HPO_4/Na_3PO_4
2. MEA, MEA/HCl
3. Boric acid, BH_3O_3/NaOH
4. Ammonium, NH_3/NH_4Cl

Each buffer was tested by:

1. Preparing buffers at different concentrations and adding Na_2S and/or HET to evaluate if the pH was kept stable, measuring pH before and after addition of reactant
2. Mixing buffer and HET and acquire spectrum to ensure the buffer peaks did not overlap
3. Made solutions of buffer and HET, and tracked for an hour, to ensure no reaction occurred

The first buffer tested was the phosphate buffer:

Phosphate buffer

Despite the Na_2HPO_4/Na_3PO_4 buffer does not obscure any peaks nor does it interfere with the reaction, cf. Figure 28, it was decided that this buffer was a poor choice to keep pH stable, because;

1. Phosphate buffers are suspected of catalysing the oxidization of sulphide (Wang 2018) and as the oxygen was present during the experiments this was undesirable.
2. The phosphate buffer has pKa values of; 2.5, 7 and 12.5. As buffers are only effective in the range of ±1 of their pKa values, these values meant that is was not possible to test the reaction in the pH range between 8 and 11.5, which is the primary pH range for the scavengers used offshore.
3. The concentration of the buffer needed to keep the pH stable was >2 M, which is close to the solubility limit of the sodium phosphate. This meant that the buffer tended to precipitate, which in turn resulted in unusable Raman spectra.
4. The concentration of the buffer also led to some of the peaks indicating HET being lost in noise of the spectra, as the buffer peaks would dominate the spectra.

For these reasons it was attempted to find a more suitable buffer.

Other buffer candidates

The MEA buffer proved to be the most effective in terms of keeping pH stable, however as this is both a constituent of the HET and a reaction product it was not a viable choice.

Boric acid proved effective in keeping pH stable as well, however, as with the phosphate buffer, the concentration had to be 2 M, for the pH to be kept stable. This created a problem with solubility.

It was then tested if Boric acid obstructs the HET peaks, cf. Figure 42.

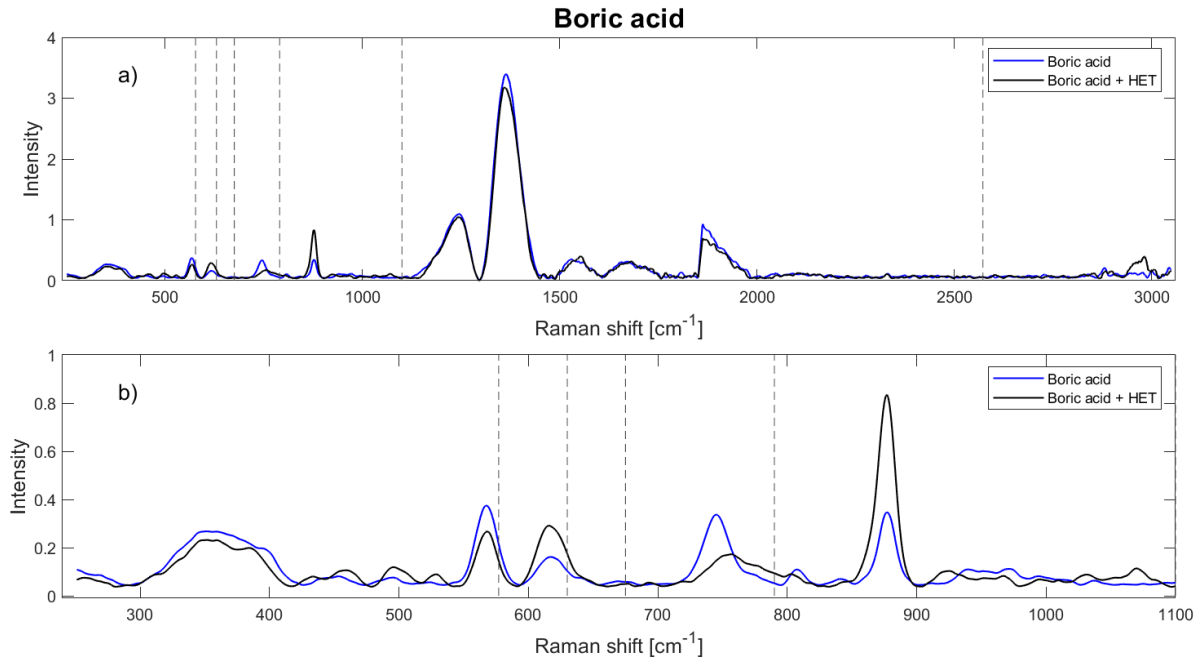

Figure 42: Raman spectra of the Buffer Boric acid (blue) and a solution of boric acid and HET (black)

From Figure 42, it is evident that boric acid has several high peaks obscuring the HET peaks, making the buffer unsuitable for use as a stabilizer for the pH in the reaction.

The last choice ammonium could keep pH stable even at lower concentrations, and the solubility was not an issue with this buffer. The Raman spectrum of ammonium did not provide any problems either, cf. Figure 43.

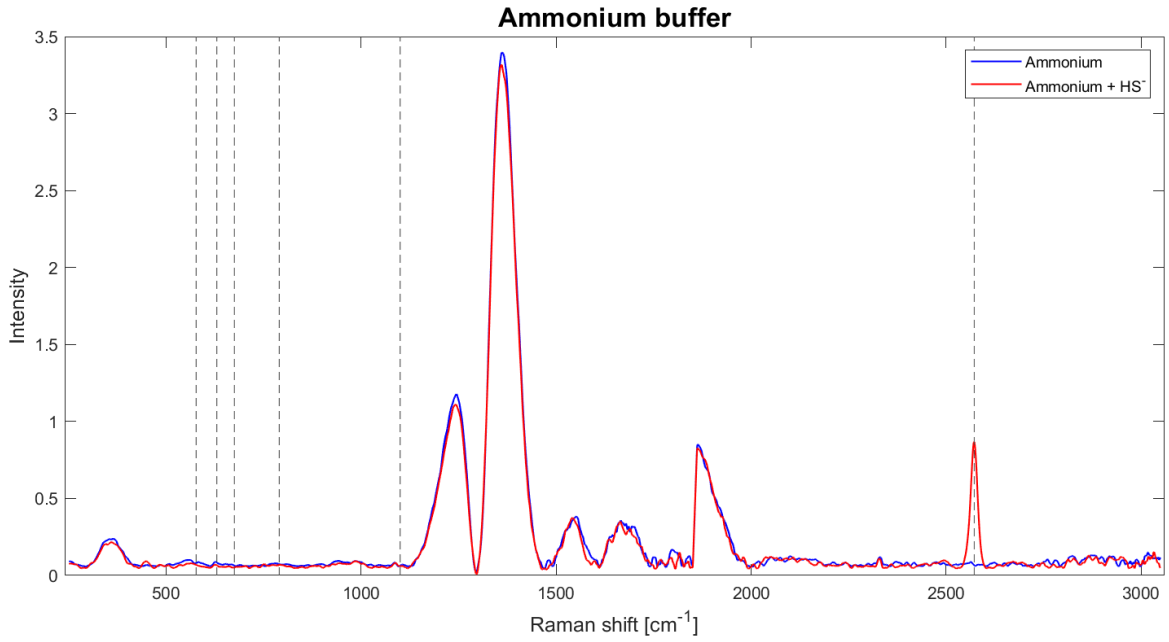

Figure 43: Raman spectra of the buffer ammonium (blue) and a solution of ammonium and HET (red)

No buffer peaks are overlapping or obscuring HET peaks, cf. Figure 44. However, from the article Wang X (Wang et al., 2018), it was suspected that the buffer itself, would react with HET. It was therefore investigated if this was the case, by preparing a solution of buffer and HET and tracking the solution with Raman for an hour, cf. Figure 44.

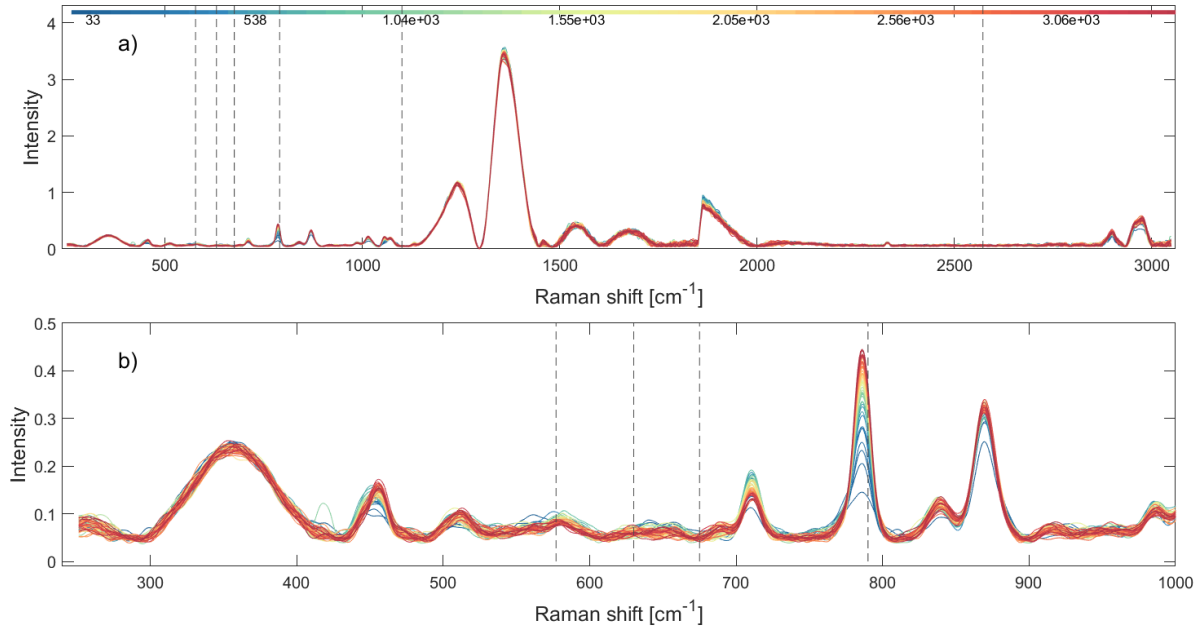

Figure 44: Raman spectra of the scavenger reaction in ammonium buffer

As it is evident from Figure 44 there are changes in the spectra, indicating a reaction occurring. As there was only buffer and HET present it is not a scavenging reaction, but as expected from the article by Wang X. et al. (Wang X. et al., 2018) a creation of a complex between buffer and HET. Therefore, ammonium was not a viable buffer candidate either.

Summary

Of the four buffer candidates available, none met the criteria for being used as a buffer for the scavenging reaction.

Phosphate buffers were not obscuring any peaks but was not usable in the desired pH range.

MEA is a reaction product and therefore not a viable candidate either. Especially since MEA is used in amine contactors and could potentially interfere with the reaction.

Boric acid could keep the desired pH range but obstructed the indicator peaks of HET in the Raman spectrum.

Ammonium could keep the desired pH range and did not obstruct any of the indicator peaks. Ammonium, however, seemingly forms complexes with HET and was therefore excluded as a buffer candidate.

As all the buffers were excluded, it was necessary to develop a method not including a buffer.

As the pH rises throughout the reaction, the lack of qualified buffer meant that the pH was not to be kept constant, but only set to an initial starting value, and then tracked throughout the reaction.

6.1.1 Calibration of product peak

To evaluate the setup and to investigate how different factors influence the consumption and production of the reactants and products, it is necessary to correlate the concentration of a species to the intensity of the Raman signal.

It has been demonstrated that Raman can mathematically be calibrated to convert the intensity of one or more peaks into a concentration of a specific chemical. These calibrations curves are then used to convert the scavenger reaction spectra into concentrations of reactants and products. These calibrations, however, are only valid for the reactants, HET and HS^-, as these were the only chemicals available in quasi-pure versions. To be able to estimate the concentration of the formed products, it was necessary to base the calibration on the reaction spectra.

As the pure scavenging products were not available to calibrate on directly, it was only possible to make estimates of the concentrations of said products. The conversion from intensity of the product indicator peaks into concentration of the product, be it thiadiazine or dithiazine, was based on the following assumptions:

- The chosen indicator peaks are the only identifiers for the product
- The reaction occurs according to the established reaction scheme – equimolar
- The calibrations of the reactants are reliable

With these three assumptions in mind, the calibration was carried out mathematically by assuming that:

$$C_{product}(t) = C_{0_{reactant}} - C_{reactant}(t) \qquad (6.1)$$

In other words, the concentration of product at a given time is, the concentration of reactant at time t subtracted from the initial concentration of reactant.

This calculation will only provide an estimate of the true concentration of product.

Raman shift 675 cm^{-1}

As the peak at 675 cm^{-1} is indictive of a C-S-C-bond it should be present in both reaction products, thiadiazine and dithiazine. Therefore, it cannot be estimated on the difference of HET, but rather on the bases of the consumed HS^-, as this needs to be consumed for either product to be formed. However, as the method used for obtaining the reaction spectra resulted in an unwanted evaporation of HS^-, equation 6.1 could not be used directly on the data for HS^-. Therefore, the equation was altered, to take the evaporation into account, cf. equation 6.2.

$$C_{675}(t) = C_{0_{HET}} - C_{HET}(1) + \left(C_{HS^-}(1) - C_{HS^-}(t)\right) \qquad \forall t \geq 1 \qquad (6.2)$$

The concentration of the product peak 675 cm^{-1}, is assumed equal to the initial concentration of HET, or the added concentration of HET, minus the concentration of HET, at the first scan, t = 1, after this point the difference in HS^- concentration from point 1 to point t, is added to estimate the concentration of the product. As the product concentration is expected to be zero at t=0, it is only necessary to calculate the concentration from timepoint 1 and forward.

The intensity of the peak was then converted into concentrations based on the quantitative data of HET and HS^-, cf. attached spreadsheet.

Unlike the calibration of HET and HS^-, PLS was not used for this calibration, as only one peak was studied, instead linear regression was used on arbitrarily chosen points of the experiments. This linear regression was then used to convert the intensity of the peak into concentrations in the remaining experiments.

6.2 Setup 1

As one method had already proven useful, this was the first method examined if it could provide reproduceable results. Moreover, the vial used have a low signal to noise ratio and does not obscure important indicator peaks.

Setup:

The setup consisted of a 12 ml glass vial with the Raman probe positioned on the outside of the glass, cf. Figure 45.

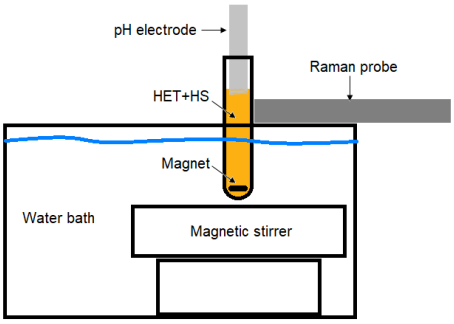

Figure 45: Setup 1

Solutions of HET and HS^- were prepared and heated separately and then mixed in the vial. The pH electrode inserted into the solution. Three scans of the solution were then acquired. After three scans, HCl was added to the solution via an automatic pipette. The addition was to the top of the solution in an open vial. As the pH electrode could only just fit into the vial, it was necessary to remove this prior to adding the acid, exposing the solution to the air in the fume hood. The time = 0 was set at the exact moment of HCl addition.

Experiments:

Several experiments were conducted using this method, cf. Table 16.

Table 16: Experimetns conducted using setup 1 varying initial pH, concentration of HET, HS^- and temperature. Conversion rates of HS^-/HET are also provided

Experiment	Time [min]	pH_{before}	$pH_{initial}$	pH_{final}	C_{HET} [M]	C_{HS-} [M]	T [°C]	HS^-/HET Conversion
S1.1	60	11.15	8.59	9.11	0.35	0.50	50	1.08
S1.2	60	11.55	9.2	10	0.17	0.31	50	1.00
S1.3	30	11.2	10.3	10.2	0.14	0.26	50	0.80
S1.4	30	11.04	9.5	9.92	0.14	0.26	50	0.71
S1.5	30	11.25	9.96	10.3	0.14	0.26	40	0.68
S1.6	30	11.47	9.35	9.75	0.14	0.26	40	1.72
S1.7	30	10.71	10.33	10.3	0.14	0.26	60	0.92
S1.8	30	10.64	9.89	10.6	0.14	0.26	60	1.58
S1.9	30	11.1	8.5	9.09	0.14	0.26	50	1.50
S1.10	30	11.07	9.3	9.82	0.14	0.26	50	1.25

All four investigated parameters were changed, as it is evident from Table 16. However, the initial pH changed regardless of identical conditions. This meant that there was little to no control with the parameters.

The conversion HS^-:HET ratio, calculated as the ratio between the consumed HS^- and HET, is between 0.8 and 1.8 for all the experiments. The experiments with ratio greater than 1, is indictive of both HET and thiadiazine reacting with HS^-, as this would make the ratio 2. However, the experiments, with ratios lower than 1, is indictive of HET being consumed with no consumption of HS^-. This could however be explained by inaccuracies in the measurements, or by sulphides equilibrium; as the pH increases more of the H_2S present in the aqueous phase would be converted to HS^-, making the concentration of HS^- increase, even with consumption by the scavenging reaction.

Results

All experiments yielded Raman spectra showing changes in the indicator peaks for both reactants and products, cf. Figure 46, for an example of an experiment.

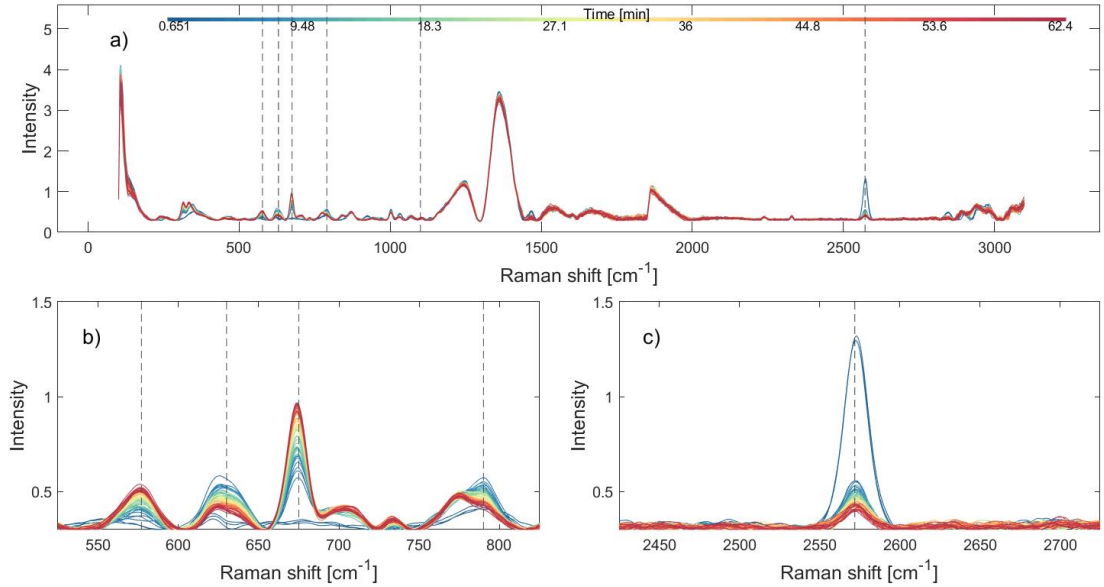

Figure 46: Raman spectra representing all experiments conducted using setup 1, experiment S1.1 to S1.10

As it is evident from Figure 46 the scavenging reaction is occurring, as the 675 cm^{-1} peak is being formed, alongside the 577 cm^{-1} peak, cf. Figure 46b. At the same time a decrease is observed in the 630 cm^{-1} and the 790 cm^{-1} peaks. These changes are corresponding with the changes in the sulphide peak, cf. Figure 46c. However, this peak drops in intensity abruptly after addition of HCl, i.e. after the first three scans. And even though the 675 cm^{-1} peak changes intensity as well in the same period, the change in the sulphide peak cannot be explained by the reaction occurring alone. This means most of the sulphide present in the solution evaporates instantaneously, this hypothesis is validated by the observable gas forming in the vial just after addition of acid.

The concentrations of HET, HS^- and the product peak 675 cm^{-1} is compared for experiments with identical starting concentrations and temperature, experiments S1.3, S1.4 and S1.9, cf. Figure 47.

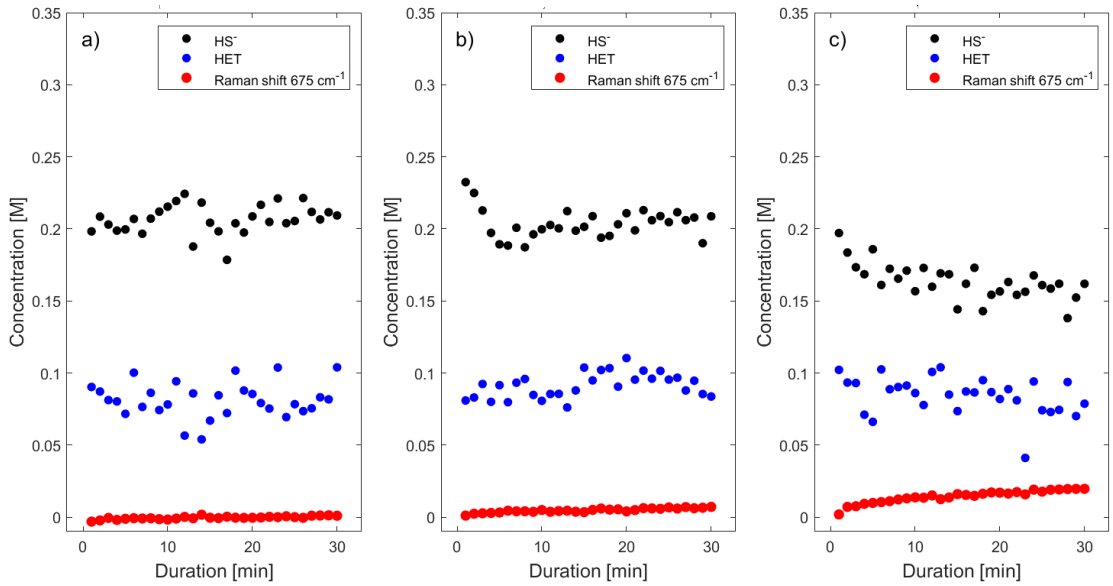

Figure 47: Concentration plots for experiments: a) S1.3 pH 10.3 b) S1.4 pH 9.5 c) S1.9 pH 8.5

From Figure 47 it is evident that there is a tendency of the lower the pH the higher the reaction rate, as the reactants are both decreasing at a higher rate at pH 8.5 than at pH 10.3. The reaction rate is therefore pH dependent.

The experiment with similar pH and temperature was examined, experiments S1.3, S1.2 and S1.1, cf. Figure 48.

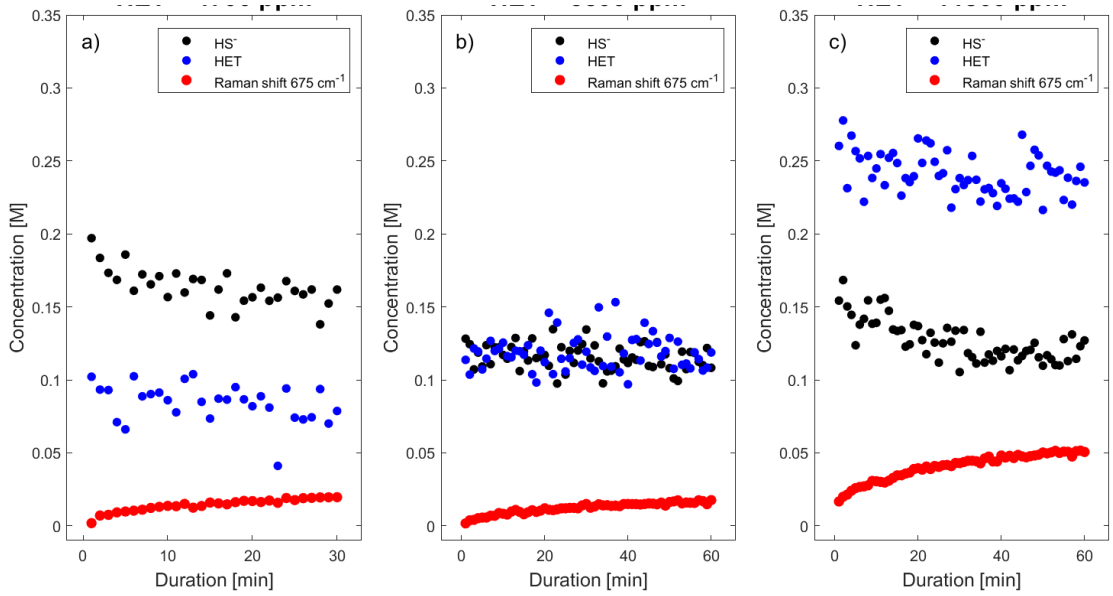

Figure 48: Concentration plots for experiments: a) S1.3 C_{HET} = 0.137 M b) S1.2 C_{HET} = 0.171 M c) S1.1 C_{HET} = 0.497 M

As it is evident from Figure 48 the product peak is increasing faster at the high HET concentration compared to the lower concentrations. This is as expected as the concentration of the

reactants is expected to influence the reaction rate. The difference between 0.137 M and 0.171 M, is not great, however, the initial pH of experiment S1.2 is higher than the other two. Hence this could be the cause of the slower reaction.

Finally, the temperatures are compared for experiments S1.5, S1.4 and S1.7 with similar pH and concentration, cf. Figure 49.

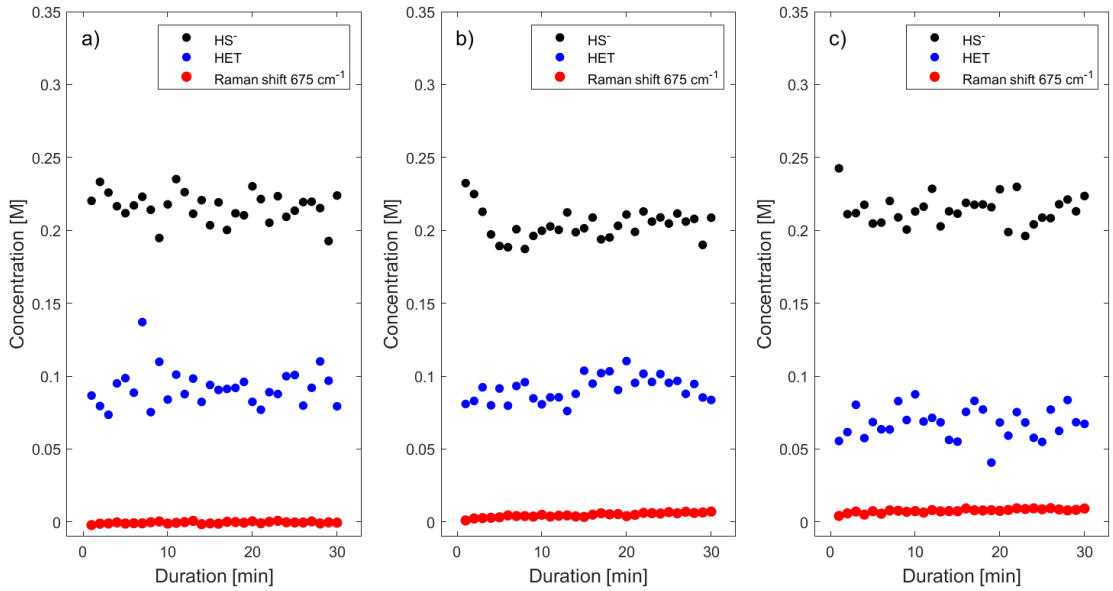

Figure 49: Concentration plots for experiments: a) S1.5, T=40°C b) S1.4, T=50°C c) S1.7, T=60°C

In Figure 49 the changes in concentration of both products and reactants are small, however there is a slight tendency of the reaction being faster at the higher temperature. As per Arrhenius this is expected.

Problems with the setup

There are two main issues with this setup; the evaporation of H_2S and the reproducibility.
As explained, most of the sulphide seemingly disappears instantaneously with addition of acid to the solution. This evaporation results in the initial concentration of sulphide being uncertain, and as control over the parameters are crucial in kinetics studies this is not a desirable result.

Another problem with this method is the reproducibility; even with identical concentrations of HET and HS^-, as well as identical volumes of HCl added, the initial pH varied, cf. Table 16. This in turn meant that there is no reproducibility of this setup, and another setup was therefore investigated.

6.3 Setup 2

To avoid the initial evaporation of the sulphide, it was attempted to lower the pH of the HET and sulphide solutions individually before mixing. If the initial pH of both solutions were around 8 it was expected that the initial pH of the mixed solution would be around 8 as well.

Setup

The setup consisted of a 12 ml glass vial with the Raman probe positioned on the outside of the glass, cf. Figure 50.

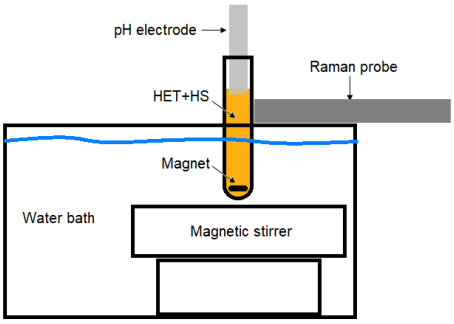

Figure 50: Setup 2

A solution of HS^- was prepared. HCl was then added slowly at the bottom of the vial, to avoid evaporation, until the desired pH was reached. The remaining concentration of HS^- was then established using Raman. A solution of HET was then prepared, and pH lowered to the desired. Both solutions were then heated separately. Finally, the two solutions were mixed in the vial. The pH electrode placed in the vial directly following the mixing, thereby sealing the system. The time = 0 was set at the exact moment of mixing, as this was the start of Raman.

Experiments

Just as with the earlier setup, several experiments were conducted with this setup, cf. Table 17.

Table 17: Experiments conducted using setup 2

Experiment	Time [min]	pH_{before}	$pH_{initial}$	pH_{final}	C_{HET} [M]	C_{HS^-} [M]	T [°C]	HS^-/HET Conversion
S2.1	60	9.02	10.37	11.10	0.150	0.621	25	0.83
S2.2	60	8.87	10.3	10.61	0.164	0.169	40	0.69
S2.3	60	8.76	10.15	10.59	0.164	0.181	50	0.89
S2.4	60	8.47	10.25	10.57	0.317	0.184	50	0.82
S2.5	60	9.55	10.14	10.54	0.317	0.154	50	0.76

All four investigated parameters were changed, as it is illustrated from Table 17. However, as it is evident from Table 17 the pH measured just after mixing of the two solutions were all above 10, regardless of the starting pH of the solutions. This meant there was little to no control of the initial pH of the reaction.

The HS^-:HET ratios are all under 1, which indicates that HET is being consumed with no HS^- being consumed. This would indicate a second reaction, possibly hydrolysis, involving HET, however the hydrolysis has been ruled unlikely, and could not be the sole cause for the low ratio. Another explanation of the low ratios could be due to the oscillations in the results, as the ratios are based on the first and last measurements.

Results

All experiments yielded Raman spectra showing very little change in the indicator peaks for both reactants and products, cf. Figure 51, an example of an experiment.

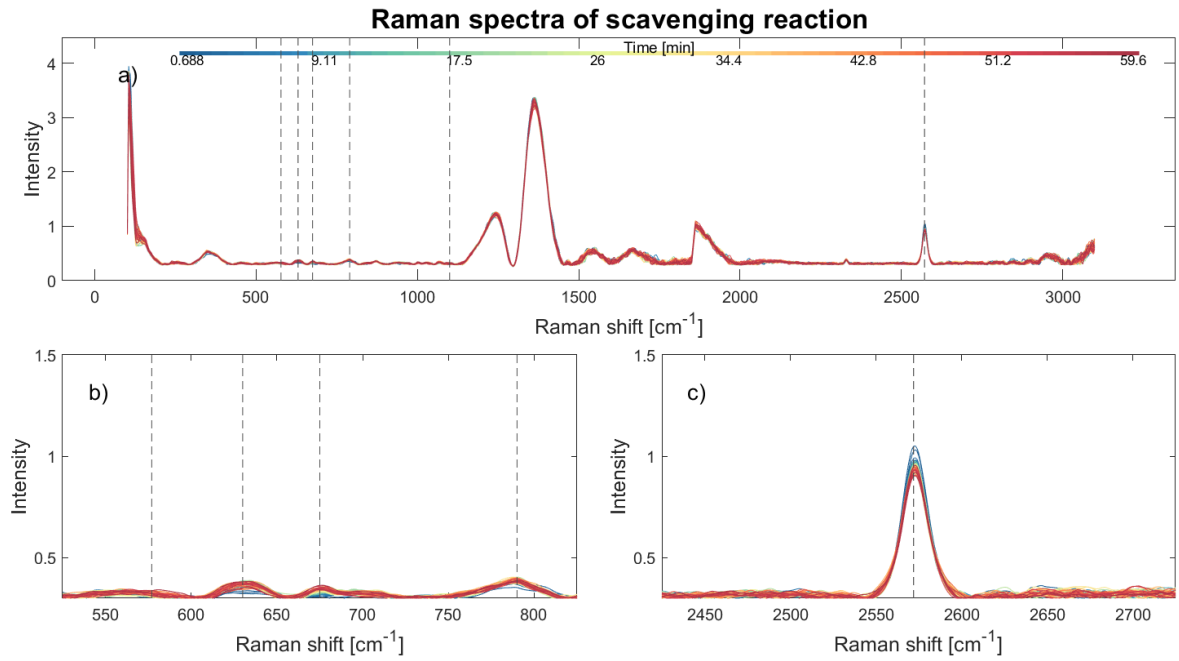

Figure 51: General Raman spectra obtained using setup 2

As it is evident from Figure 51 there is a slight difference in the sulphide peak, and a corresponding slight change in the indicator peak at 675 cm^{-1}. However, unlike previous results, there appears to be an increase in the 630 cm^{-1} peak. It is evident from Figure 51 that the reaction is occurring, however, the rate is very low. The fact that the initial pH was 10 and only a very slow reaction is occurring, indicates the importance of protonating triazine for the reaction to occur.

Problems with the setup

The main problem with this setup, is that the pH is the same in every experiment and is therefore not controllable. Even if both solutions are at initial pH values of 8, the pH is 10 immediately after mixing of the two solutions. This means the initial pH is not controllable and therefore is not ideal for kinetics studies. Another setup was therefore investigated, although this setup proved to be somewhat reproduceable.

6.4 Setup 3

Another attempt to avoid the evaporation of sulphide and avoiding the sudden increase of pH after mixing, was to add diluted HCl instead of concentrated acid. This was expected to limit the amount of evaporation and still allowing a controllable initial pH.

In order to define how diluted the acid needed to be, to obtain the desired pH with different concentrations, a series of preliminary experiments were conducted.

As the desired experiments included three different levels of pH and of concentration of reactants, each combination of these three parameters had to be investigated.

A solution with the desired concentrations of reactants were prepared and added a diluted acid solution. This method was repeated until all combinations of pH and concentrations had an established dilute solution, cf. Appendix 4.

After the determination of how much the acid should be diluted the experiments were carried out.

Setup

The setup consisted of a 12 ml glass vial with the Raman probe positioned on the outside of the glass, cf. Figure 52.

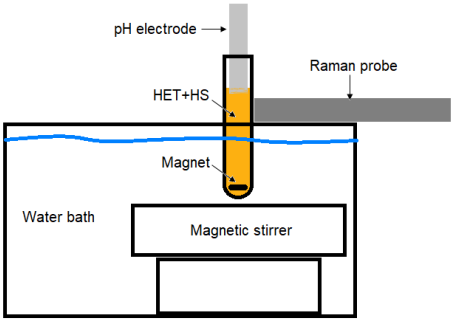

Figure 52: Setup 3

A solution with the desired concentrations of reactants were prepared. A solution of acid with the matching dilution was prepared. Both solutions were then heated separately. Finally, the two solutions were mixed in the vial. The pH electrode placed in the vial directly following the mixing, thereby sealing the system. The time = 0 was set at the exact moment of mixing, as this was the start of Raman.

Experiments

Just as with the earlier setup, several experiments were conducted with this setup, cf. Table 18.

Table 18: Experiments conducted using setup 3 varying initial pH, HET concentration and HS^- concentration.

Experiment	Time [min]	$pH_{initial}$	pH_{final}	C_{HET} [M]	C_{HS^-} [M]	T [°C]
S3.1	60	9.20	9.73	0.293	0.443	45
S3.2	60	8.83	8.85	0.293	0.147	45
S3.3	60	9.49	10.33	0.147	0.443	45
S3.4	60	8.46	9.42	0.147	0.293	45
S3.5	60	8.44	8.79	0.147	0.147	45
S3.6	60	9.09	9.70	0.147	0.293	45
S3.7	60	8.49	8.72	0.293	0.293	45
S3.8	60	8.83	8.86	0.293	0.147	45

pH and concentration of HET and HS^- was investigated, as it is evident from Table 18. As expected, the pH was kept as desired, and there was no visible evaporation of H_2S. Only a couple of the planned experiments were carried out, as there was no visible reaction in the experiment where the HS^- concentration was low.

Results

All experiments with low or medium concentration of sulphide yielded similar Raman spectra, cf. Figure 53 for an example of an experiment.

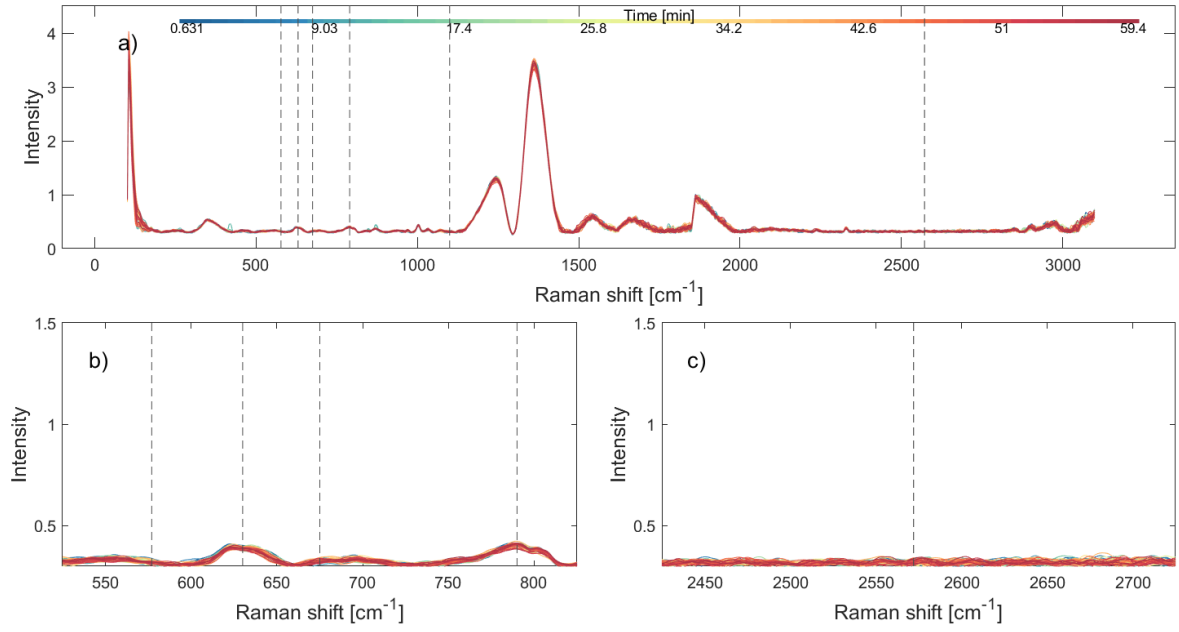

Figure 53: General Raman spectra of experiments conducted with low HS^-concentration.

As illustrated on spectra in Figure 53 no reaction is happening. This can be explained by the complete lack of sulphide in the solution, cf. Figure 53c. This indicates that even though no

visible evaporation of H_2S occurred the gas must have evaporated. This method was therefore not suitable for studying the scavenger reaction.

However, at higher concentrations of HS^- a reaction occurred, and an example is illustrated in Figure 54.

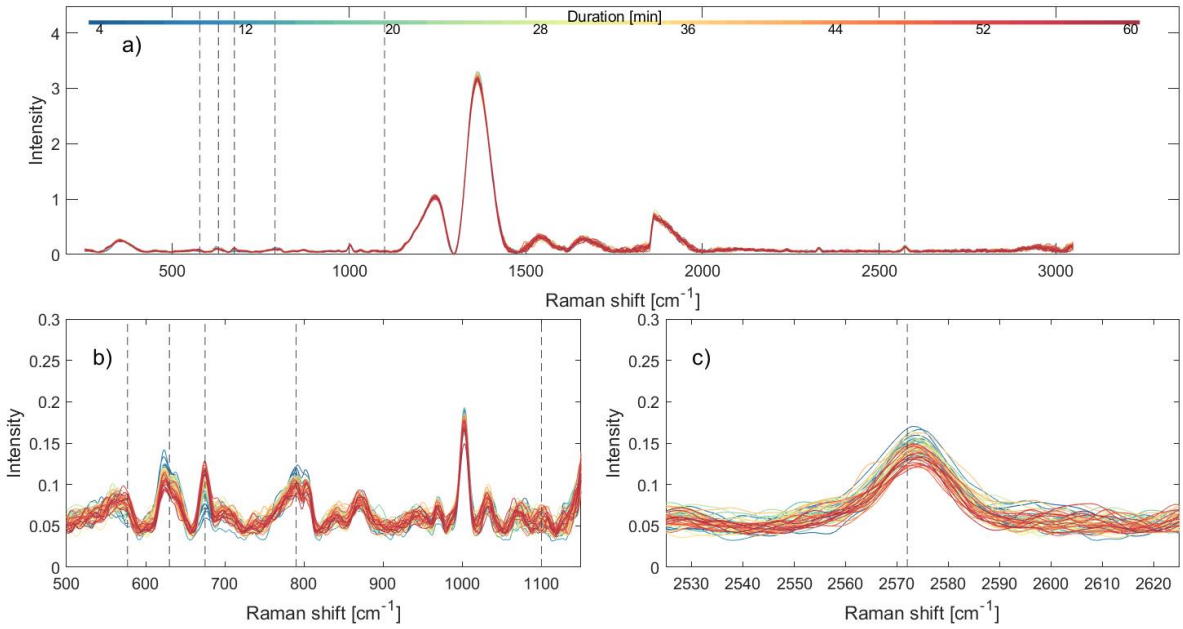

Figure 54: General Raman spectra of an experiment where the concentration of HS^- was not low.

As it is evident from Figure 54 a reaction is occurring, as the 675 cm^{-1} peak is increasing, and there is a slight decrease in the 2572 cm^{-1} peak.

Problems with the setup

This method proved useful in setting the desired pH, however, the sulphide evaporated completely in several of the experiments in this setup. This resulted in no reaction occurring, making this method unfeasible.

6.5 Setup 4

As one of the main issues with the tried setups had been the evaporation of sulphide partly due to the locally low pH, and the open container, the system should be closed. Another issue would be the high detection limit caused by the glassware used, this could be abated by submerging the Raman probe in the solution, thereby removing the glass related peaks from the spectra altogether.

If the system was near completely closed, no H_2S should be able to evaporate regardless of any low pH value, locally or not. Furthermore, if the acid was added deep within the liquid the gas should dissolve back into the liquid before evaporating, due to the high pH of the liquid. If the glass peaks were eliminated, the detection limit of both sulphide an especially HET should decrease, resulting in greater volumes being available.

This meant that a completely new setup was required.

Setup

To be able to close the system completely a container with as little a surface as possible was needed, however, it needed to be able to accommodate both the Raman probe, the pH electrode as well as a device for adding the acid. The only glassware that suited these requirements were a measuring cylinder, making the new setup as illustrated in Figure 55.

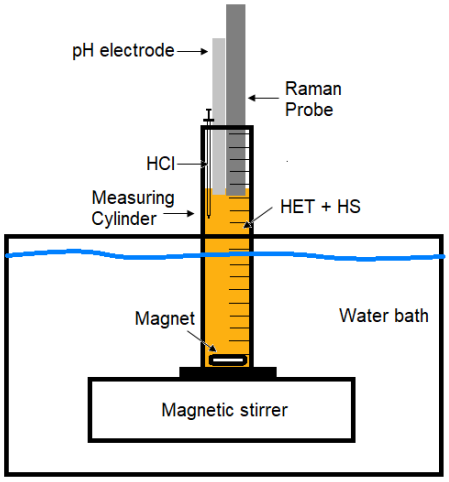

Figure 55: Setup 4

For adding the acid, a plastic syringe was chosen. Solutions of HET and HS^- was prepared and heated separately. Both solutions were mixed in the measuring cylinder. The Raman probe, pH electrode and syringe were submerged into the solution. The container was sealed with para-film. One Raman scan was acquired. The syringe was emptied into the solution. The time t=0 was set to the exact time of injection of acid.

Experiments

As with all other setups, several experiments were carried out, cf. Table 19.

Table 19: Experiments conducted using setup 4 varying pH and time

Experiment	Time [min]	pH_{before}	$pH_{initial}$	pH_{final}	C_{HET} [M]	C_{HS^-} [M]	T [°C]	HS^-/HET Conversion
S4.1	45	11.35	8.9	9.88	0.044	0.09	40	1.15
S4.2	45	11.43	9.48	10.26	0.044	0.09	40	0.92
S4.3	45	11.40	9.33	10.28	0.044	0.09	40	1.88
S4.4	45	11.31	9.47	10.38	0.044	0.09	40	1.92
S4.5	45	11.27	9.3	10.2	0.044	0.09	40	1.82
S4.6	45	11.26	9.49	10.43	0.044	0.09	40	1.88
S4.7	45	11.35	9.56	10.47	0.044	0.09	40	1.95
S4.8	45	11.28	9.34	10.09	0.044	0.09	40	1.72
S4.9	45	11.29	9.14	9.86	0.044	0.09	40	1.84
S4.10	120	10.57	9.5	10.42	0.044	0.09	40	1.14
S4.11	120	11.46	9.56	10.46	0.044	0.09	40	1.72
S4.12	120	11.42	8.99	9.97	0.044	0.09	40	2.29

All experiments were run at the same temperature, and with the same concentrations of both HET and HS^-. There is a slight variation in the initial pH, however there are several runs with the same initial pH values, making this setup a fairly reproduceable method.

With conversion HS^-:HET ratios between 1.1 to 2 for the all the experiments, not including S4.3, and S4.12, with ratios of 0.9 and 2.3 respectively, the indication of both HET and thiadiazine reacting with HS^- is strong. The low ratio for the experiment nyefors3, could be explained by inaccuracies of the calculation of the concentrations. The very high conversion ratio could be due to the same, or this might indicate an evaporation of H_2S mid reaction. However, there is the possibility, as this is a two-hour experiment, that the high conversion ratio is due to the formation of trithiane, thus making the ratio 3, and not 2.

Results

All experiments yielded similar Raman spectra, cf. Figure 56 an example of an experiment.

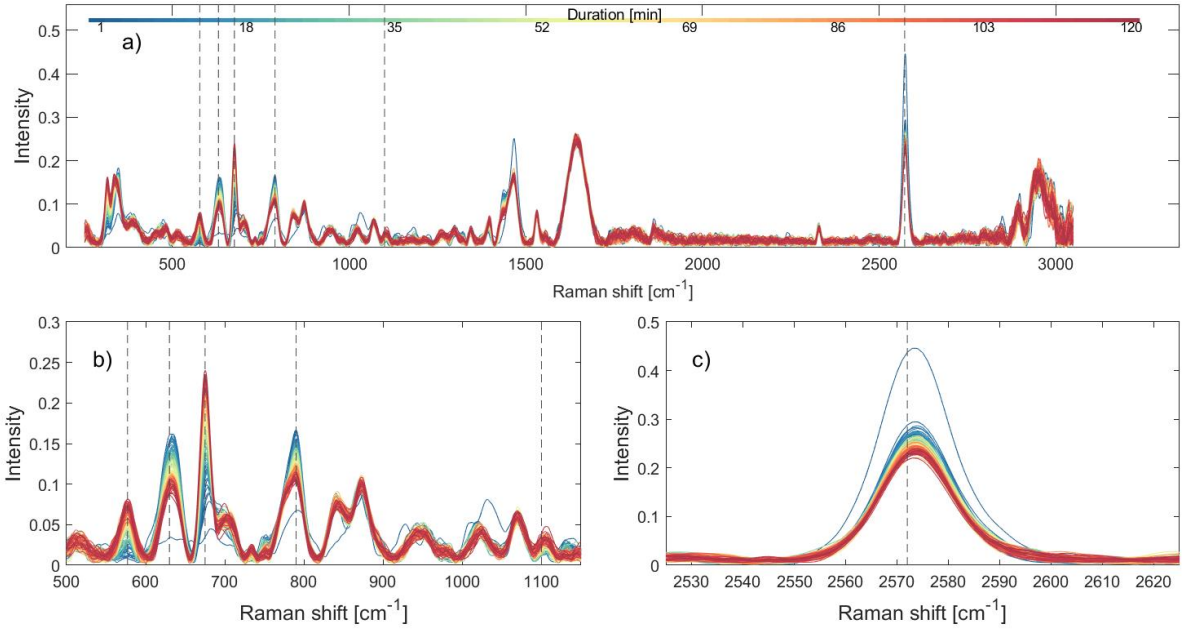

Figure 56: General Raman spectra of all experiments conducted using setup 4

As illustrated in the Raman spectra in Figure 56 some evaporation of H_2S still occurs, however, the amount of evaporation is lessened compared to the other setups. Furthermore, this setup has a lot lower detection limit for HET, making the peaks easier identifiable. However, the first scan is obtained before the addition if acid, but after the insertion of the syringe, and in the spectrum the peak at 675 cm^{-1} is already present at the first scan, indicating the reaction already starting. This could be due to the acid escaping the syringe an lowering the pH locally.

Experiments S4.3, S4.5 and S4.7 was compared, as these were identical, cf. Figure 57.

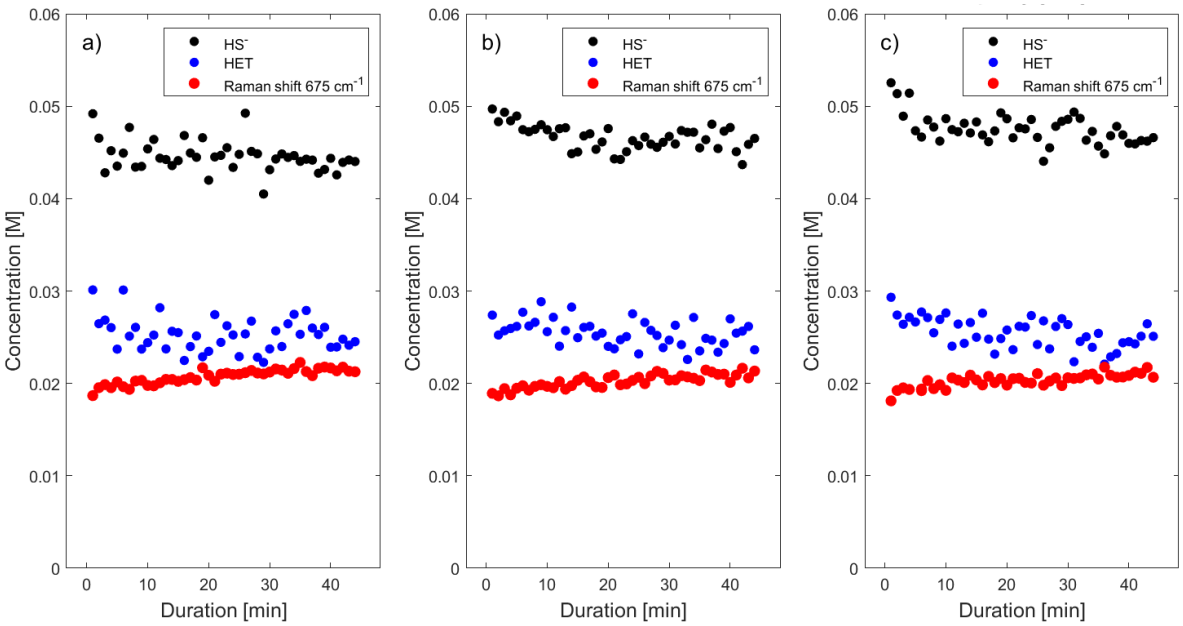

Figure 57: experiments a) S4.3, b) S4.5, c) S4.7

As it is evident from Figure 57 the experiments yielded almost identical results, indicating that this setup is repeatable. However, there is a slight difference in the concentration of HS^-, which proves problems with evaporation of H_2S.

Experiments S4.8, S4.6 and S4.12 was compared, as these differ in pH, cf. Figure 58.

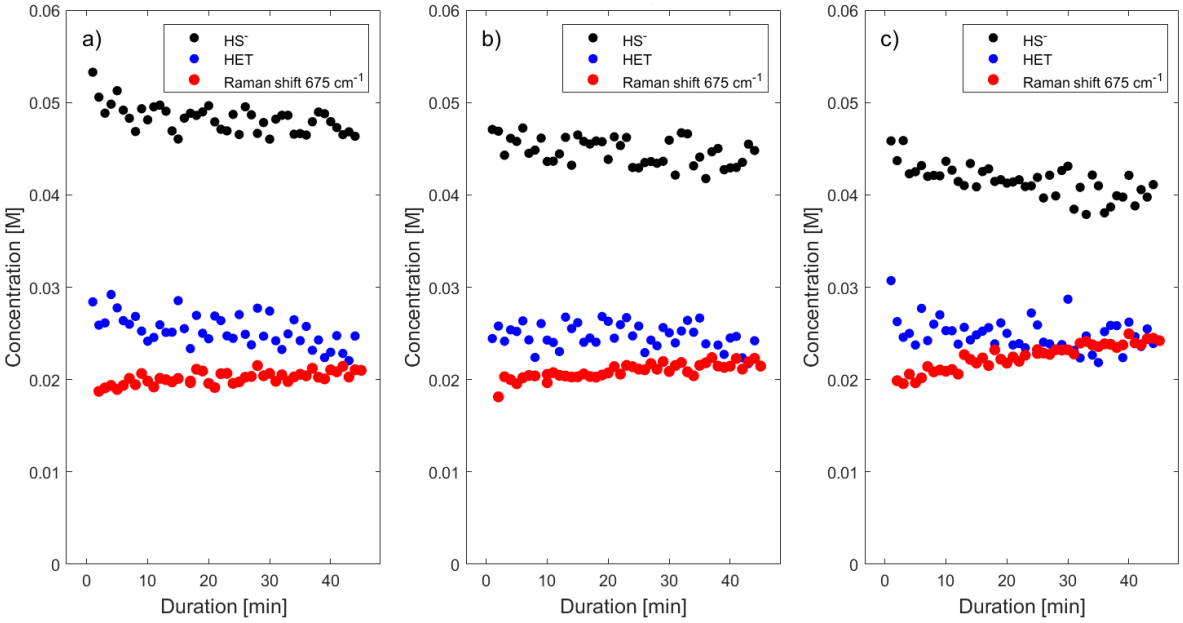

Figure 58: a) S4.8, pH = 9.56, b) S4.6, pH = 9.3, c) S4.12, pH = 8.9

As it is evident from Figure 58 the reaction is pH dependent, as the reaction is faster the lower the initial pH. The reactants decrease faster and the product is formed faster at pH 8.9 than pH

9.6. It is also evident from Figure 58 that the lower the pH the more H_2S evaporates, as the initial concentration of HS^- in S4.12 is lower than for the experiment at higher pH.

Problems with the setup

The fourth setup gives reproducible results for similar conditions. However, the H_2S is evaporating, making the initial concentration of HS^- unknown. Further, the initial time, t = 0, is not possible to determine, as it appears the reaction starts before the injection of the acid.

6.6 Concluding remarks

The main challenge of the setup for obtaining kinetics data is to keep pH stable. Buffers with buffer capacity within the pH range of 8 to 10 was proven not to be practical. Not having a buffer to keep pH stable and low enough to initiate the reaction, HCl was added to the solution. Addition of the acid caused an immediate evaporation of H_2S, due to the locally low pH when added.

Setup 1 proved useful for qualitatively studying the reaction, however, the evaporation of H_2S in this setup was large, and the initial conditions were not repeatable.

In setup 2, the evaporation of H_2S was not an issue, however, in this setup the main issue, was to keep the initial pH, as the mixing of the two solutions resulted in an immediate rise in pH.

Setup 3 was repeatable regarding the initial pH, however in this method the evaporation of H_2S was great, often resulting in the complete disappearance of sulphide in the solution. Thus, no reaction occurred.

The final setup, setup 4, proved repeatable regarding initial pH, and the evaporation was limited, however, still occurring. The setup is not a viable method for obtaining reliable kinetics data, however, as the initial time, t = 0, is unknown, due to the untimely initiation of the reaction.

Chapter 7

Evaluation of reaction kinetics

To establish the reaction kinetics of a reaction it must first be determined if the reaction is elementary or consists of a sequence of elementary reactions. From this a proposed expression for the reaction kinetics must be derived and tested to evaluate if it fits the data acquired experimentally.

Reaction 7.1 is expected to be the scavenging reaction occurring:

$$HET + HS^- \rightarrow Thiadizine + MEA \qquad (7.1)$$

A HS^-/HET ratio of between 1 and 2 are obtained from the experimental data, and HS^- is consumed faster than HET. This indicates more than one scavenging reaction is occurring, and equation 7.2 is the expected reaction based on literature:

$$Thiadizine + HS^- \rightarrow Dithiazine + MEA \qquad (7.2)$$

If a rate expression for the consumption of HS^- both these reactions needs to be considered, for HET only reaction 7.1 is needed.

It was examined if the scavenging reaction consuming HET is elementary.

For a reaction to be elementary it must (Roberts, 2009):

- Have non-fractional molecules
- Be unimolecular or bimolecular
- Have less than four bonds breaking or forming

In reaction 7.1 HET and HS^- reacts one to one, and does therefore comply with the first screening criteria, secondly it is bimolecular as two reactants collide to form products. The third screening criteria is, however, not met, as there are more than four bonds forming or breaking in the reaction mechanism, cf. Figure 59.

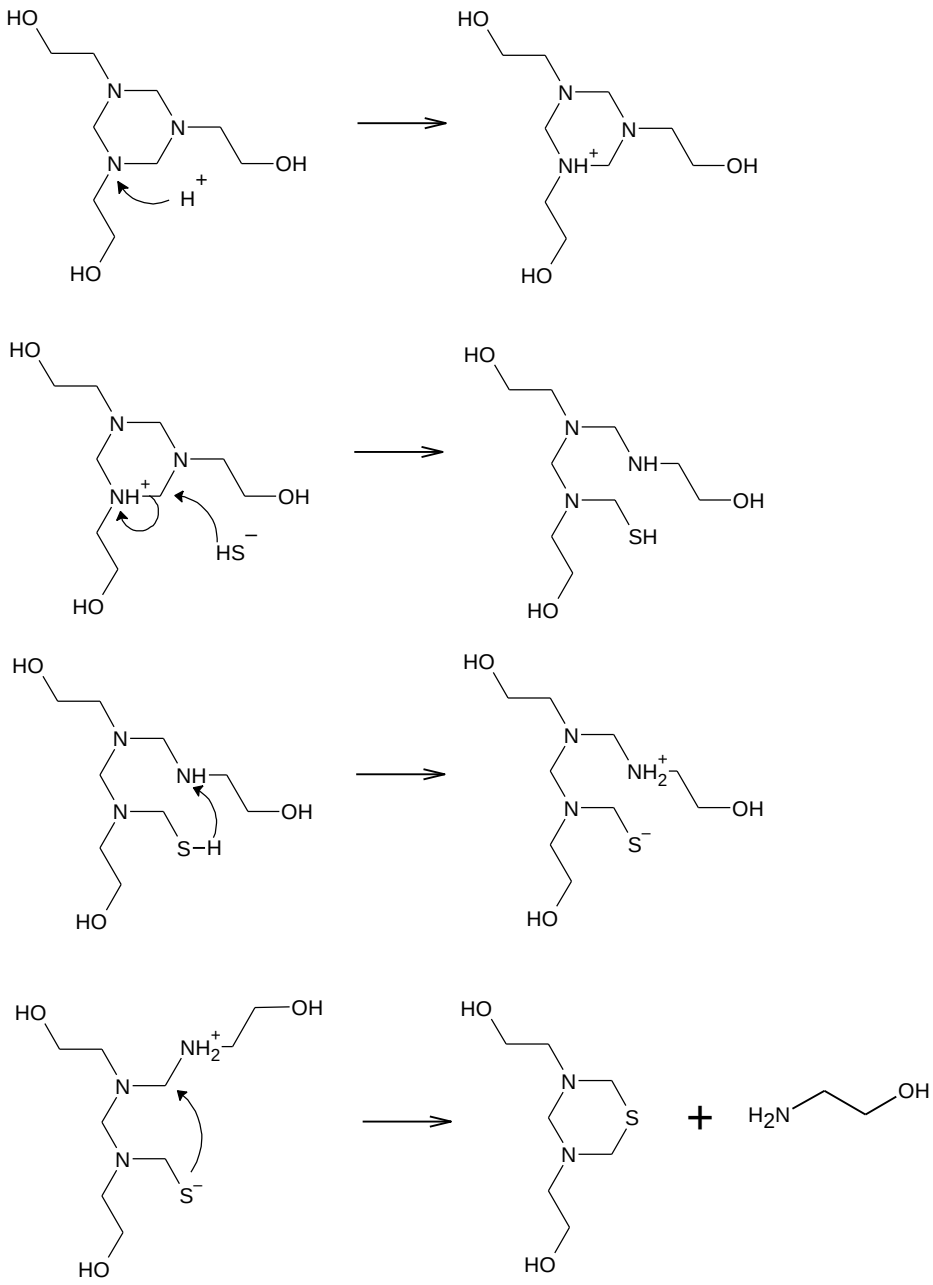

Figure 59: Proposed reaction mechanism for HETs reaction with HS^-, inspired by (Madsen, 2011)

The scavenging reaction cannot be considered an elementary reaction, and it must be attempted to describe the reaction with a sequence of reactions. Based on the reaction mechanism from Figure 59, reactions 7.3 to 7.6 must be occurring:

$$HET + H^+ \overset{k_1}{\rightarrow} HET^+ \quad (7.3)$$

$$HET^+ + HS^- \overset{k_2}{\rightarrow} HET_R \quad (7.4)$$

$$HET_R + H^+ \overset{k_3}{\rightarrow} HET_N^+ \quad (7.5)$$

$$HET_N^+ \overset{k_4}{\rightarrow} Thiadiazine + MEA \quad (7.6)$$

HET is only a reactant in reaction 7.3 and the rate expression should therefore be:

$$-r_{HET} = k_1 \cdot C_{HET} \cdot C_{H^+} \quad (7.1)$$

From equation 7.1 The consumption of HET is not dependent on the concentration of HS^-. This can further be established by finding an expression for the disappearance of HS^-. If only the scavenger reaction involving HET is considered, HS^- is consumed in reaction 7.2 Only. This gives the expression:

$$-r_{HS^-} = k_2 \cdot C_{HET^+} \cdot C_{HS^-} \quad (7.2)$$

HET^+ is an intermittent reactant, and the concentration is established using steady state approximation. This assumes that the consumption, $-r_{HS^-}$, and forming, r_{HET}, of HET^+ are equal and the rate =0:

$$-r_{HET^+} = 0 = k_1 \cdot C_{HET} \cdot C_{H^+} - k_2 \cdot C_{HET^+} \cdot C_{HS^-} \quad (7.3)$$

Isolating the concentration of HET^+ gives:

$$C_{HET^+} = \frac{k_1 \cdot C_{HET} \cdot C_{H^+}}{k_2 \cdot C_{HS^-}} \quad (7.4)$$

Inserting the concentration of HET^+ in the rate expression for HS^- gives the reaction rate for HS^-, equation 7.5:

$$-r_{HS^-} = k_1 \cdot C_{HET} \cdot C_{H^+} \quad (7.5)$$

As expected, the rate of consumption of HS^- is equal to the rate of consumption of HET, but neither of the rate expression are dependent of the concentration of HS^-.

The rate expression for the consumption of HET must be:

$$-r_{HET} = k_1 \cdot C_{HET} \cdot C_{H^+} \qquad (7.6)$$

The consumption is therefore dependent on the concentration of H^+. This is in line with the pH dependency the reaction exhibited in the experimental work. Equation 7.6 is tested on the experimental data obtained in the project.

As the experimental data in this project is concentration vs. time, the instantaneous rates and concentrations had to be established first. The reaction between HET and HS^- is considered homogeneous and the rates are calculated using equation 7.7 (Roberts, 2009).

$$-r_A = \frac{C_A(t_1) - C_A(t_2)}{t_2 - t_1} \qquad (7.7)$$

With r_A as the rate of disappearance of A, $C_A(t_1)$- $C_A(t_2)$ being the difference in concentration measured at time 1 and 2, and t_2-t_1 is the time interval.

The rate is the difference between to experimental data points over the time period between the two datapoints. The concentrations are, however, measured at each datapoint, and an average of the two datapoints are then needed, cf. equation 7.8 (Roberts, 2009):

$$C_A = \frac{C_A(t_1) + (t_2)}{2} \qquad (7.8)$$

With equations 8.7 and 8.8 the rates of disappearance of HET and corresponding concentrations of the reactants; HET and H^+, was obtained, and used in equation 7.6.

It was assumed that the reaction is first order with respect to each of the two reactants. The rate constants are found mathematically; At 40℃ the rate constant, k, was found to be $2.73 \cdot 10^6 \left[\frac{1}{M \cdot s}\right]$ and at 50℃ it was $2.43 \cdot 10^5 \left[\frac{1}{M \cdot s}\right]$, cf.

Table 20: Calculated rate constants for experiments at 40℃ and 50℃. Standard deviation is listed for each.

Table 20: Calculated rate constants for experiments at 40℃ and 50℃. Standard deviation is listed for each.

Temperature	Rate constant, k $\left[\frac{1}{M \cdot s}\right]$	Standard deviation $\left[\frac{1}{M \cdot s}\right]$
40 ℃	$4.38 \cdot 10^6$	$\pm 2.12 \cdot 10^6$
50 ℃	$5.17 \cdot 10^6$	$\pm 3.73 \cdot 10^6$

The rate constants for the reaction is increasing with temperature, which is in accordance with the faster consumption of HET at higher temperatures. However, the standard deviations indicate a high difference in the datasets. The rate constants are deviating more than 50 % and is therefore not reliable.

To ensure the rate constants found match the data, the constants are inserted into the reaction rate expression for the consumption of HET:

$$-r_{HET,40℃} = -4.17 \cdot 10^6 \cdot C_{HET} \cdot C_{H^+} \qquad (7.9)$$

$$-r_{HET,50℃} = -5.17 \cdot 10^6 \cdot C_{HET} \cdot C_{H^+} \qquad (7.10)$$

Equations 7.9 and 7.10 are plotted against the measured values of rate of consumption of HET, cf. Figure 60 for experiments at 40℃ and Figure 61 for 50℃.

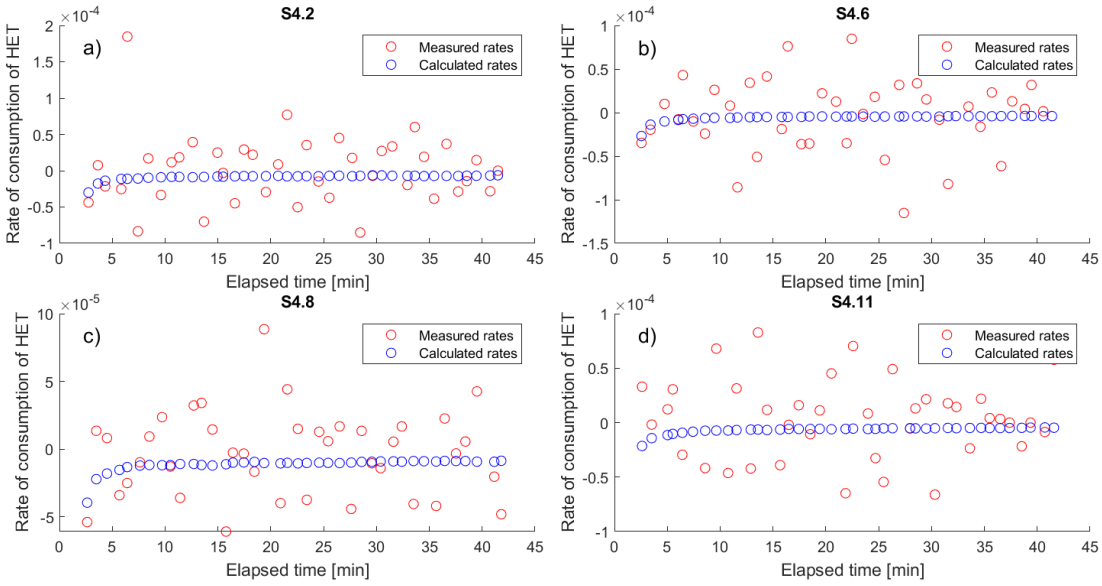

Figure 60: Calculated and measured rate of consumption for experiments at 40℃: a) Experiment S4.2, b) Experiment S4.6, c) Experiment S4.8, d) Experiment S4.11

As it is evident from Figure 60 the calculated rates are overlapping with the measured rates. This indicates that the kinetics expression is probable. However, the measured values are scattered, and a trend is not clear. One cause of the scatter is the scatter in the Raman signal. The differences in the measured concentration of HET results in scattered reaction rates. Figure 60a is the experiment with the best fitted curve; however, it is not possible from the experimental data in this project to ascertain with certainty that the kinetics expression is valid.

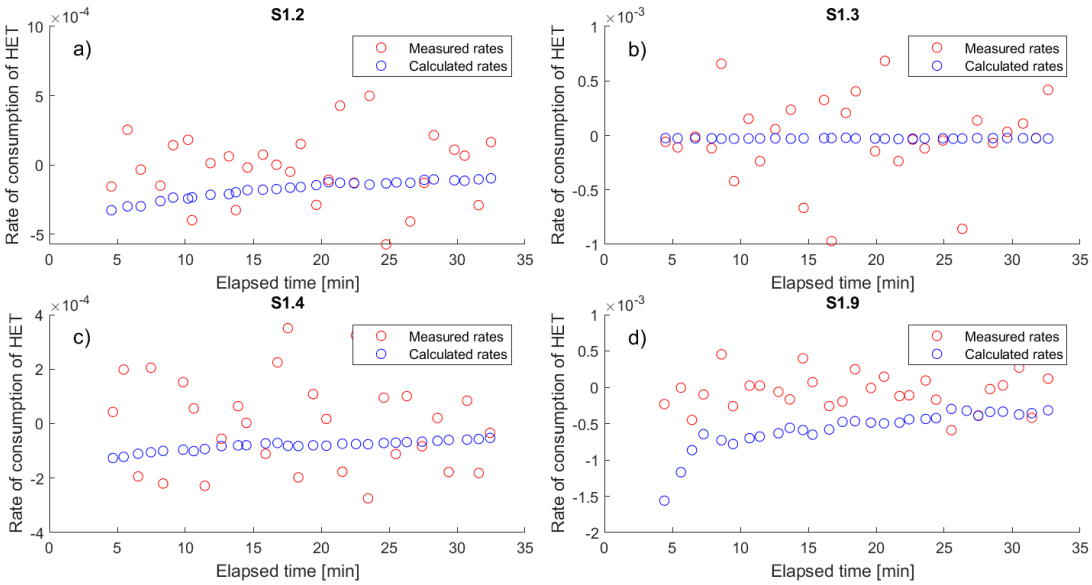

Figure 61: Calculated and measured rate of consumption for experiments at 50℃: a) Experiment S1.2, b) Experiment S1.3, c) Experiment S1.4, d) Experiment S1.9,

The calculated reaction rates are overlapping with the measured values and indicate a validity of the kinetics expression. As with the experiments at 40℃ the plots are dominated by scattered measurements and it is not possible to obtain a confident fitting of the data. Figure 61d is the least good fit of the calculated data and the measured rates.

Since rate constants are estimated at two different temperatures, it is possible to estimate the activation energy of the reaction from the Arrhenius equation 7.11 (Roberts, 2009):

$$\ln\left(\frac{k_2}{k_1}\right) = -\frac{E_a}{R} \cdot \left(\frac{1}{T_2} - \frac{1}{T_1}\right) \qquad (7.11)$$

With a gas constant of 8.31 $\frac{J}{mol \cdot K}$ the activation energy is estimated to be 18.1 kJ/mol. This indicates a fast reaction.

The experimental data obtained in this project indicates that the reaction rate is only dependent on the concentration of HET and pH. The data is not suitable for a definite conclusion of the proposed kinetics expression for the consumption of HET is valid, and the data is not appropriate to estimate a rate expression for the consumption of HS^-.

Chapter 8
Discussion

In this project one of the main questions has been if Raman spectroscopy is a feasible method of obtaining kinetics data of the scavenging reaction between 1,3,5-tri-(2-hydroxyethyl)-hexa-hydro-s-triazine, HET, and HS^-. Little information regarding the qualitative aspect of the scavenging reaction is available in the literature and less information is available about the quantitative aspect. The kinetics of the widely used scavenger is therefore lacking.

The scavenging reaction is heterogeneous; consist of both absorption into the aqueous phase and of the reaction in the aqueous phase. The focus of the experimental work was the reaction in the aqueous phase.

From the experimental work of this project it has proven challenging making the reaction occur and obtaining repeatable quantitative data, and thereby obtaining information regarding the kinetics of the scavenger reaction.

It is possible to distinguish between the two reactants, HET and HS^-, in the solutions, as these chemicals resulted in different peaks in the Raman spectrum. Especially HS^- was easily identifiable as it results in only one completely isolated peak at Raman shift 2572 cm^{-1}. HET yielded several peaks in the Raman fingerprint region, < 1500 cm^{-1}, and above 2900 cm^{-1}. This made the two chemicals discernible from one another. However, HET was not easily discernible from the by-product MEA, as these chemicals have similar bonds, since MEA is a constituent of HET. The similar bonds resulted in similar Raman responses, and made the differentiation between the two difficult. However, each chemical had indicator peaks unique to each species; HET had a distinctive peak at 790 cm^{-1} and MEA one at 1100 cm^{-1}. The difficulties in distinguishing the two chemicals is further explained by the 75 % purity of the chemical HET; most of this impurity is suspected, but not known, to be water, however, some of the impurities are suspected of being MEA, as HET is prepared from MEA. The presence of MEA in the chemical, and thereby every solution of HET, resulted in the MEA peaks being challenging to separate from the peaks caused by HET.

The correlation between intensity of the peaks and the concentration of the chemical was found by calibrating Raman on each chemical. HS^- was affected by the peak at 2572 cm^{-1} as

expected and resulted in R^2-value of 0.99. HET was calibrated based on several peaks, however in order to take the peaks overlapping with MEA into account, the solutions used to calibrate HET was a combination of MEA and HET. This ensured that the peaks MEA overlapped did not influence the calibration. However, without the pure HET, the calibration may not exclude MEA completely. The correlation between concentration and peak intensity was linear and had R^2-value of 0.98.

The detection limit of each component was estimated during the calibration, and it was found that the solutions, which yielded no reaction, was above the threshold of the detection. The detection limit was therefore not the reason for the lack of reaction. The detection limit changed with different setups and needed to be accounted for with each changing setup.

Raman and the sensor from Unisense yielded similar results; a decrease in the sensor data yielded a decrease in the Raman intensity, however, Raman showed a stronger decreasing tendency compared to the sensor. The sensor measured the neutral H_2S and not HS^-, which have different responses in Raman spectra: H_2S = 2590 cm^{-1} and HS^- = 2572 cm^{-1}, an additional calibration was needed. This calibration proved challenging, and only yielded R^2-value of 0.5, the low value indicates a poor fit between the intensity and the concentration. However, as the concentration of H_2S varied due to evaporation, the concentration values were not accurate. This could explain the differences in the results from the sensor and the data from Raman. The sensor also proved susceptible to HET and water and the results of may have been affected by this, making the sensor data less reliable.

Temperature and pH did not influence the reaction individually, as no reaction occurred with varying temperature or pH. With a combination of lower pH and higher temperature a reaction was observed, and new peaks was formed. The most important peak being the peak at 675 cm^{-1}, as this was identified as a C-S-C-bond, corresponding to the expected scavenger products. In this project it has not been establish which scavenger product was formed, as a C-S-C-bond is present in all expected scavenger products. Several other peaks were formed throughout the experiments, these peaks remain to be identified.

Another aspect of the project was to develop a setup that could provide kinetics data of scavenging reaction. The reaction is both pH and temperature dependent, and a setup including both a higher temperature than ambient, and a lower pH than 10 needed to be developed.

Four different setups were tested, however, none proved useful, as they all had disadvantages.

None of the setups provided the opportunity to stabilize pH, as pH increases during the reaction and no buffer proved suitable. The buffers either had overlapping peaks with the chemicals, solubility problems or reacted with the chemicals. It was therefore necessary to lower pH by direct addition of acid, and then tracking pH throughout the reaction. This resulted in unwanted and uncontrollable evaporation of HS^-, and in uncertainties regarding the initiation time, t = 0, of the reaction. Two of the setups proved repeatable, however in these setups the initial conditions were not controllable. Further work regarding the setup is therefore needed in order to obtain reliable and repeatable results.

From the experimental data obtained during the project period several observations regarding the reaction was made. The reaction appears very pH dependent, as the consumption of both reactants are faster the lower the pH. All experiments with initial pH below 9.5 had a higher and faster consumption of HET and HS^-, compared to experiment with initial pH above 9.5. Experiments with pH below 9.5 also showed a faster formation of products, compared to experiments with higher pH. The faster formation of products and equally faster consumption of reactants indicate a strong pH dependency of the scavenging reaction. As the initial concentration of HS^- varied after the injection of acid, the different concentration might have an impact on the reaction rate, the results are therefore not directly comparable. However, as the reaction was not occurring at pH levels above 11, the likelihood of the reaction being pH dependent increases. The pH dependency can be explained by the reaction mechanism of the scavenging reaction proposed in literature; the scavenger molecule needs to be protonated in order to react with the sulphide. The lower pH results in higher concentration of H^+-ions and the likelihood of HET being protonated increases.

The reaction rate also appears to be influenced by the concentration of HET, as the rate of consumption of HET and HS^- increased with increasing concentration of HET.

From HS^-/HET conversion ratios between 1 and 2, it was observed that HS^- was being consumed faster than HET, which indicated that more than one scavenging reaction occurs. From the literature it is expected that the scavenger product thiadiazine is also able to react with HS^- in a scavenger reaction, and the higher consumption rate of HS^- was therefore to be expected. Some experiments had conversion ratios below 1, indicating more HET being consumed than HS^-. This could be due to the equilibrium of sulphide, as the concentration of HS^- will

increase with an increase in pH. It could also be caused by HET decomposing due to locally low pH. The hydrolysis is not observable at pH above 7, however at pH below 1, a change in the Raman spectrum of HET is observed. As locally low pH would only be occurring in the early stages of the reaction, just succeeding the addition of acid, hydrolysis should not be an issue later in the reaction.

From the literature-based reaction mechanism a kinetics expression for the consumption of HET was proposed, and the rate of consumption is solely dependent on the concentration of HET and H^+. This is in line with the experimental work, were a strong pH dependency and a dependency of concentration of HET is observed. Observation regarding the concentration of HS^- was not made conclusively, yet it does not appear to have an effect. A repeatable setup with control over initial concentrations, pH and the initiation time of the reaction was not possible to obtain during the project. Nevertheless, an estimation of the rate constants at different temperatures was made. The rate constants had deviations of more than 50 % and is not reliable, which was expected from the experimental data. To obtain less deviating rate constants a new setup is needed. However, the rate constants found did provide an overlap between the calculated rates of HET consumption and the measured rates. The kinetics expression proposed can therefore not be excluded as a possible rate expression for the consumption of HET. Further work is needed to confirm if the expression is correct.

Chapter 9

Conclusion

The project results confirmed Raman spectroscopy as a feasible technique of qualitatively and quantitatively investigation of the aqueous phase reaction between 1,3,5-tri-(2-hydroxyethyl)-hexahydro-s-triazine, HET, and HS^-. It is possible to distinguish between the reactants and products in the Raman spectrum, as each chemical yield unique peaks. A correlation between the intensity and the concentration of the chemicals can be made, and the concentrations of reactants at any given time during the reaction can be determined.

None of the tested setups are deemed fully adequate; each one presents advantages and disadvantages, further improvement on the setup is needed.

From the experimental data a strong pH dependency of the reaction was evident: the reaction did not occur at pH above 11, and the consumption of HET and the formation of products was faster at initial pH levels below 9.5 compared to higher pH values. A dependency of the concentration of HET was also observed from the experimental work; a HET concentration of 0.35 M yielded a faster consumption compared to concentrations below 0.17 M.

A kinetics expression for the consumption of HET was proposed based on the reaction mechanism:

$$-r_{HET} = k \cdot C_{HET} \cdot C_{H^+}$$

The experimental data yielded an activation energy of the scavenging reaction of 18 $\frac{kJ}{mol}$, based on rate constants:

$$k(40℃) = 4.38 \cdot 10^6 \pm 2.1 \cdot 10^6 \frac{1}{M \cdot s}$$

$$k(50℃) = 5.17 \cdot 10^6 \pm 3.7 \cdot 10^6 \frac{1}{M \cdot s}$$

The proposed reaction rates for the consumption of HET proved a fair fit with the experimental data and must be considered probable.

Chapter 10

Further work

The experimental work in this project indicate that the reaction rate of the scavenging reaction is strongly dependent on pH and the concentration of the scavenger. However, to determine the rate with certainty, stable reproducible results are a necessity, and a new setup is needed.

A setup must provide control over the initial concentrations of HET, HS^- and H^+, and not interfere with the Raman spectrometer. Further the initial time, $t = 0$, of the reaction must be well established.

To examine the rate of the scavenging reaction kinetics expression for both the consumption of HET and HS^- must be determined experimentally. Further the forming of the reaction products must be examined as well. The reaction products should be identified and quantified to propose a kinetics expression for the formation of all reaction products.

The identification of both products and reactants needs to be verified using other analytical methods than Raman spectroscopy, and the possibilities must be exhaustedly examined. A second method of analysing the components of the reaction will provide a more precise measurement of the chemicals in the reaction, and it will verify the use of Raman as a feasible method of tracking the scavenging reaction.

One of the issues in the project was the impurities of the chemicals, and further study of the reaction kinetics and the reaction in general should be conducted on pure substances. As the availability of HET is low a method of obtaining the pure chemical would be to synthesize the chemical in the lab. This further requires reliable methods of qualitative and quantitative analysis of HET.

An improved setup with Raman and a secondary analysis method will result in a deeper comprehension of not only the pure components, but also the mixture of the chemicals. Mixing the chemicals provides additional challenges regarding identification and quantification and must be fully understood before a complete kinetics expression can be obtained. For further work this effect must be investigated.

H^+ is found to be a reactant in the scavenging reaction and the concentration of the ion must be determined with equally high accuracy as the other reactants. The use of a pH logger will improve the accuracy of the pH measurements.

The hydrolysis of HET was not observed as an issue in this project, however, as the literature is conflicting on this subject the hydrolysis of HET must be further investigated. A deep comprehension of the hydrolysis will further enhance the understanding of the reaction mechanisms of the scavenging reaction, and thereby result in a more accurate kinetics expression.

An expression of the rates of consumption of HET, HS^- and H^+, and rates of forming of the products, will result in more accurate expressions of the aqueous phase reaction between HET and HS^-. However, to fully comprehend the scavenging reaction, the absorption of H_2S into the aqueous HET must be examined. It must be examined if the absorption or the scavenging reaction is the limiting step in the scavenging of the toxic gas. Further it must be examined if the rate of absorption can be optimized.

If the rate limiting step is identified and an expression for the rate of the entire scavenging process is obtained, the process can be optimized, and preferably lead to a decrease in the use of scavenger in the offshore oil and gas production.

Chapter 11

Literature

Agbroko O.W., Piler K., Benson T.J., 2017, A comprehensive review of H2S scavenger technologies from oil and gas streams, ChemBioEng Reviews, Vol. 4:6, 339-359.

Arnaut L., Formosinho S., Burrows H., 2007, 1, Chapter 9, Chemical Kinetics, Amsterdam, Netherlands, Elsevier.

Bakeev K.A., 2010, Process Analytical Technology, 2nd ed., Chichester, England, John Wiley & Sons, LTD.

Bakke J.M., Buhaug J., Riha J., 2001, Hydrolysis of 1,3,5-Tris(2-hydroxyethyl)hexahydro-s-triazine and Its Reaction with H2S, Ind. Eng. Chem. Res., Vol. 40, p.6051-6054

Bashipour F., Rahimi A., Khorasani S.N., Naderinik A., 2017, Experimental Optimization and Modeling of Sodium Sulfide Production from H2S-Rich Off-Gas via Response Surface Methodology and Artificial Neural Network, IFP Energies nouvelles, Vol. 72, 9

Beredskabsstyrelsen, Fakta om Hydrogensulfid, [online] Available at: https://brs.dk/beredskab/eksperter/kemisk_beredskab/inf_kemiske_stoffer/Documents/Faktaark_hydrogensulfid.pdf (Accessed: June 3rd 2019)

Bothamly M., 2004, Offshore Processing options vary widely, Oil and Gas Journal, Vol. 102, iss 45.

Buhaug J.B., 2002, Investigation of the Chemistry of Liquid H2S Scavengers, Ph.D. Thesis, Norwegian University of Science and Technology, Trondheim, Norway.

Chemical Kinetics: From Molecular Structure to Chemical Reactivity, Elsevier, Amsterdam, Netherlands.

Cline J.D., Richards F.A., 1969, Oxygenation of Hydrogen Sulfide in Seawater at Constant Salinity, Temperature, and pH, Environmental Science & Technology, 09/1969, Vol. 3(9), pp.838-843

Doeller J.E., Isbell T.S., Benavides G., Koenitzer J., Patel H., Patel R.P., Lancaster Jr. J.R., Darley-Usmar V.M., Kraus D.W., 2005, Polarographic measurement of hydrogen sulfide production and consumption by mammalian tissues, analytical Biochemistry, Vol. 341, p. 40-51.

dthreetechnology, [online] Available at: http://www.dthreetechnology.com/h2s_scavenger.html?fbclid=IwAR3zT8knguF1H75AkyCZ_efYlvszFfkGusMB6W18Kjq8qUkF1VUwM1Y5iEg (Accessed: 6th of June 2019)

Eilers P.H.C., 2003, A perfect smoother, Analytical Chemistry, Vol. 75, 3631-3636

Gammelby M., Johansen L.N., Kloster L., 2018., Placering af H2S-sensor til produktions-strømme offshore, Semester project, Aalborg University Esbjerg.

Johansen L.N., Kloster L., Andreasen A. Kucheryavskiy S., Nielsen R.P., Maschietti M., 2019, Raman Spectroscopy for Monitoring Aqueous Phase Hydrogen Sulphide Scavenging Reactions with Triazine: A Feasibility Study, Chemical Engineering Transactions, Vol. 76.

Kelland M.A., 2014, Production Chemicals for the Oil and Gas Industry, Chapter 15, Boca Raton, USA, CRC Press, Taylor and Francis Group

Kucheryavskiy S., 2019, Multivariate Data Analysis for Chemometrics [Online], available at: https://cran.r-project.org/web/packages/mdatools/mdatools.pdf (Accessed: 2 May 2019)

Liss P.S., 1972, Process of gas exchange across an air-water interface, Deep-sea Research, Pergamon Press, Vol. 20, 221-238

Madsen H.T., 2011, Investigation of Fouling Formation during H2S Scavenging with 1,3,5-tri-(2-hydroxyethyl)-hexahydro-s-triazine, Master thesis, Aalborg University Esbjerg

Madsen H.T., Søgaard E., 2012, Use of ESI-MS to determine reaction pathway for hydrogen sulphide scavenging with 1,3,5-tri-(2-hydroxyethyl)-hexahydro- s-triazine, European Journal of Mass Spectrometry, Vol. 18, p. 377-383.

Mathesongas, [online] Available at: https://www.mathesongas.com/pdfs/products/Lower-(LEL)-&-Upper-(UEL)-Explosive-Limits-.pdf (Accessed: 6 June 2019)

Murison J., Schneider F., Muller T., Punga V., Löw M. Peerlings H., Feustel M., Taylor G., Wylde J., Kelly C., 2016, Laboratory simulation of gas sweetening,[online] available at: https://doi.org/10.31224/osf.io/63nq7 (5 May 2019)

Perez-Pineiro R., Cruz-Perez D., Hoshowski J., Zhang H., Hendry J., 2018, H2S scavenger tower operational efficiency achieved through onsite compositional analysis, NACE Corrosion Conference & Expo, Phoenix, Arizona, USA, Paper No. 11553,1-7, NACE International.

Rinnan Å., van den Berg F., Engelsen S.B., 2009, Review of the most common pre-processing techniques for near-infrared spectra, TrAC Trends in Analytical Chemistry, Vol. 28(10), 1201-1222

Roberts G.W., 2009, Chemical Reactions and Chemical Reactors, Chapter 5 and 6, Hoboken, USA, John Wiley & Sons, Inc.

Socrates G., 2001, Infrared and Raman Characteristic Group Frequencies: Tables and Charts, 3rd ed., John Wiley & Sons, LTD, Chichester, England.

Sumestry M., Tedjawidjaja H., 2013, Case Study—Calcium-Carbonate-Scale Inhibitor Performance Degradation Because of H2S-Scavenger Injection in Semgoa Field, Oil and Gas Facilities, Vol. 2(01), P. 40-45

Taylor G.N., Wylde J.J., Müller T., Murison J., Schneider F., 2017, Fresh insight into H2S Scavenging Mechanism of MEA-Triazine vs. MMA-Triazine, SPE International Conference on Oilfield Chemistry, Montgomery, Texas, USA, Paper No. SPE-184529-MS

Unisense A/S, [online] Available at: https://sulfilogger.com/products/ (Accessed: May 30th, 2019)

Wang X., Zheng Y., Shi J., Gong X., Ji Y., Han W., Jiang Y., Austin E.D., Fang X., Zhang Z., 2018, Elucidating the Reaction Mechanisms between Triazine and Hydrogen Sulfide with pH Variation Using Mass Spectrometry, Vol. 90, p. 11138-11145.

Östlund H.G., Alexander J., 1963, Oxidation rate of sulphide in seawater – A preliminary study, Journal of Geophysical Research, Vol.68(13), pp.3995-3997

Appendices

Deoxygenation

Preliminary investigations were conducted trying to limit the amount of oxygen in the system. The reasoning being that offshore production is anoxic and free oxygen can oxidize Sulphur into Sulphite and Sulphate.

A glove box was not available for this project.

First the water was deoxygenized by a N_2 gas flow through a pipe into the demineralized water, detecting the oxygen concentration with an oxygen measuring instrument. It was throughout the experiment observed the oxygen level decreasing with time, cf. Table 21.

Table 21: Deoxygenation of demineralised water over time

Time [min]	Measured O_2 [mg/L]	Temperature [°C]
0	6.26	22.9
6	3.70	22.5
10	2.97	22.2
15	2.85	22.0
20	3.09	21.8
26	3.20	N/A
41	0.87	20.1
62	0.80	N/A

Table 21 illustrates that it was quite time consuming to deoxygenate the demineralized water. Furthermore, two challenges were presumed to impact the oxygen concentration in the solution:

1) Stirring of the solution, to ensure homogeneous conditions.

2) During the experiment the deoxygenated water was going to be poured into different glassware

These two conditions were therefore further investigated. First it was investigated if stirring of the water had any effect on the oxygen level, cf. Table 22 For this experiment no deoxygenation of the demineralized water was performed.

Table 22: Measurement of oxygen content in demineralized water with and without stirring

Measured O_2 [mg/L] without stirring	Measured O_2 [mg/L] with stirring	Measuring point in solution
6.81	8.68	Top
6.91	8.67	Bottom

From Table 22 an increase of oxygen in the solution is observable and as first presumed the stirring of solution also has an effect, increasing the oxygen level. Moreover, the importance of stirring, for a homogeneous solution, is also underlined by Table 22 as there is a bigger variation in the solution with no stirring compared with the solution being stirred.

Secondly it was examined if the pouring affected the oxygen level in the water, cf. Table 23.

Table 23: Transfer of deoxygenated water from one glassware to another

Point in time	Measured O_2 [mg/L]	Temperature [°C]
Deoxygenated water	1.02	19.8
First transfer	3.70	N/A

As Table 23 illustrates even at first attempt to carefully pour the deoxygenated water from one glassware to another caused a significant increase in the oxygen level of almost 400 %.

After these investigations it was concluded that it would be challenging to keep the system near anoxic without a glovebox. The presumption was that at least one transfer of the deoxygenated water was needed as the oxygen measurement instrument wouldn't fit the size of glassware preferred. The rise in oxygen level of the solution when transferred could again be deoxygenated, however, after det addition of the Sulphur, deoxygenation would be at risk of eliminating the Sulphur species. Another attempt to keep oxygen from absorbing back into the solution was tested, but with no success. For this attempt a flow of N_2 over the solution was to limit the absorbance of oxygen.

Experimental specifications

In this appendix the experimental specifications are listed.

All masses are weighed on an analytical balance.

All volumes from 5 ml and above are measured using volumetric flasks with the uncertainties of ± 0.04 ml.

All volumes under 5 ml are measured with an automatic pipette with uncertainties of ± 0.01 ml.

Segment A

Table 24: Experimental specifications

Experiment	Scavenger	$V_{scavenger}$ [µl]	Sulphur salt	m_{salt} [g]	V_{total} [ml]
A.1	MMAT	246	Na_2S	0.2426	100
A.2	MMAT	164	Na_2S	0.2426	100
A.3	MMAT	246	Na_2S	0.3645	100
A.4	MMAT	164	Na_2S	0.3651	100
A.5	MMAT	246	Na_2S	0.2440	100
A.6	MMAT	246	Na_2S	0.3646	100
A.7	MMAT	246	Na_2S	0.2433	100
A.8	MMAT	246	Na_2S	0.2441	100
A.9	MMAT	246	Na_2S	0.3648	100
A.10	MMAT	164	Na_2S	0.2445	100
A.11	MMAT	164	Na_2S	0.2447	100
A.12	MMAT	164	Na_2S	0.2448	100
A.13	MMAT	246	Na_2S	0.3659	100
A.14	MMAT	164	Na_2S	0.3657	100
A.15	MMAT	164	Na_2S	0.3643	100
A.16	MMAT	164	Na_2S	0.3650	100
A.17	MMAT	73	Na_2S	0.7763	100
A.18	MMAT	73	Na_2S	0.7763	100

Segment E

Table 25: Experimental specifications

Experiment	Scavenger	$m_{scavenger}$ [g]	Sulphur salt	m_{salt} [g]	V_{total} [ml]
E.1	HET	1.0023	Na_2S	0.5032	100
E.2	HET	1.0132	Na_2S	0.5003	100
E.3	HET	1.0004	Na_2S	0.5005	100

Table 26:: Experimental specifications

Experiment	Scavenger	$V_{scavenger}$ [µl]	Sulphur salt	m_{salt} [g]	V_{total} [ml]
E.4	MMAT	1000	Na_2S	0.5131	100
E.5	MMAT	1000	Na_2S	0.5024	100
E.6	MMAT	1000	Na_2S	4.8808	100
E.7	MMAT	1000	NaHS	1.6949	100
E.8	MMAT	1000	Na_2S	0.9230	100

Segment F

Table 27: Experimental specifications

Experiment	Scavenger	$V_{scavenger}$ [µl]	Sulphur salt	m_{salt} [g]	V_{total} [ml]
F.1	MMAT	100	Na_2S	0.8	100

Table 28: Experimental specifications

Experiment	Scavenger	$m_{scavenger}$ [g]	Sulphur salt	m_{salt} [g]	V_{total} [ml]	V_{HCl} [ml]
F.2	HET	1	Na_2S	1	10	1
F.3	HET	0.5085	Na_2S	0.5067	10	1.5
F.4	HET	1.0152	Na_2S	1.0143	10	1
F.5	HET	1	Na_2S	1	10	1
F.6	HET	1.0205	Na_2S	0.6610	10	0.9

Segment G

Table 29: Experimental specifications

Experiment	Scavenger	$m_{scavenger}$ [g]	Sulphur salt	m_{salt} [g]	V_{total} [ml]	V_{HCl} [ml]
G.1	HET	0.0599	~	~	3	0.01
G.2	HET	0.1798	~	~	3	0.01
G.3	HET	0.1199	~	~	3	0.03
G.4	HET	0.1199	~	~	3	0.01
G.5	HET	0.1199	~	~	3	0.02
G.6	HET	0.1798	~	~	3	0.02
G.7	HET	0.1798	~	~	3	0.03
G.8	HET	0.0599	~	~	3	0.02
G.9	HET	0.0599	~	~	3	0.03
G.10	HET	1.0024	~	~	10	1
G.11	HET	1.0142	~	~	10	2

Setup 1

Table 30: Experimental specifications

Experiment	Scavenger	$m_{scavenger}$ [g]	Sulphur salt	m_{salt} [g]	V_{total} [ml]	V_{HCl} [ml]
S1.1	HET	1.0169	Na_2S	0.8068	10	1
S1.2	HET	0.4996	Na_2S	0.4993	10	0.5
S1.3	HET	0.4020	Na_2S	1.0004	10	1
S1.4	HET	0.4004	Na_2S	1.0012	10	1
S1.5	HET	0.3998	Na_2S	1.0005	10	1
S1.6	HET	0.4009	Na_2S	1.0005	10	1
S1.7	HET	0.4028	Na_2S	1.0005	10	1
S1.8	HET	0.4015	Na_2S	1.0005	10	1
S1.9	HET	0.4018	Na_2S	1.0013	10	1
S1.10	HET	0.4020	Na_2S	1.0000	10	1

Setup 2

Table 31: Experimental specifications

Experiment	Scavenger	$m_{scavenger}$ [g]	Sulphur salt	m_{salt} [g]	V_{total} [ml]
S2.1	HET	0.4468	Na_2S	1.001	10
S2.2	HET	0.4836	Na_2S	1.0006	10
S2.3	HET	0.4893	Na_2S	1.0006	10
S2.4	HET	0.4024	Na_2S	0.9994	10
S2.5	HET	0.4020	Na_2S	1.0008	10

Setup 3

Table 32: Experimental specifications

Experiment	Scavenger	$m_{scavenger}$ [g]	Sulphur salt	m_{salt} [g]	V_{total} [ml]
S3.1	HET	0.8572	Na_2S	0.3718	10
S3.2	HET	0.8572	Na_2S	0.1250	10
S3.3	HET	0.4031	Na_2S	0.3731	10
S3.4	HET	0.4031	Na_2S	0.2486	10
S3.5	HET	0.4292	Na_2S	0.1247	10
S3.6	HET	0.4253	Na_2S	0.2465	10
S3.7	HET	0.8586	Na_2S	0.2482	10
S3.8	HET	0.8573	Na_2S	0.1235	10

Setup 4

Table 33: Experimental specifications

Experiment	Scavenger	$m_{scavenger}$ [g]	Sulphur salt	m_{salt} [g]	V_{total} [ml]	V_{HCl} [ml]
S4.1	HET	0.8348	Na_2S	0.9437	65	0.8
S4.2	HET	0.8342	Na_2S	0.9447	65	0.8
S4.3	HET	0.8339	Na_2S	0.9447	65	0.8
S4.4	HET	0.8350	Na_2S	0.9449	65	0.8
S4.5	HET	0.8360	Na_2S	0.9441	65	0.8
S4.6	HET	0.8362	Na_2S	0.9449	65	0.8
S4.7	HET	0.8360	Na_2S	0.9443	65	0.805
S4.8	HET	0.8367	Na_2S	0.9446	65	0.81
S4.9	HET	0.8366	Na_2S	0.9448	65	0.845
S4.10	HET	0.8365	Na_2S	0.9442	65	0.8
S4.11	HET	0.8362	Na_2S	0.9448	65	0.85
S4.12	HET	0.8364	Na_2S	0.9443	65	0.9

Calibration

For each of the different setups, individual calibrations were carried out.

14.1.1 Setup 1-3

For setups 1-3 the calibrations for HET, HS^- and peak 675 cm^{-1} were as follows:

HET

Prediction performance for Conc:

	X expvar	Y expvar	RMSE	Bias	Slope	R2	RPD
Comp 1	45.5	99.3	0.0187	3.49e-17	0.993	0.993	12.1
Comp 2	2.15	0.431	0.0114	8.11e-17	0.997	0.997	19.9

Results for cross-validation

Prediction performance for Conc:

	X expvar	Y expvar	RMSE	Bias	Slope	R2	RPD
Comp 1	41.6	99.2	0.0204	-0.000557	0.97	0.992	11.1
Comp 2	0.269	-0.0578	0.0212	-0.000826	0.979	0.991	10.7

Figure 62: PLS results for HET

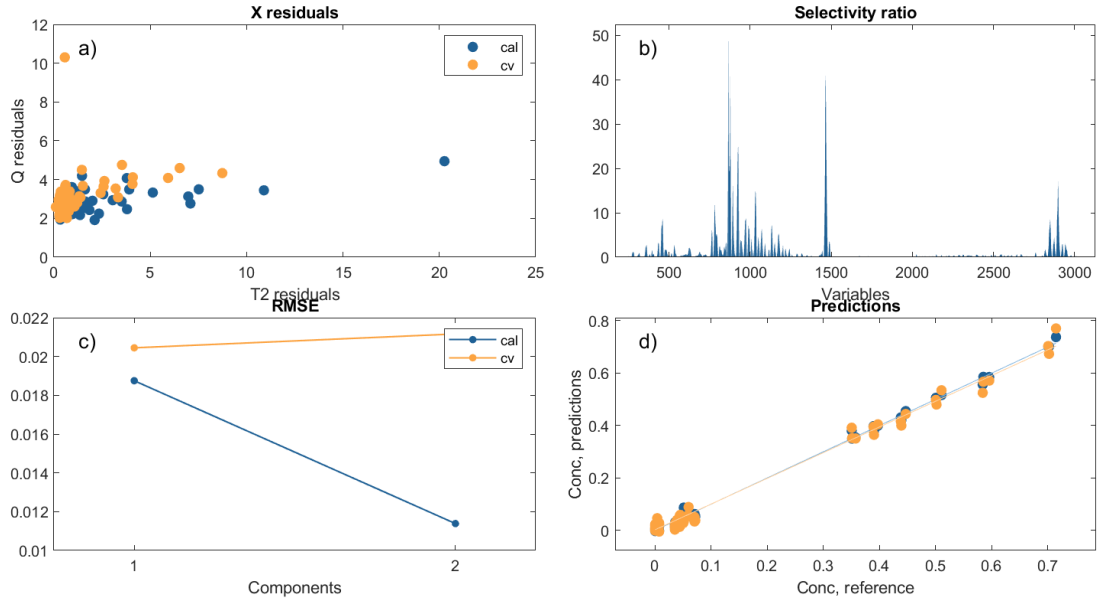

Figure 63: PLS results for HET

HS^-

Prediction performance for Conc:

	X expvar	Y expvar	RMSE	Bias	Slope	R2	RPD
Comp 1	77.6	98.3	0.0326	5.75e-17	0.983	0.983	7.75

Results for cross-validation

Prediction performance for Conc:

	X expvar	Y expvar	RMSE	Bias	Slope	R2	RPD
Comp 1	76.5	97.9	0.0369	2.69e-05	0.978	0.979	6.86

Figure 64: PLS results for HS^-

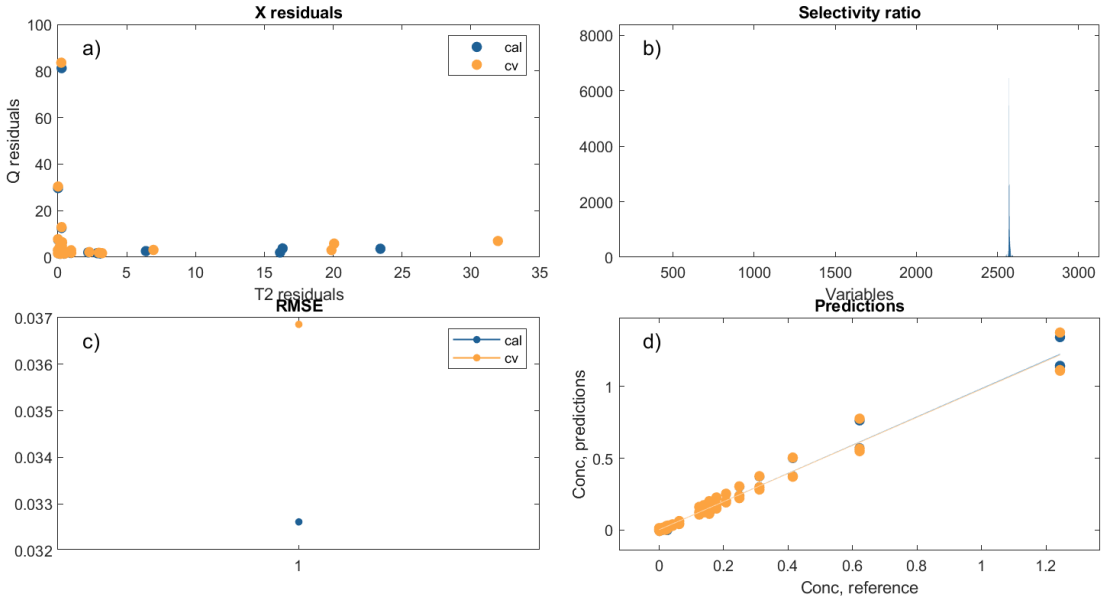

Figure 65: PLS results for HS^-

Peak 675 cm^{-1}

Linear regression model:
y ~ 1 + x1

Estimated Coefficients:

	Estimate	SE	tStat	pValue
(Intercept)	-0.0118196441362375	0.00203113147656282	-5.81924128133709	0.0101047736551026
x1	0.0907667381643027	0.00445592147051374	20.3699142287258	0.000258671123713874

Number of observations: 5, Error degrees of freedom: 3
Root Mean Squared Error: 0.00142
R-squared: 0.993, Adjusted R-Squared 0.99
F-statistic vs. constant model: 415, p-value = 0.000259

Figure 66: Regression results for peak 675 cm^{-1}

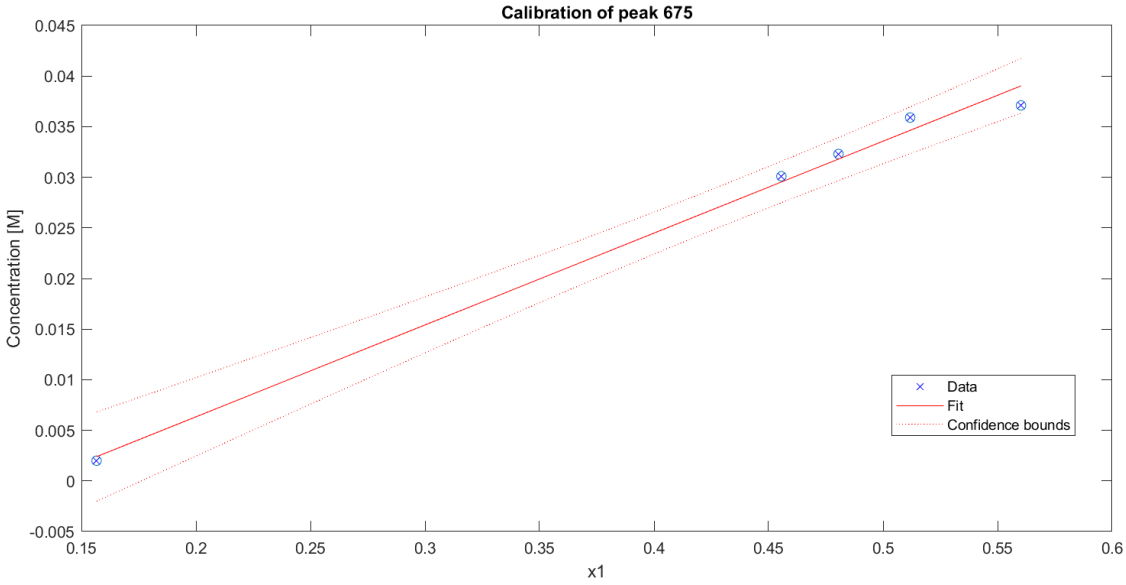

Figure 67: Regression of peak 675 cm^{-1}

14.1.2 Setup sensor

For the setup involving the sensor a calibration on both HS^- and H_2S was required. A series of solutions of HS^- was prepared and scanned. Then HCl acid was added to lower the pH and thereby create H_2S. As the system was nearly completely closed the equilibrium was assumed reached. Figure 68 illustrates the Raman spectra of the experiments.

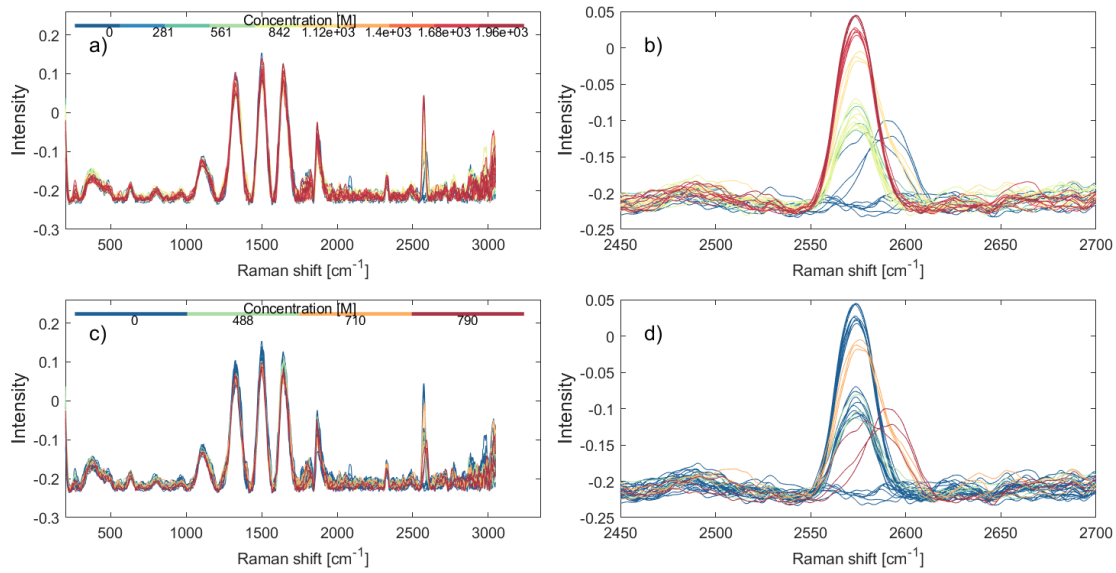

Figure 68: a) Full spectrum coloured on the basis of concentration of HS^-, b) Zoom-in of a), c) Full spectrum coloured on the basis of concentration of H_2S, b) Zoom-in of c)

HS^-

Prediction performance for Conc:

	X expvar	Y expvar	RMSE	Bias	Slope	R2	RPD
Comp 1	29.5	92.1	205	1.07e-13	0.921	0.921	3.56

Results for cross-validation

Prediction performance for Conc:

	X expvar	Y expvar	RMSE	Bias	Slope	R2	RPD
Comp 1	20.1	89.4	238	0.0974	0.837	0.898	3.07

Figure 69: PLS results for HS^-

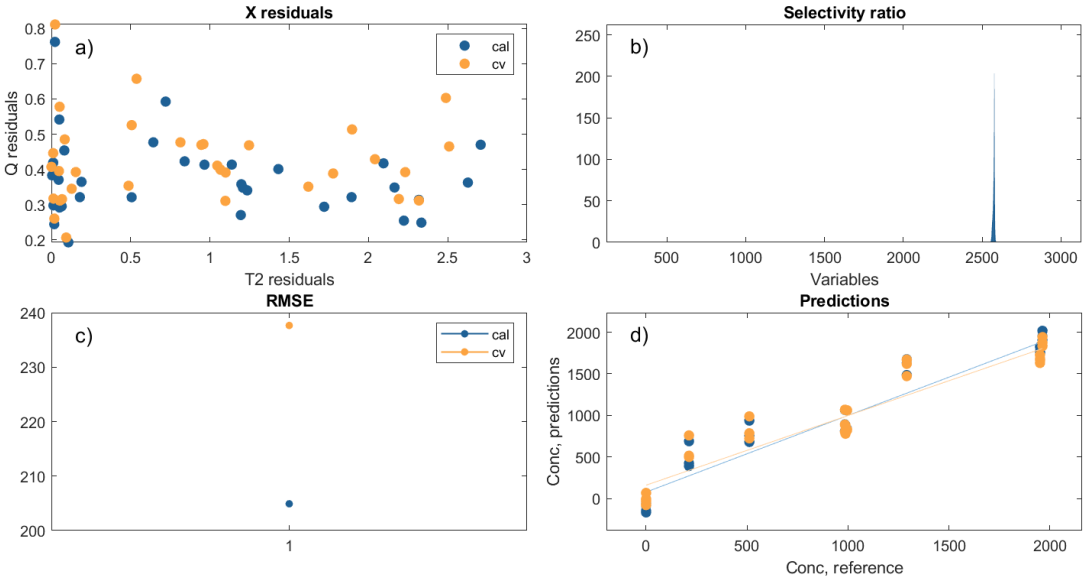

Figure 70: PLS results for HS^-

H_2S

Prediction performance for Conc:

	X expvar	Y expvar	RMSE	Bias	Slope	R2	RPD
Comp 1	8.29	77.9	144	6.03e-15	0.779	0.779	2.13

Results for cross-validation

Prediction performance for Conc:

	X expvar	Y expvar	RMSE	Bias	Slope	R2	RPD
Comp 1	-7.32	43.9	230	7.8	0.35	0.471	1.34

Figure 71: Regression results for H_2S

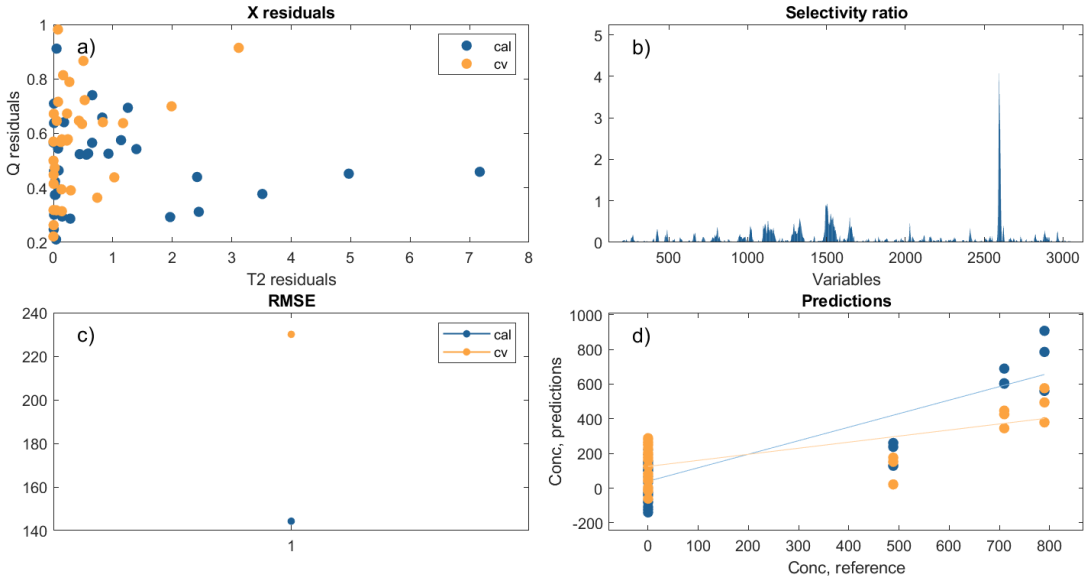

Figure 72: Regression results for H2S

14.1.3 Setup 4

For setup 4 the calibrations for HET, HS^-, MEA and the peak 675 cm^{-1} were as follows:

HET

Prediction performance for Conc:

	X expvar	Y expvar	RMSE	Bias	Slope	R2	RPD
Comp 1	78.9	92.5	0.00665	-6.17e-18	0.925	0.925	3.66
Comp 2	5.95	6.49	0.0024	2.57e-19	0.99	0.99	10.2

Results for cross-validation

Prediction performance for Conc:

	X expvar	Y expvar	RMSE	Bias	Slope	R2	RPD
Comp 1	75.5	91.2	0.00721	-1.72e-05	0.912	0.912	3.38
Comp 2	5.45	7.24	0.003	-2.03e-05	0.97	0.985	8.14

Figure 73:: Regression results for HET

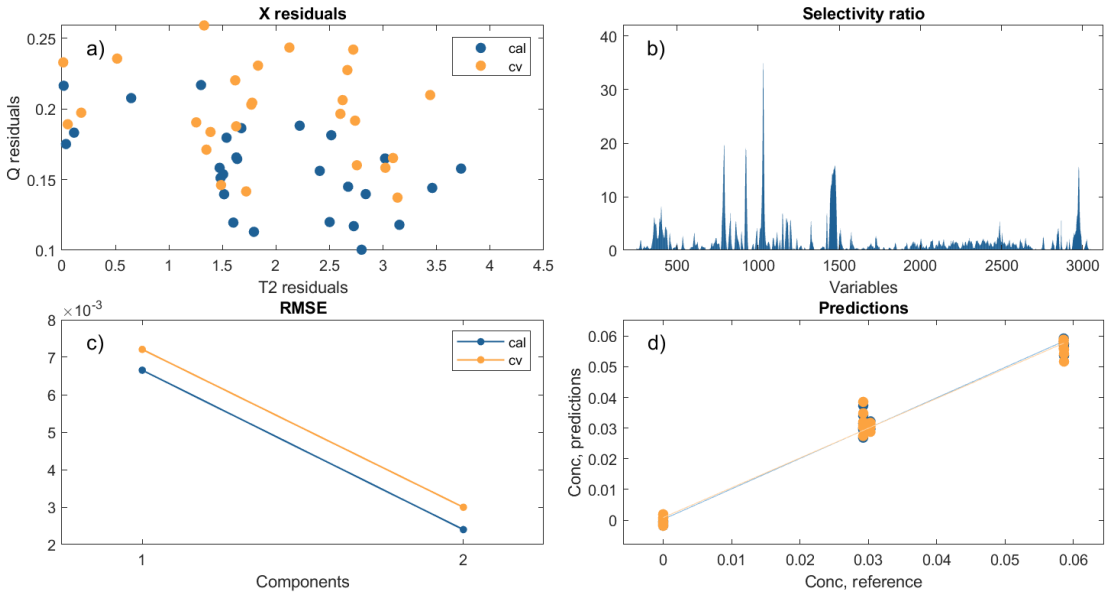

Figure 74: Regression results for HET

HS^-

Prediction performance for Conc:

	X expvar	Y expvar	RMSE	Bias	Slope	R2	RPD
Comp 1	52.6	99.5	0.00147	5.62e-18	0.995	0.995	14.2

Results for cross-validation

Prediction performance for Conc:

	X expvar	Y expvar	RMSE	Bias	Slope	R2	RPD
Comp 1	42.5	99.1	0.002	-5.8e-05	0.945	0.993	10.4

Figure 75: Regression results for HS^-

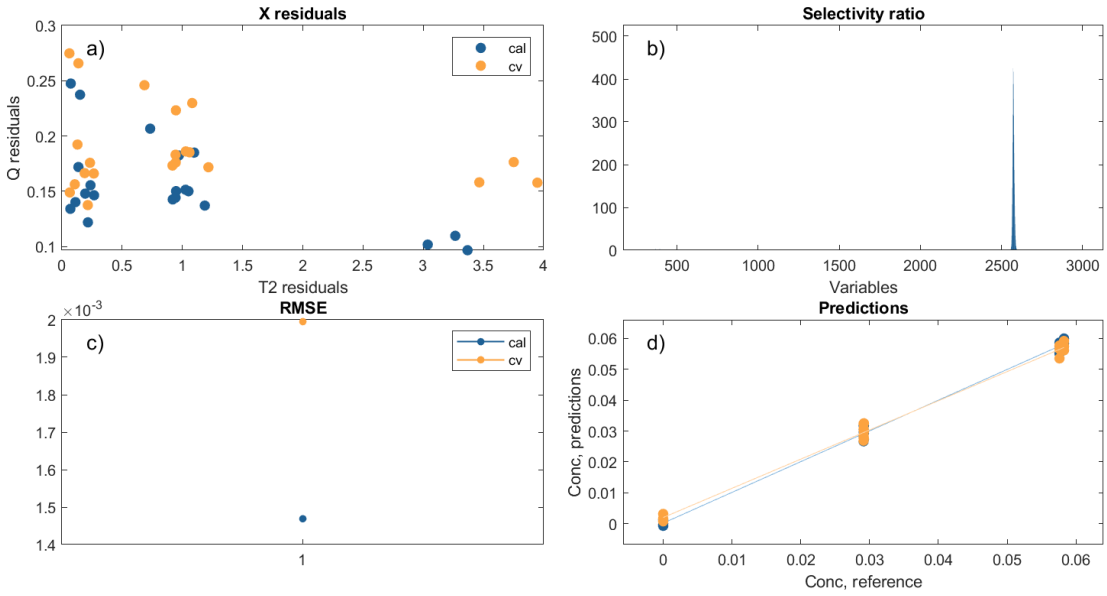

Figure 76: Regression results for HS^-

MEA

Prediction performance for Conc:

	X expvar	Y expvar	RMSE	Bias	Slope	R2	RPD
Comp 1	74.5	24.9	0.021	6.42e-18	0.249	0.249	1.15
Comp 2	10.4	71.1	0.00486	6.23e-18	0.96	0.96	4.98

Results for cross-validation

Prediction performance for Conc:

	X expvar	Y expvar	RMSE	Bias	Slope	R2	RPD
Comp 1	72.5	14.7	0.0223	-5.63e-05	0.213	0.162	1.08
Comp 2	8.41	77.8	0.00662	-0.000126	0.851	0.932	3.65

Figure 77: Regression results for MEA

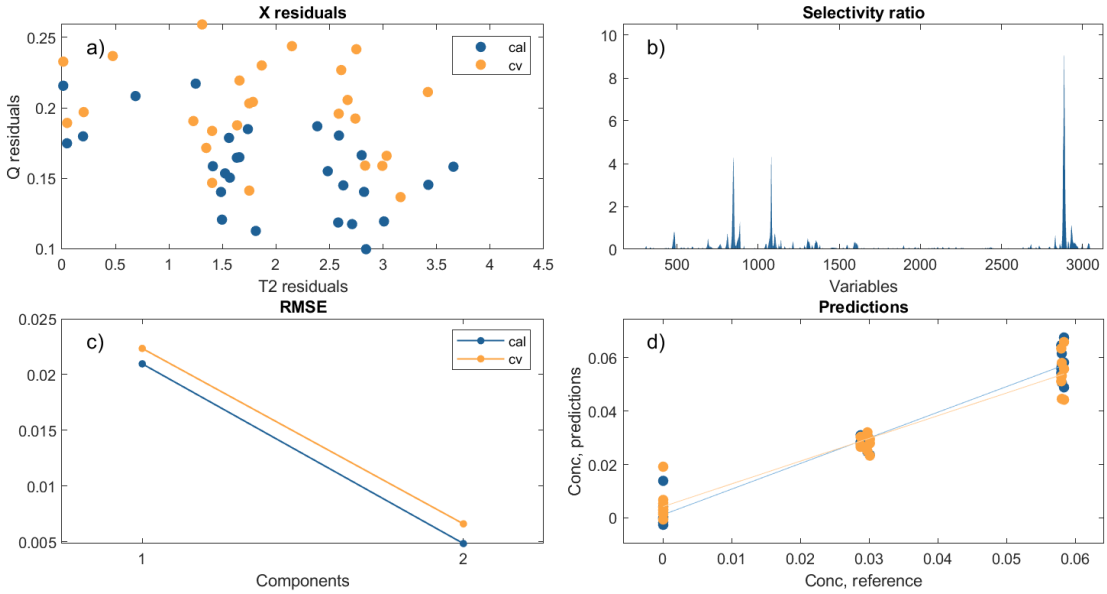

Figure 78: Regression results for MEA

Peak 675 cm^{-1}

Linear regression model:
y ~ 1 + x1

Estimated Coefficients:

	Estimate	SE	tStat	pValue
(Intercept)	0.014849136938984	0.00255344240840204	5.81534045574054	0.0101237883272786
x1	0.0776755492452057	0.0145725359855527	5.33026985297641	0.0129050555403176

Number of observations: 5, Error degrees of freedom: 3
Root Mean Squared Error: 0.00176
R-squared: 0.904, Adjusted R-Squared 0.873
F-statistic vs. constant model: 28.4, p-value = 0.0129

Figure 79: Regression results for peak 675 cm^{-1}

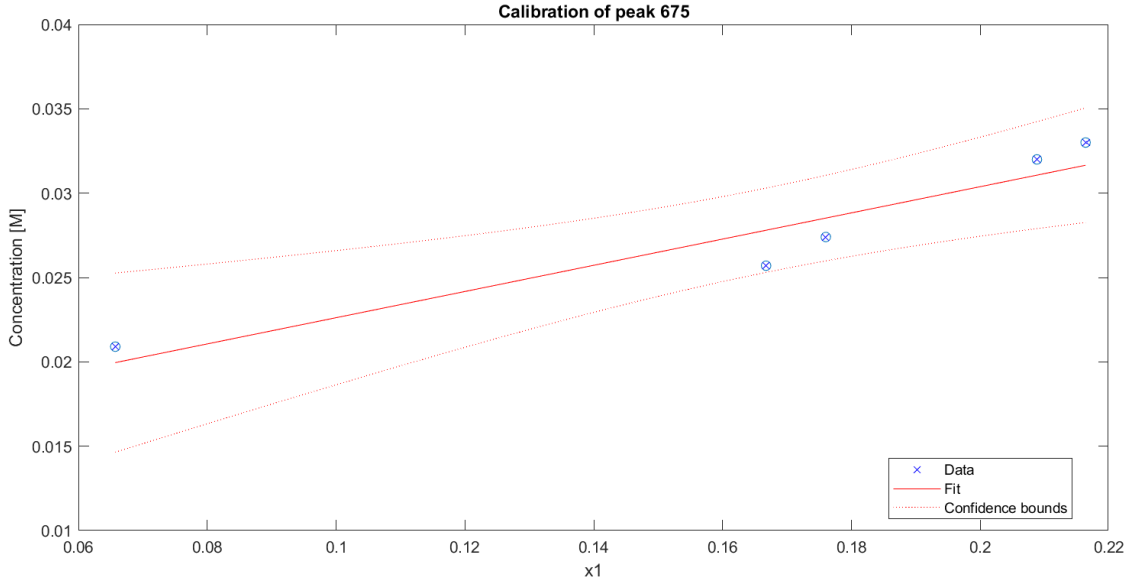

Figure 80: Regression results for peak 675 cm^{-1}

Solutions of HCl

Dilution of HCl

To set the initial pH of the reaction solution without evaporating the Sulphur, a series of experiments were conducted trying to ascertain the HCl/H_2O ratio of a solution to set the pH. By diluting HCl in demineralized water the theory was that no sudden evaporation of H_2S would occur. The pH levels wanted was 8.8, 9.2 and 9.6. and with three different concentration levels of both HET and HS^-.

The dilution ratios found in Table 34 were obtained by trial and error.

Table 34: HCl/H_2O ratios for different combinations of reactant concentrations

NaHS [M]	HET [M]	HCl/H_2O ratio at pH 8.8	HCl/H_2O ratio at pH 9.2	HCl/H_2O ratio at pH 9.6
1.43	1.43	1:15	1:18	1:25
0.95	0.95	1:23	1:29	1:90
0.48	0.48	1:45	1:56	1:71
1.43	0.95	1:23	1:29	1:36
1.43	0.48	1:36	1:45	1:63
0.95	1.43	1:20	1:23	1:29
0.95	0.48	1:40	1:45	1:56
0.48	1.43	1:36	1:42	1:56
0.48	0.95	1:40	1:45	1:56

As it is evident from Table 34 different the different concentrations of HET and HS^- influenced the ratios immensely.

Volume experiments

It was also investigated if the addition of HCl would change the volume of the solution, as this was undesirable since kinetic studies in batch reactors are favourably conducted under constant volume conditions.

HCl does not change the volume of the solution when added, due to its low density however, this is assured by experiments, cf. Table 35-Table 37.

Table 35: Addition of 37% HCl solution to demineralized water

Experiment	m_{MMAT} [g]	V_{MMAT} [mL]	V_{H2O} [mL]	V_{HCl} [mL]	V_{Total} after HCl
Experiment 1	0.0957	0.1	2	0	2.1
Experiment 1	0.0957	0.1	2	0.1	2.1
Experiment 2	0.6035	0.6	2	0	2.6
Experiment 2	0.6035	0.6	2	0.1	2.6
Experiment 2	0.6035	0.6	2	0.2	2.6
Experiment 3	0.6092	0.6	2	0	2.6
Experiment 3	0.6092	0.6	2	0.05	2.6
Experiment 3	0.6092	0.6	2	0.1	2.6

Table 36: Addition of diluted HCl. 100 µL acid in 10 mL water

Experiment	m_{MMAT} [g]	V_{MMAT} [mL]	V_{H2O} [mL]	V_{HCl} [mL]	V_{Total} after HCl
Experiment 4	0.6039	0.6	2	0	2.6
Experiment 4	0.6039	0.6	2	0.1	2.6
Experiment 4	0.6039	0.6	2	0.2	2.6
Experiment 4	0.6039	0.6	2	0.3	2.6
Experiment 4	0.6039	0.6	2	0.4	2.6
Experiment 4	0.6039	0.6	2	0.5	2.6
Experiment 4	0.6039	0.6	2	0.6	2.6
Experiment 4	0.6039	0.6	2	0.7	2.6
Experiment 4	0.6039	0.6	2	0.8	2.6
Experiment 4	0.6039	0.6	2	0.9	2.6
Experiment 4	0.6039	0.6	2	1.0	2.6
Experiment 4	0.6039	0.6	2	1.5	2.6
Experiment 4	0.6039	0.6	2	2	2.6

Table 37: Addition of diluted HCl. 1 mL acid in 10 mL water

Experiment	m_{MMA} [g]	V_{MMA} [mL]	V_{H2O} [mL]	V_{HCl} [mL]	V_{Total} after HCl
Experiment 5	0.6089	0.6	2	0	2.6
Experiment 5	0.6089	0.6	2	0.1	2.6
Experiment 5	0.6089	0.6	2	0.2	2.6